

Development of Novel, Potent and Selective Small Molecular Weight PI3K/mTOR Inhibitors for the Treatment of Cancer

Inauguraldissertation

zur

Erlangung der Würde eines Doktors der Philosophie

vorgelegt der

Philosophisch-Naturwissenschaftlichen Fakultät

der Universität Basel

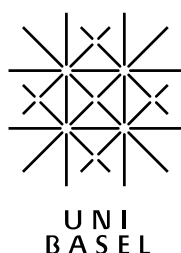
von

Nataša Cmiljanović

aus

Serbien

Basel 2011



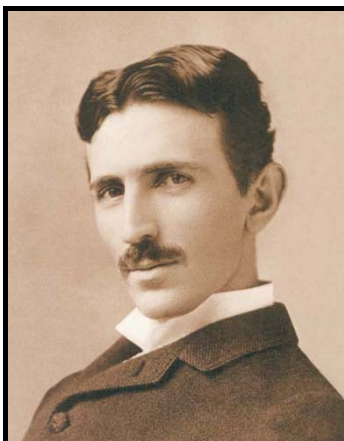
Genehmigt von der Philosophisch-Naturwissenschaftlichen Fakultät
auf Antrag von

Prof. Dr. Bernd Giese

Prof. Dr. Edwin Constable

Basel, den 22.06.2010

Prof. Dr. Eberhard Parlow
Dekan



“Of all the frictional resistance, the one that most retards human movement is ignorance; the friction which results from ignorance can be reduced only by the spread of knowledge and the unification of the heterogeneous elements of humanity. No effort could be better spent.”

Nikola Tesla

This work is a result of research guided by Prof. Dr. Bernd Giese and Prof. Dr. Matthias Wymann during the period from March 2007 to August 2010 in the Department of Chemistry and Department of Biomedicine, University of Basel.

The research results obtained during my PhD thesis are protected by several patent applications:

Cmiljanovic, V., Cmiljanovic, N., Giese, B., Wymann, MP., *Triazine, Pyrimidine and Pyridine Analogs and their use as therapeutic agents and diagnostic probes*. UK Patent ***.

Cmiljanovic, V., Cmiljanovic, N., Giese, B., Wymann, MP., *Triazine, Pyrimidine and Pyridine Analogs and their use as therapeutic agents and diagnostic probes*. International WTO Patent ***.

Cmiljanovic, V., Cmiljanovic, N., Giese, B., Wymann, MP., *Spirocyclic compounds and their use as therapeutic agents and diagnostic probes*. UK Patent ***.

Cmiljanovic, V., Cmiljanovic, N., Giese, B., Wymann, MP., *Piperazinotriazines*. UK Patent ***.

ACKNOWLEDGMENTS	7
1. INTRODUCTION	9
2. THEORETICAL BACKGROUND	12
2.1. PHOSPHOINOSITIDE 3-KINASES	12
2.1.1. Class I PI3Ks.....	14
2.1.2. Class II PI3Ks	15
2.1.3. Class III PI3Ks	15
2.1.4. Class IV PI3Ks.....	15
2.2. PI3K INHIBITORS	16
2.2.1. Natural PI3K Inhibitors.....	16
2.2.2. Synthetic First Generation of PI3K Inhibitors.....	18
2.2.3. Synthetic Second Generation of PI3K Inhibitors	20
3. RESEARCH PROJECT	23
4. DISCUSSION AND RESULTS	24
4.1. ZSTK474 DERIVATIZATION	24
4.1.1. Triazine Chemistry.....	24
4.1.2. Fragment Validation Step as an Effective Method in Process of Creating Novel and Active ZTSK474 Derivatives	27
4.1.3. Synthesis of Novel, Active and Selective ZSTK474 Derivatives	32
4.2. STRUCTURE-BASED DESIGN OF IRREVERSIBLE PI3K INHIBITORS.....	43
4.2.1. Benefits of Covalent Binding Mechanism	43
4.2.2. Published Irreversible Kinase Inhibitors	44
4.2.3. Michael Addition of Amine and Thiol Nucleophiles to the Acryl Containing Probe VCA20 in Water	47
4.2.4. Selectivity Filter Approach for Successful Design of Irreversible Inhibitors	49
4.2.5. Chemistry and Biology of Irreversible ZSTK474 Derivatives.....	51
4.3. PI3K INHIBITOR ACTIVITY AGAINST HUMAN GLIOBLASTOMA	65
4.3.1. PI3K Inhibitor Efficacy in Colony Formation Assay on Malignant Glioma Cell Lines	68
4.4. TRIAZINE AND PYRIMIDINE DERIVATIVES	70
4.4.1. Chemistry and Biology of Di-Morpholine-Containing Triazine and Pyrimidine Derivatives	71
4.4.2. Chemistry and Biology of Linked Triazine and Pyrimidine Derivatives	86
4.5. GRAPHICAL OVERVIEW OF THE BEST DI-MORPHOLINE-CONTAINING AND LINKED TRIAZINE AND PYRIMIDINE DERIVATIVES.....	96
4.6. CRYSTAL STRUCTURES OF PI3K/MTOR INHIBITORS	98
5. SUMMARY AND OUTLOOK	103
6. EXPERIMENTAL PART	104
6.1. GENERAL WORK CONDITIONS	104
6.2. CONDITIONS OF MEASUREMENTS	104

6.3. BIOLOGICAL METHODS AND PARAMETERS.....	106
6.3.1. In Cell Western High Throughput Screening Assay	106
6.3.2. Kinase Glo Luminescent Assay	108
6.3.3. In cell Western Inhibition Assay on Bone Marrow Derived Mast Cells	110
6.3.4. Covalent PI3K γ Inhibitors.....	110
6.3.5. Colony Formation Assay.....	112
6.4. CRYSTALLIZATION AND INHIBITOR SOAKS	113
6.4.1. Data Collection and Structure Determination	113
7. REFERENCES	115
Curriculum Vitae, Natasa Cmiljanovic	121

Acknowledgments

I would like to acknowledge Prof. Dr. Bernd Giese and Prof. Dr. Matthias Wymann for giving me opportunity to be a member of their groups and to work on highly interesting projects in fields of medicinal chemistry, bioorganic chemistry and chemical biology. Due to their enthusiasm and expertise in our research field, I was able to broaden my scientific horizons.

Next, I would like to thank Prof. Dr. Edwin Constable for kindly accepting to be the referee for this thesis.

Especially my gratefulness goes to my brother Vladimir Cmiljanović for his great support over all these years. His untiring dedication to this project, enthusiasm, creativity, positive attitude, advice and exchange of knowledge always encouraged me and motivated during my thesis.

I would like to thank our master students: Jasmina Bogdanović, Alexander Sele, Manuela Jörg, Valentina Volić, Gabriel Schäfer, Heiko Gsellinger and Samantha Brianza for their valuable contribution to the project, their engagement and very nice atmosphere during the time we worked together.

Great thanks go to Dr. Romina Marone (research group of Prof. Dr. Matthias Wymann) for providing us biological analysis data and great cooperation. Her professional and precise work significantly contributed to the success of the project. Also I would like to thank Ann Mertz (research group of Prof. Dr. Matthias Wymann) for developing of high-throughput screening assays and Dr. Thomas Bohnacker (research group of Prof. Dr. Matthias Wymann) for the fast and effective work on the project of covalent inhibitors.

Next, I would like to thank Dr. Marketa Zvelebil from The Institute of Cancer Research, Breakthrough Breast Cancer Research Centre, London, UK, for doing structural studies (computational studies and high-throughput molecular modeling studies). I am grateful also to Prof. Dr. Roger L. Williams and Xuxiao Zhang from MRC Laboratory of Molecular Biology, University of Cambridge, UK for the complicated X-ray structure elucidation of several enzyme-inhibitor complexes.

Many thanks to Dr. Serdar Korur from Department of Biomedicine, University of Basel, University Hospital Basel, for successful testing of our inhibitors on malignant glioblastoma cell lines.

I am grateful to all people from analytical support for their valuable scientific investigations. Special thanks go to Dr. Daniel Häussinger for NMR analyses and to Mr Werner Kirsch for elemental analyses as well as to Dr. Markus Neuburger for X-ray structural analyses.

Many thanks go to the lab 101 for nice work atmosphere and collegial support in any situation. Also I would like to thank all former members of the Giese and the Wymann groups for exchange of knowledge and nice work atmosphere.

I am also grateful to technical staff at the Department of Chemistry for helping me to solve upcoming technical problems.

I would like to thank Office of Technology Transfer, University Basel (Wissens und Technologietransferstelle der Universität Basel) especially to Mr Mathias Weiss and Ms Hannah Greiner for their professional work on patent protection of our research results obtained during my thesis.

Last but not least, I would like to thank my parents and Miljan for their great support, encouragement and trust during all the time of my thesis.

1. Introduction

The desire to provide appropriate medications dates back to the origin of human beings, when diseases were cured by using mainly plant extracts. Generally, far in the past the efforts invested in finding new drugs were based on intuition and empirical observation. From the pharmaceutical point of view, the period to 1800s is called *the age of botanicals*, while natural product extracts, particularly those derived from botanical species, provided the main source of folk medicine. However, over the last two centuries, progress in understanding human biology and new technology has dramatically changed the approach to finding drugs. During and especially in second half of nineteenth century, development of pharmaceutical companies contributed to the rapid progress of drug development. Also, synthesis of the first synthetic pharmaceutical drug, aspirin occurred in the latter half of the nineteenth century. First half of the twentieth century provided the production of vitamins, antibiotics and unification of various scientific disciplines that led to the development of new technologies and reducing of gap in knowledge. The second half of twentieth century is characterized by linking new technologies with understanding of the human body functioning and the structure of DNA, allowing new approaches to drug improvement. Further expansion of computing technology, improving of instrumentation and examination the causes of diseases helped to the further progression of science. Eventually, emerging of genetic engineering and biotechnology in the late nineties led to rational drug design. Following development of combinatorial chemistry based on the rapid synthesis of a large number of different but structurally related molecules in order to produce some potentially biologically active compounds has also influenced the acceleration process of drug development. Practically, the end of the twentieth century provided an abundant source of medicinal information due to the incredibly rapid development of the computer technology, the existence of more powerful pharmaceutical companies and expansion of knowledge in the field of human biology. Thanks to that efficient methods for finding new drugs have been enabled. The beginning years of the new millennium continued to improve in drug discovery based on state-of-the art chemistry and chemical genetics, new advances in biology, enzyme-based molecular syntheses, proteomics and genomics, recombinant biomolecules, high-throughput screening, and gene and cell therapy [1], [2].

The usual process of drug discovery consists from several crucial stages on their way from research laboratories to the market (Figure 1). It starts with identifying cellular and genetic factors that play a role in specific diseases. Once a target is identified, the next step involves discovery of some suitable drug candidates that can block or activate a desired target [3]. The most commonly used

methods in finding the promising drug candidates, with possibility to test a large number of different compounds in a short way, using robotics, data processing, control software, liquid handling devices and sensitive detectors in order to identify active compounds are high-throughput screening (HTS) methods.

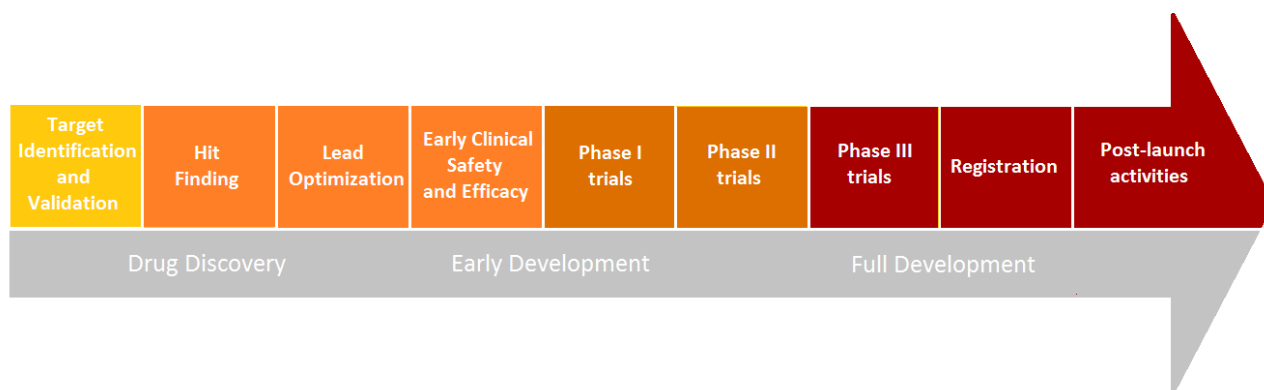


Figure 1. Overview of the most important stages in drug discovery and development process [4].

Found active compounds, so-called hits are subject of further optimization and modification in aim of creating a lead structure. This lead will then be further optimized via a medicinal chemistry project, resulting in one or two compounds which will be proposed for early drug development phase, referring to establish an initial safety profile of drug. In next proof of concept step and phase I trial, drug for a first time is given to human in order to confirm a mechanism of action, examine a safety, determine appropriate dosing and identify side effects. Phase II studies are designed to determine effectiveness and further study the safety of the candidate drug, by testing on a larger number of people (100-300). Phase III studies include even more detailed testing of efficacy and safety with several hundreds to thousands of volunteer patients. After a process of approving the drug by regulatory authorities, a new drug can be made commercially available to patients. Post-approval studies test a marketed drug in new age groups or patient types and focusing on previously unknown side effects or related risk factors in order to accomplish better effectiveness and safety [4]. The process of launching drug to the market takes an average of 10 to 12 years and roughly 900 million dollar costs [3].

Each year is estimated that 10.9 million people worldwide are diagnosed with cancer and there are 6.7 million deaths from the disease [5]. In the last decades, extreme interest in finding more effective treatments against cancer is continuously growing (Figure 2). Therefore, one of the most competitive and challenging fields in medicinal chemistry is cancer research. In recent years, phosphoinositide 3-kinases (PI3Ks) have become extremely attractive target of industry and the

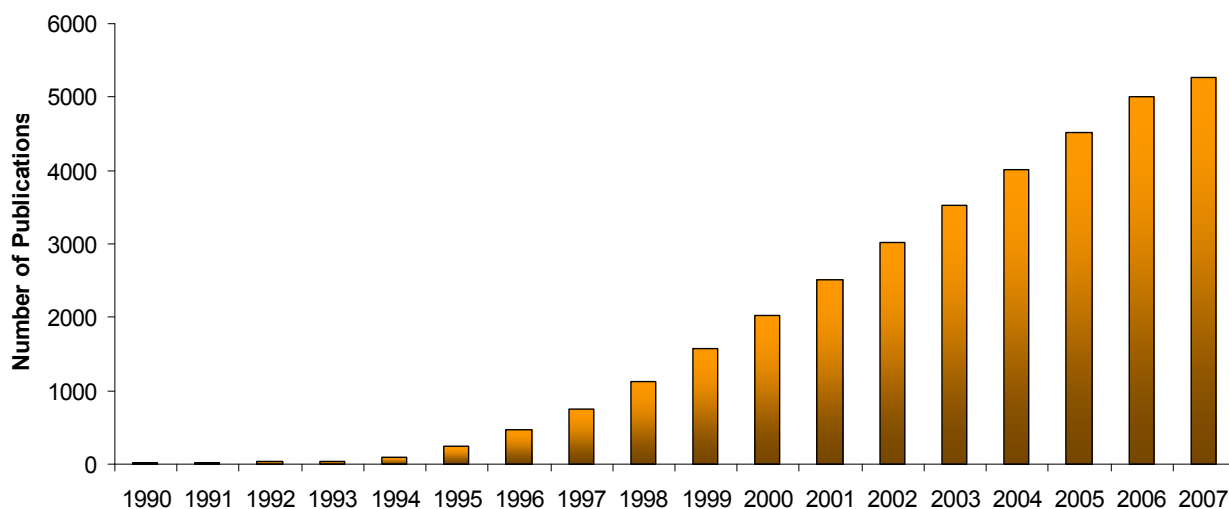


Figure 2. Accumulated numbers of published papers where wortmannin was used as a PI3K inhibitor [6].

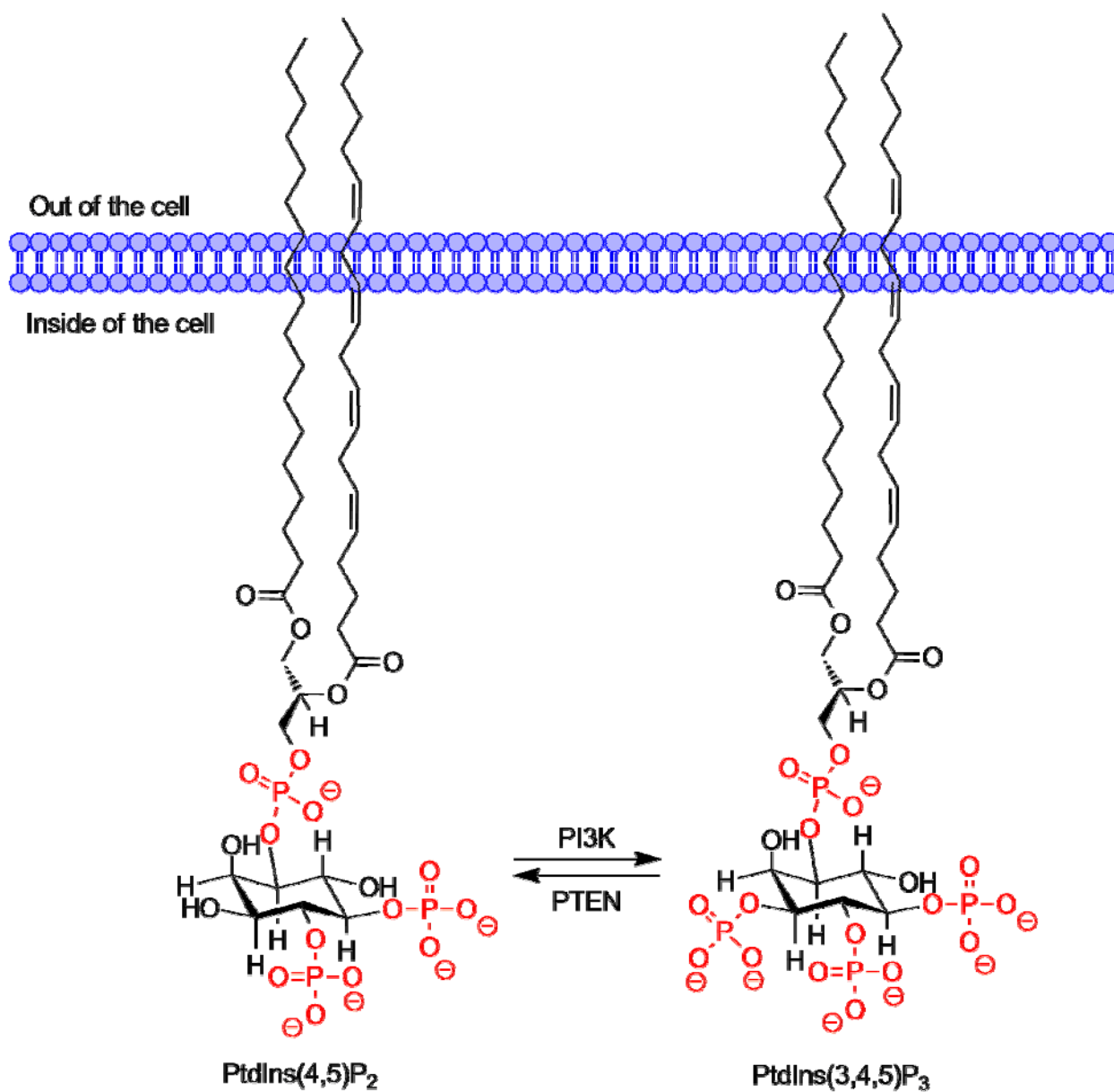
academy as well due to their possibility to modulate diverse biological process such as cell survival, growth and metabolic control by influencing many human diseases including allergy, inflammation, metabolic diseases and cancer [6]. This contributed to the development of a numerous PI3K inhibitors and many of them have established the potential usefulness as therapeutics for treatment of cancer. Several of them have already entered clinical trials. Currently two of the main interests in medicinal chemistry are: research of new, more active and selective inhibitors and the optimization of known compounds, as well as improving their pharmacodynamic and pharmacokinetic properties.

2. Theoretical Background

2.1. Phosphoinositide 3-Kinases

The phosphoinositide 3-kinases (PI3Ks) belong to a family of lipid kinases, which are implicated in signal transduction pathways and modulation of fundamental cellular activities such as cell growth, proliferation, differentiation, motility, survival and metabolism. The biochemical function of PI3Ks is the phosphorylation of the 3'-OH position of the inositol ring of PtdIns(4,5)P₂, leading to PtdIns(3,4,5)P₃, which is involved in a variety of cell signal cascades as second messenger [7]. The involvement of PI3Ks in such important biological processes can lead in case of their deregulation to development of various diseases including diabetes, thrombosis, inflammatory and autoimmune diseases as well as cancer [8], [9].

At the moment there have been eight different PI3Ks identified, categorized into III classes, according to their structural features and *in vitro* lipid substrate specificity [6]. Additionally there is a class IV of PI3Ks, comprised from PI3K-related proteins such as mTOR, DNA-PK_{cs}, ATM, ATR, SMG-1 and TRRAP [10].

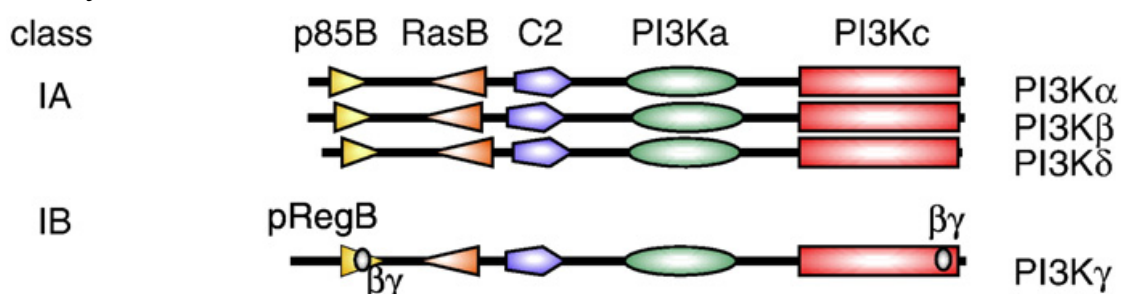


Scheme 1. Schematic representation of PI3K functionality: Phosphorylation of the 3-hydroxyl position of the inositol ring of PtdIns(4,5)P₂ leads to PtdIns(3,4,5)P₃.

2.1.1. Class I PI3Ks

The class I PI3Ks is the most extensively studied class within lipid kinases family due to its association with tumorigenesis, inflammation, cardiovascular and metabolic diseases. Therefore their activation and biological function is best understood among all PI3K classes. This class is divided into two subclasses IA and IB based on their regulatory subunit and upstream activator. There are three isoforms in Class IA, namely PI3K α , PI3K β and PI3K δ , with the respective p110 catalytic subunit bound to the p85 regulatory subunit. Class IB PI3K consists of catalytic subunit p110 γ and a regulatory subunit p101 or p84 [6]. *In vitro* they are capable to convert PtdIns to PtdIns-3-P, PtdIns-4-P to PtdIns(3,4)P₂, and PtdIns(4,5)P₂ to PtdIns(3,4,5)P₃, but *in vivo* substrate is PtdIns(4,5)P₂. Activation of Class IA PI3Ks is caused by diverse receptor tyrosine kinases, while Class IB PI3Ks is activated by G-Protein Coupled Receptors (GPCRs). This activation leads to the production of PtdIns(3,4,5)P₃, which recruits proteins containing pleckstrin-homology (PH)-domains as protein kinase B (PKB/Akt). Activation of PKB/Akt by their phosphorylation causes further phosphorylation of many proteins (involved in various cellular processes), regulating their activity in positive or negative manner [6], [11].

Catalytic subunits



Regulatory subunits

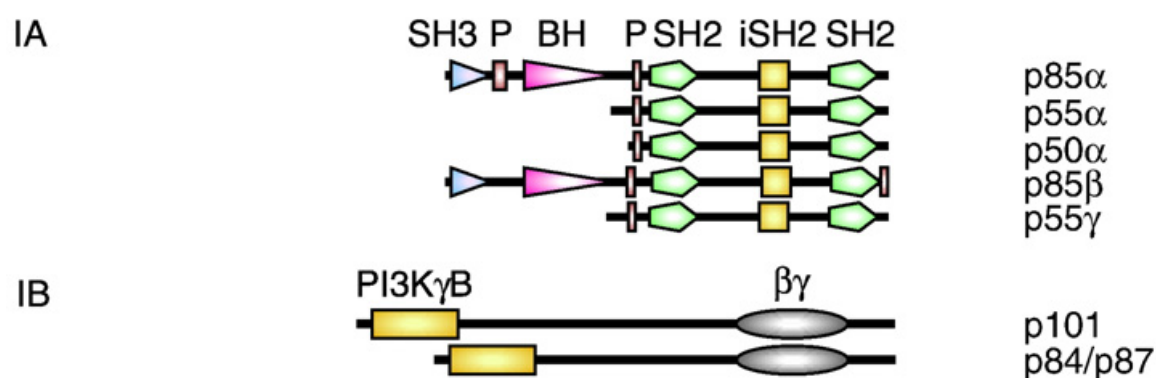


Figure 3. Catalytic and regulatory subunits of class I PI3Ks [6]

The activation of the PI3K pathway is negatively regulated by the action of two phosphoinositide phosphatases. The SH2-domain-containing inositol phosphatase (SHIP), hydrolyzes PtdIns(3,4,5)P₃ to PtdIns(3,4)P₂ and phosphatase and tensin homolog (PTEN) reverses PtdIns(3,4,5)P₃ to PtdIns(4,5)P₂. The most frequent aberrations of PI3K signalling are loss or decreasing of PTEN function and mutations in PI3K α . Loss of PTEN function is usually a late step in tumour progression, occurring in advanced tumour stages [6], [12], [13], [14].

2.1.2. Class II PI3Ks

This class of large (170-200 kDa) enzymes comprises three catalytic isoforms (C2 α , C2 β , and C2 γ) and no regulatory proteins. *In vitro*, class II PI3Ks preferentially phosphorylates PtdIns and PtdIns-4-P to form PtdIns-3-P and PtdIns(3,4)P₂, respectively. The relevancy of class II PI3Ks by *in vivo* processes is still under investigation. The distinct feature of class II PI3Ks is the C-terminal C2 domain, which is Ca²⁺ insensitive due to the lack of a conserved aspartate residue. Their mode of action is still poorly understood and no adaptor molecules have been identified yet [6].

2.1.3. Class III PI3Ks

Class III PI3Ks is capable to phosphorylate specifically PtdIns to PtdIns-3-P. The only one member of Class III PI3Ks is Vps34, which is in human cells associated with a regulatory subunit p150. Vps34 was first identified in a *Saccharomyces cerevisiae* (budding yeast) and has been shown to play an essential role in the trafficking of proteins and vesicles. In recent years a lot of attention was given to the requirement of Vsp34 in the induction of autophagy in nutrient, amino acids, as well as glucose-deprived cells [6].

2.1.4. Class IV PI3Ks

The PI3Ks related proteins of class IV are high molecular enzymes with a catalytic core similar to PI3Ks. As already mentioned Class IV includes the protein mTOR, DNA-PK_{cs}, ATM, ATR, SMG-1 and TRRAP, which might be involved either in cell growth control, genome transcriptome surveillance or DNA damage responses [6].

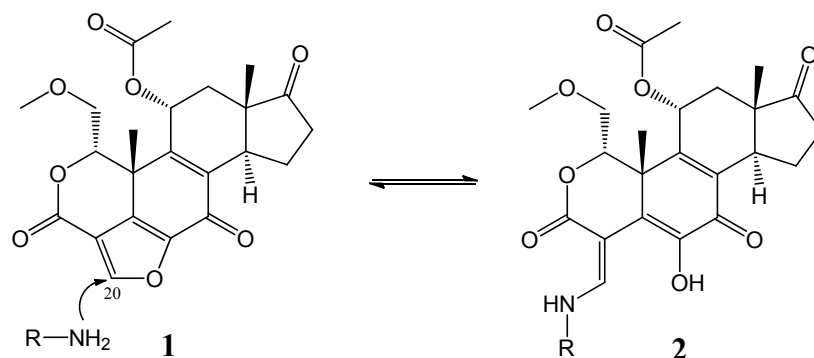
2.2. PI3K Inhibitors

Twenty years ago was discovered association of PI3K enzymatic activity with viral oncoproteins. During the next period, understanding about biological role of these enzymes has developed rapidly. Today, it is known that PI3Ks are involved in many vital cell functions and their deregulation is connected to development of various disorders. Since PI3Ks are shown to be important target in cancer as well as other disease, interest in development of PI3K inhibitors has significantly increased. The elucidation of PI3K γ crystal structure, free and in a complex with ATP, wortmannin, LY294002 and other kinase inhibitors has accelerated further drug design. The development of PI3K inhibitors as potential therapeutic agents has made a great leap forward in the past several years. Several promising PI3K inhibitors have entered into clinical trials for cancer therapy and other diseases. Recently, researchers started to believe that treatment with an isoform specific inhibitor might lead to reduction of side effects without loss of efficiency. However, the advantage in using isoform specific inhibitors is still under investigation. The following chapter presents an overview of some natural and synthetic PI3K inhibitors from the public domain, their mechanism of action and biological function.

2.2.1. Natural PI3K Inhibitors

Wortmannin (**1**) is a fungal metabolite, which was first isolated from *Penicillium wortmanni* in 1957 by Brian and co-workers as an anti-inflammatory agent [15], while its structure was elucidated 15 years later by Petcher and co-workers [16]. Wymann and co-workers have identified wortmannin (**1**) as a potent PI3K inhibitor against Class I, II and III PI3Ks as well as other related PI3K kinases [17]. Interestingly, unlike most known kinase inhibitors, wortmannin (**1**) inhibits PI3K in an ATP-non competitive manner by covalent binding with PI3K. The mechanism of PI3K inhibition was elucidated by the group of Prof. Matthias P. Wymann in 1996, basing on formation of an enamine after nucleophilic attack of Lys-802 residue of PI3K α to the C-20 position of wortmannin. This enamine is in equilibrium with an imine (Schiff base), which is relatively stable at physiological pH, but is easily hydrolyzed under acidic conditions [18]. SAR studies of wortmannin (**1**) demonstrated that furan ring is essential for its activity and modifications of the electrophilicity of furan ring lead to serious changes in inhibitor activity [6]. Wortmannin (**1**) is low nanomolar inhibitor ($IC_{50} \sim 5$ nM), which has shown anti tumour effect both *in vitro* and *in vivo*. However, the liver toxicity, poor solubility and low stability have limited wortmannin (**1**) for

therapeutic use, but still wortmannin (**1**) has been widely used for investigating of diverse signal transduction processes involving PI3K [19].



Scheme 2. Mechanism of PI3K inhibition by wortmannin (**1**). The nucleophile Lys-802 in PI3K α (Lys-833 in PI3K γ) within the ATP binding pocket attacks the furan ring of wortmannin (**1**) at C20, resulting in stable wortmannin-PI3K adduct (**2**) [6]

Other natural compounds with PI3K inhibition activity are demethoxyviridin (**3**), liphagal (**4**) and resveratrol (**5**). Demethoxyviridin (**3**) was isolated from *Nodulisporium hinnuleum* and inhibits PI3Ks at low molecular concentrations with similar reaction mechanism as wortmannin, due to the identical furan ring system [20], [21]. Liphagal (**4**) was extracted from the sponge *Aka coralliphaga* and can inhibit PI3K α and PI3K γ , whereas the inhibition of PI3K α already appears at 10-fold lower concentrations (0.1 vs. 1.0 μ M) [22]. Resveratrol (**5**) is a plant hormone isolated for the first time in 1940 from the roots of *Veratrum grandiflorum*. The production of resveratrol by grapevines is one of the plant's defence mechanisms against environmental stress, such as pruning or attack by a microorganism. Current studies indicate that resveratrol inhibits class IA PI3K by displacing ATP, also it is shown that resveratrol is absorbed rapidly into the body, meaning that the molecule reaches the bloodstream fast and is on a hand to act on cells [23], [24].

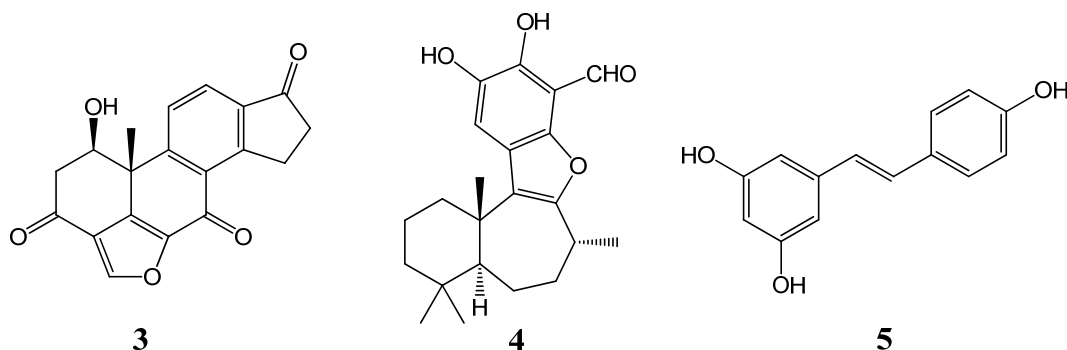


Figure 4. Chemical structures of natural PI3K inhibitors: demethoxyviridin (**3**), liphagal (**4**) and resveratrol (**5**).

2.2.2. Synthetic First Generation of PI3K Inhibitors

LY294002 (**6**) as a first synthetic PI3K inhibitor was synthesized by Lilly in the early nineties [6], with a chemical structure modified from quercetin, a compound which was previously demonstrated to inhibit PI3K as well as various protein kinases [25], [26]. Compared to wortmannin (**1**), LY294002 (**6**) has a 500-fold higher IC_{50} value (1.4 μ M) for class I PI3Ks, but the advantage of better chemical stability. The structure of LY294002 (**6**) in complex with PI3K γ has been elucidated by X-ray crystallography and it was shown that the morpholine oxygen forms a hydrogen bond with the backbone amide of Val-882. This interaction is shared by most current PI3K inhibitors as well as ATP. Further experiments revealed that modification of the morpholine group in LY294002 (**6**) leads to a decrease in inhibitor activity. Additional interactions occur with Lys-833, Met-804, Trp-812 and Met-953 [27]. LY294002 (**6**) also showed both anti-angiogenic activity and antitumor efficacy *in vivo*. However, dermal toxicity together with poor solubility, low bioavailability and poor inhibitor activity prevented enter of LY294002 (**6**) to the clinical trial [28], [29].

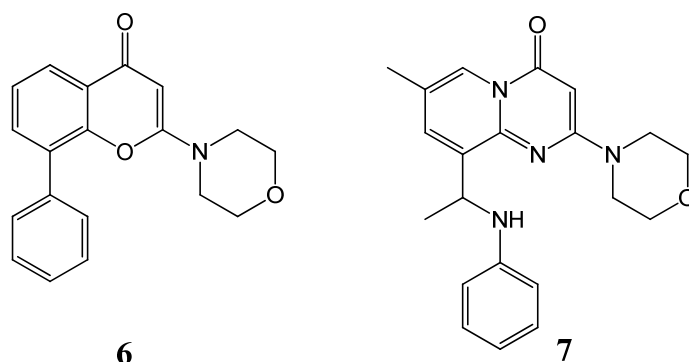


Figure 5. Chemical structures of the synthetic first generation inhibitors: LY294002 (**6**) and TGX-221 (**7**).

TGX-221 (**7**), which is structural derivative of LY294002 (**6**), is able to inhibit selectively the PI3K β isoform *in vitro*. The inhibition potency of TGX-221 (**7**) to PI3K β is approximately 1000-fold over those observed for PI3K α and PI3K γ and about 20 fold over PI3K δ . Administration of TGX-221 (**7**) showed a favorable antithrombotic effect by eliminating occlusive thrombus formation without prolonging bleeding time [30].

IC87114 (**8**) is a first PI3K δ -specific inhibitor that inhibits PI3K δ with an IC_{50} of 0.5 μ M, 58-fold more potently than PI3K γ , and over 100-fold more potently than PI3K α and PI3K β [31]. Originally, IC87114 (**8**) was used for investigations against inflammation and autoimmune diseases [32], but recently, there have been reported anti-leukemia activities of IC87114 (**8**) [33]. Derivatization of

IC87114 (**8**) led to new inhibitors such as PIK-39, PIK-293 and PIK-294. Molecular modelling of PIK-39 (**9**) and IC87114 (**8**) in complex with PI3K γ showed that the adenine moiety of these molecules interacts with Val-882 and Glu-880 within the ATP bonding pocket. It was also found that PIK-39 (**9**) is able with its own ligand conformation to induce a conformational switch of Met-804, opening a novel hydrophobic pocket. Further optimizations of PIK-39 (**9**) led to PIK-294 (**10**) that is also able to induce the conformational switch of Met-804, which makes PIK-294 (**10**) selective to PI3K δ . Additionally, PIK-294 (**10**) is able to fill with its phenol ring the hydrophobic “affinity” pocket of the enzyme leading to a 60-fold increase in inhibitor activity [34].

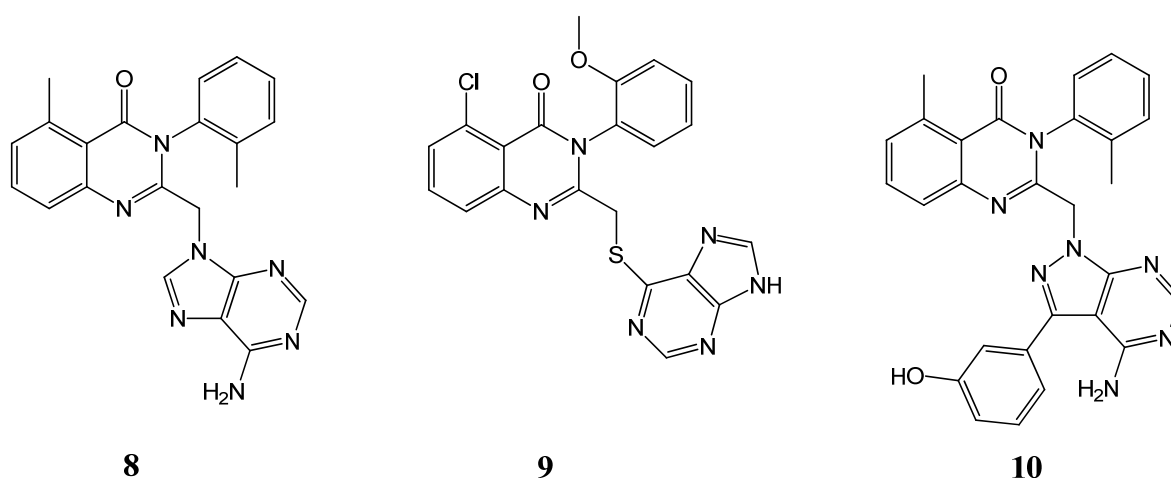
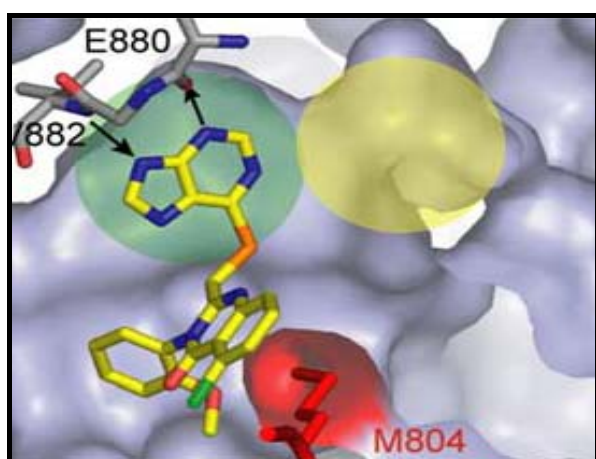


Figure 6. Chemical structures of the synthetic first generation inhibitors: IC87114 (**8**), PIK-39 (**9**), PIK-294 (**10**).

A. PIK-39



B. PIK-294

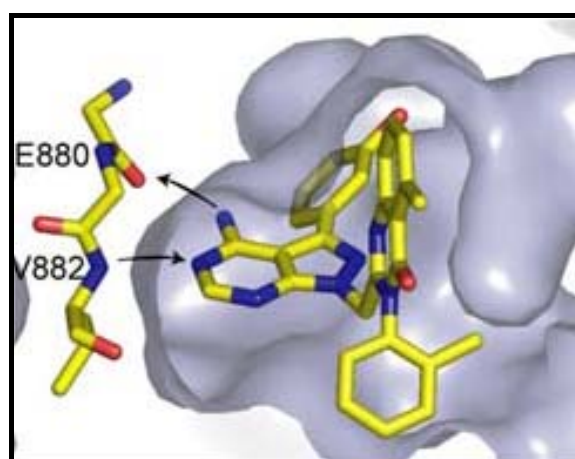


Figure 7. A) Crystal structure of isoform-selective PI3K inhibitor PIK-39 (**9**) bound to p110 γ ; B) predicted binding mode for PIK-294 (**10**), where hydrogen bonds are indicated by arrows [34].

2.2.3. Synthetic Second Generation of PI3K Inhibitors

Previously presented compounds did not reach the clinical trials due to their toxicity and poor physicochemical properties, but they contributed to the examination of biological function and structural properties of PI3Ks, what was essential for further process of PI3K inhibitor development. Therefore, further improvements of already existing compounds or the syntheses of entirely new structures have led to the emergence of novel second generation of PI3K inhibitors. The development of new generation PI3K inhibitors is accomplished by combination of various approaches such as structure-activity relationship (SAR) analysis, *in silico* modeling studies based on three-dimensional structures of already known inhibitors bound to the catalytic site of PI3K γ , classical activity-driven medicinal chemistry analogue preparation and screening of chemical libraries with novel enzymatic high-throughput screening assays (HTS). Some of the members of second generation PI3K inhibitors will be described in the following part of this chapter.

PI-103 (**11**), discovered by Japanese company Yamanouchi, is one of the novel dual PI3K and mTOR inhibitor with slight better selectivity to a PI3K α and selectivity of 6, 11, and 19 fold over PI3K δ , β , γ isoform, respectively. It was reported antitumor activity *in vivo* without any obvious side effects, and its effect was attributed to its ability to target both kinases. Also it was shown that PI-103 (**11**) reduced proliferation of glioma, breast, ovarian and cervical tumour cells in xenograft mouse models. Unfortunately, unfavourable pharmacokinetics as well as rapid metabolism have been found, pointed out to necessity of further structural optimization [35], [36], [37].

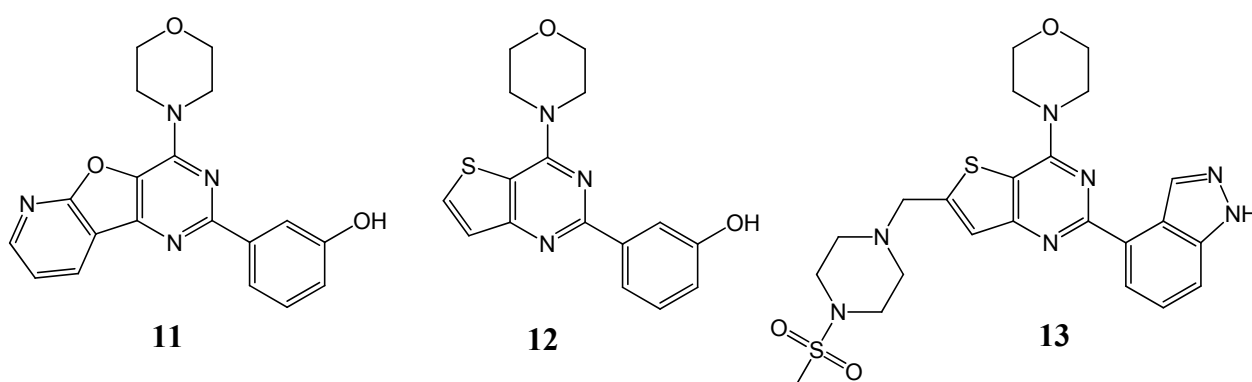


Figure 8. Chemical structures of the synthetic second generation inhibitors: PI-103 (**11**), 15e (**12**) and GDC-0941 (**13**).

15e (**12**) is a next example of the second generation of PI3K inhibitors, belonging to the group of thieno[3,2-*d*]pyrimidine derivatives, developed by Yamanouchi Pharmaceutical. 15e (**12**) suppresses tumour cell proliferation and is pan-class I PI3K inhibitor. The poor pharmacokinetic

profile and the short half-life time of less than 10 minutes are reasons for limited application possibilities of 15e (**12**) *in vivo* [38].

Further optimization of 15e (**12**) resulted in a GDC-0941 (**13**) as a highly selective inhibitor against Class I PI3Ks. GDC-0941 (**13**) inhibited PI3K α , β , δ and γ with IC₅₀ of 3, 33, 3 and 75 nM, respectively. An anti-angiogenic effect, *in vitro* and *in vivo*, has been also reported. Replacement of the 3-hydroxylphenyl group with 4-indazolylgroup decreased the issue of glucuronidation and resulted in an acceptable oral bioavailability. GDC-0941 (**13**) has entered clinical phase I in 2008 for the treatment of cancer [10], [39].

AS-252424 (**14**), AS-605240 (**15**), AS-604850 (**16**) are thiazolidinedione derivatives and first examples of selective PI3K γ inhibitors. It was showed in mouse models in case of rheumatoid arthritis that these inhibitors decreased progression of joint destruction. Co-crystallization of these compounds with PI3K γ helped in description and identification of their selectivity features. Based on these experiments, it was discovered that thiazolidinedione nitrogen makes a salt-bridge interaction with a side chain of Lys-833, oxygen of the 1,3-benzodioxole ring of AS-604850 (**16**) makes H-bond with the backbone amide of Val-882, while the nitrogen of the quinoxaline ring of AS-605240 (**15**) forms the link to Val-882. In case of AS-252424 (**14**), SAR studies showed that the central furan and hydroxyl group play essential role for the PI3K γ activity [40], [41].

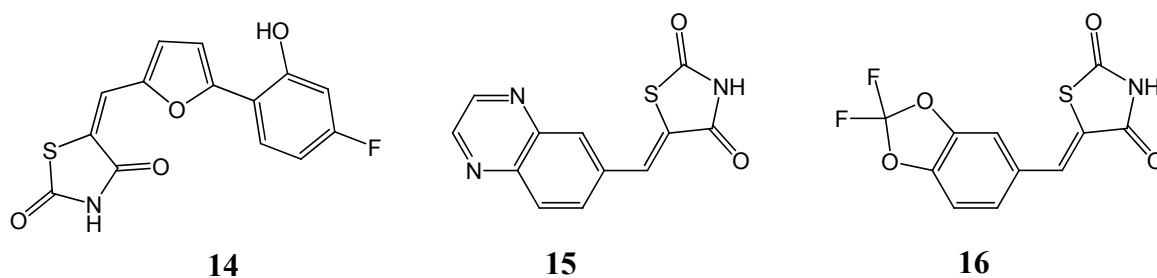


Figure 9. Chemical structures of the synthetic second generation inhibitors: AS-252424 (**14**), AS-605240 (**15**) and AS-604850 (**16**).

ZSTK474 (**17**) is a triazine derivative, identified as PI3K inhibitor by Zenyaku Kogyo, which inhibited all four isoforms, with IC₅₀ values of 16, 44, 5, 49 nM for PI3K α , β , δ , and γ , respectively. It was reported that ZSTK474 (**17**) showed weaker inhibition against mTOR and DNA-PK and no inhibition over a panel of 139 protein kinases. Preclinical studies have shown potent anti-tumour activity in xenograft models *in vivo* at both early and advanced stages, without obvious toxicity [42], [43]. Due to the good results of ZSTK474 (**17**), it can be assumed that the effectiveness of an inhibitor is not associated with its absolute isoform selectivity. Since most human diseases are not

the result of one single pathological process it could be argued that less selective inhibitors acting on a wider variety of cellular processes could be more beneficial for multi-factorial diseases [44].

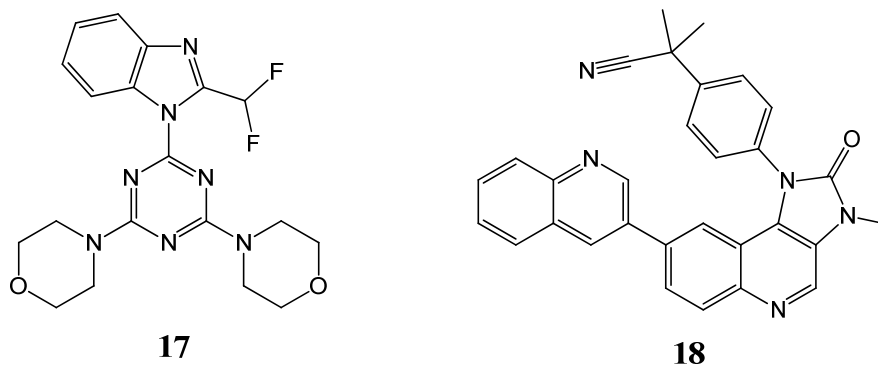


Figure 10. Chemical structures of the synthetic second generation inhibitors: ZSTK474 (**17**) and NVP-BEZ235 (**18**).

NVP-BEZ235 (**18**) is an imidazo[4,5-c]quinoline derivative, identified as a pan-PI3K inhibitor with IC_{50} values of 4, 76, 5, and 7 nM for PI3K α , β , δ , and γ , respectively. Its potent inhibition against mTOR was also confirmed. In addition, NVP-BEZ235 (**18**) also inhibited growth of a panel of cancer cells *in vitro* and showed anti-angiogenic activity. By oral administration, obvious toxicity was not observed. NVP-BEZ235 (**18**) is now in phase I/II clinical trials for the treatment of advanced breast, prostate and brain cancers [45], [46].

3. Research Project

Over the last decade, the rapid increase of interest for PI3K pathway is a consequence of the intense research efforts of many pharmaceutical companies as well as academy. Most of these companies established PI3K drug development programs, which helped to arise promising molecules and some of them have already entered clinical trial for treatment of cancer and other diseases. On the basis of recent data, it does seem that isoform selectivity would be a key point for PI3K inhibitor development, but often impressive inhibitor selectivity *in vitro*, usually requires further optimization *in vivo*. Therefore, the biggest challenge for the development of an effective inhibitor is to find the right balance in terms of isoform selectivity and potency, to combine maximum efficacy in a given disease with minimal unwanted side effects.

At the beginning of our project, it was not clear whether the targeting of one or all PI3K isoforms or maybe PI3K/mTOR will be successful in cancer therapy. Many of the PI3K inhibitors that are currently in clinical development inhibit all isoforms of class I PI3Ks whereas others inhibit only individual isoforms. For example, IC87114 (**8**) is PI3K δ specific inhibitor and has shown promising pharmacological activities. Since the most frequent PI3K α gene mutation is found in human cancers, it is assumed that cancer therapy should be based on selective PI3K α inhibitors. However, many examinations have confirmed that other isoforms are also involved in tumor genesis, suggesting that pan-PI3K inhibitors may enhance their therapeutic properties in curing against cancer.

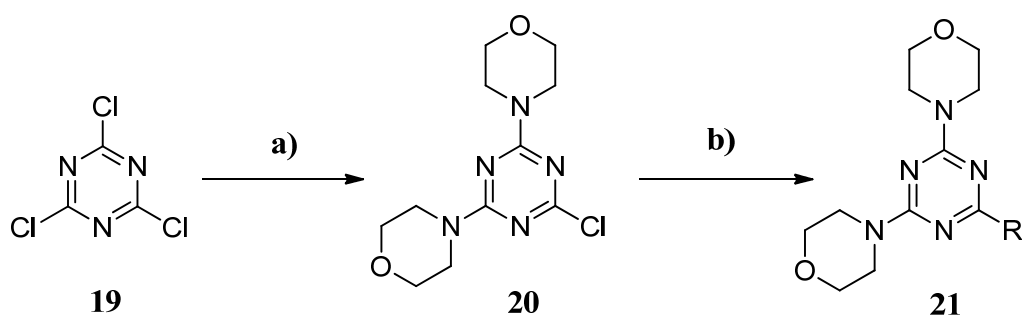
In order to answer to this oncology question, we started with intensive patent search (>400 patents, ~100-300 pages per patent!) to identify compounds, which are under pharmaceutical development such as dual pan-PI3K/mTOR inhibitor PI-103 (**11**) (Intellectual Property (IP) of Piramed/Genentech/Roche, UK/USA/CH) and selective pan-PI3K inhibitor ZSTK474 (**17**) (IP of Zenyaku, Japan). We synthesized these compounds in multi-gram scale and successfully proved their anti-tumor activity *in vitro* and *in vivo* as well as their selectivity effect on melanoma cancer. Their binding mode was successfully obtained through the structure activity relationship studies and X-ray structure elucidation in complex with PI3K γ . Using all information from previously performed research, we could rationally design novel highly active compounds. Interestingly, by changing a specific group of atoms or even a single atom by the known inhibitors we could have an affect in increase of both selectivity as well as potency.

4. Discussion and Results

4.1. ZSTK474 Derivatization

Until now, the emphasis is placed on targeting of specific isoforms within the Class I in order to provide selective inhibitors, which contribute to reduction of toxicity without loss of efficiency. Stimulated by the same fact, we tried to increase isoform selectivity and to improve physicochemical properties from already known pan-PI3K inhibitor ZSTK474 (**17**) identified by Japanese pharmaceutical company Zenyaku Kogyo. We tried to increase the selectivity against PI3K α by using all information obtained from structure-activity relationship (SAR) studies, X-ray crystal structure of ZSTK474 (**17**) in complex with PI3K γ and PI3K δ and modeling studies. Compared to other novel PI3K inhibitors, ZSTK474 (**17**) displayed significantly less activity against the mTOR, DNA-PK and no inhibition against panel of 139 protein kinases [39], [42]. Therefore, selective targeting of PI3K family and unpublished SAR studies of ZSTK474 (**17**) from the competitor, prompted us to improve its selectivity profile activity within the class I PI3K family.

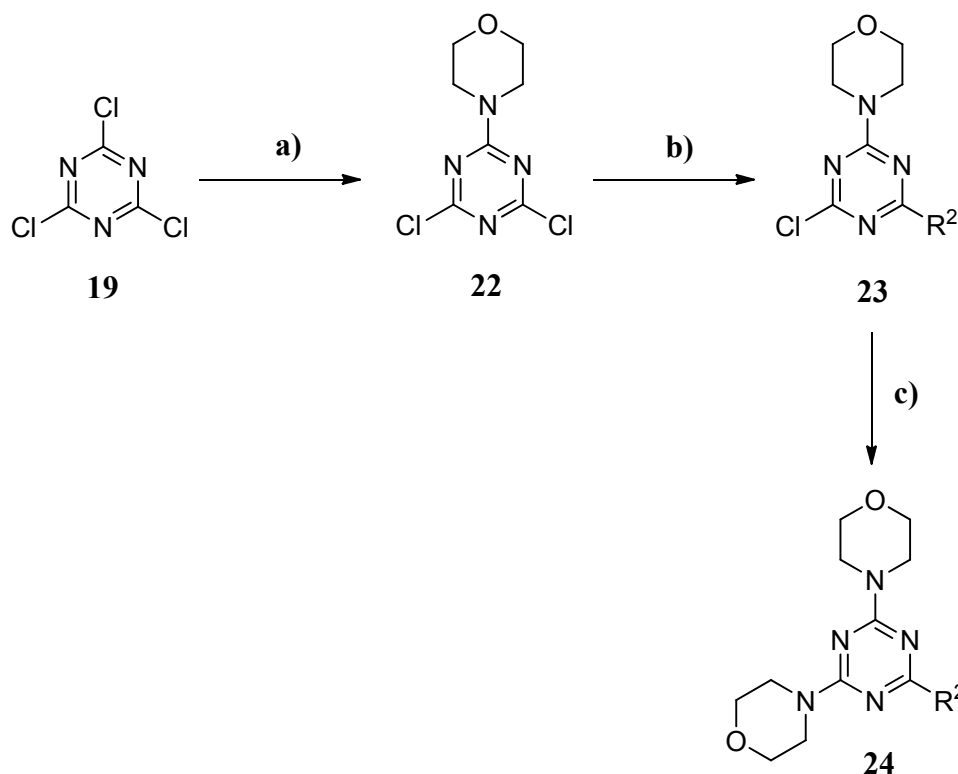
4.1.1. Triazine Chemistry



Scheme 3. Reagents and conditions: a) cyanuric chloride (1.0 eq.), morpholine (4.5 eq.), DMF, 0 °C, 20 minutes, 56 %; b) amine (1.1 eq.), DMF, NaH (60% in mineral oil, 1.5 eq.) added at 0 °C, 30 minutes at room temperature, then reflux at 153 °C for 3.5 - 5.5 hours, 13 – 77 %.

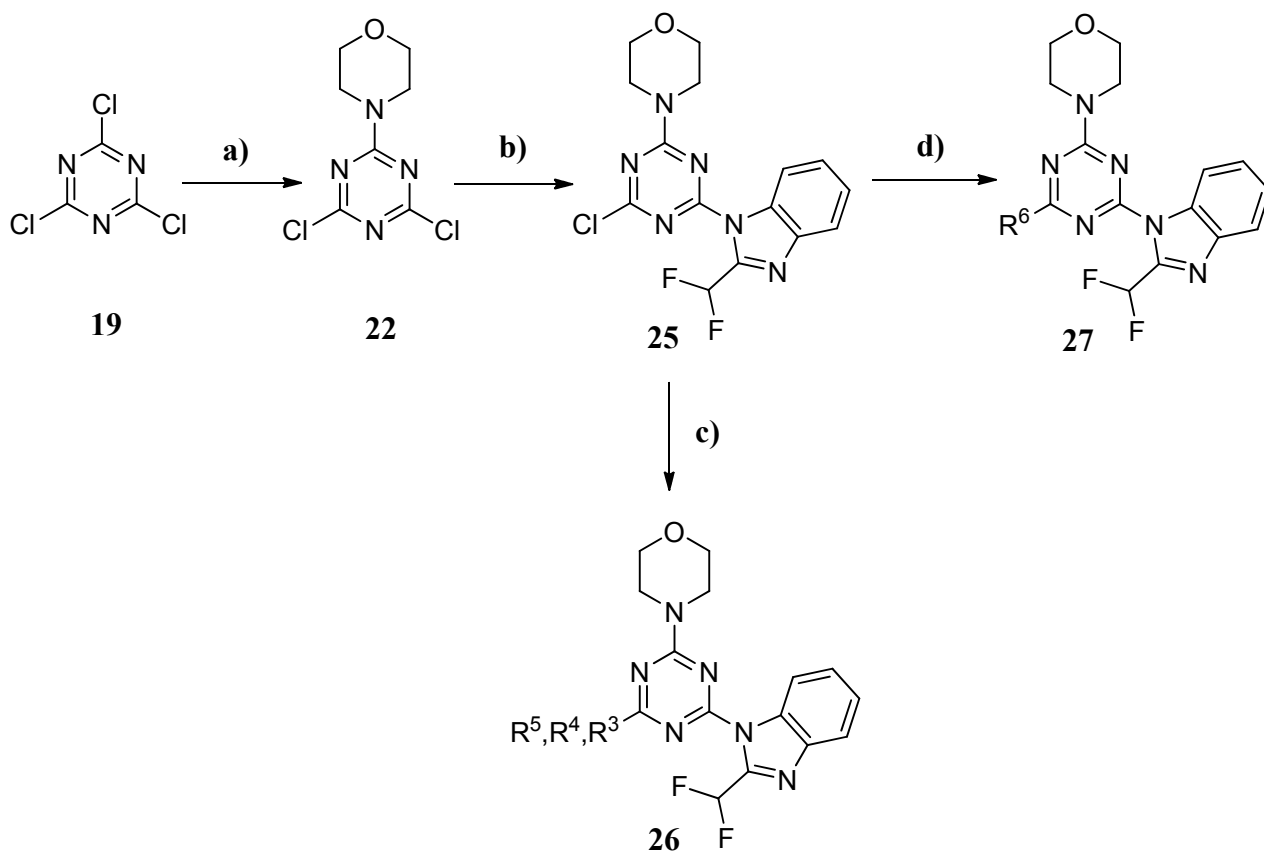
Compounds (**28-33**) (Table 1) are produced as presented in (Scheme 3). Cyanuric chloride (**19**) was substituted by two morpholine units in DMF, at 0 °C for 20 minutes, giving the intermediate (**20**). Further replacement of the third chlorine was done by nucleophilic substitution with several

heterocyclic aromatic amines, in presence of NaH as a base and DMF as a solvent, refluxing at 153 °C for 3.5 - 5.5 hours.



Scheme 4. Reagents and conditions: a) morpholine (1.0 eq.), CH_2Cl_2 , $-50\text{ }^\circ\text{C}$, 20 minutes, 28 %; b) K_2CO_3 , (1.44 eq.), heterocyclic aromatic compound (1.4 eq.), DMF, 30 minutes at $-5\text{ }^\circ\text{C}$, 3 - 4 hours at room temperature, 60 – 80 %; c) morpholine (1.2 eq.), K_2CO_3 (3.2 eq.), DMF, room temperature, 45 minutes - 2 hours., 60 - 95 %.

Compounds (**34-50**) (Table 2, 3, 5, 6 and 8) have been synthesized following the procedure reported in Schemes 4 and 5. Cyanuric chloride (**19**) was substituted by morpholine in methylene chloride at $-50\text{ }^\circ\text{C}$ for 20 minutes to give intermediate (**22**). Replacement of the second chlorine center with 2-difluoromethyl-1H-benzimidazole or a heterocyclic aromatic amine in presence of K_2CO_3 in DMF, at $-5\text{ }^\circ\text{C}$ for 30 minutes and further stirring at room temperature for 3 - 4 hours led to intermediates (**23**) (Scheme 4) and (**25**) (Scheme 5). The final step gave products (**24**) (Scheme 4) and (**26**) (Scheme 5) by process of amination in presence of K_2CO_3 and DMF at room temperature for 45 minutes, or products with the general structure (**27**) (Scheme 5) by Suzuki coupling of intermediate (**25**) with appropriate boronic acid pinacol esters, dichloro 1,1'-bis(diphenylphosphino)ferrocene-palladium(II)dichloride dichloromethane complex as a catalyst in 1,2-dimethoxyethane:2M Na_2CO_3 (3:1) as a solvent and stirring overnight at $90\text{ }^\circ\text{C}$.



Scheme 5. Reagents and conditions: a) morpholine (1.0 eq.), CH₂Cl₂, -50 °C, 20 minutes, 28 %; b) K₂CO₃, (1.44 eq.), 2-difluoromethyl-1H-benzimidazole (1.4 eq.), DMF, 30 minutes at -5 °C, 3 - 4 hours at room temperature, 60 – 80 %; c) amine (1.2 eq.), K₂CO₃ (3.2 eq.), DMF, room temperature, 45 minutes - 2 hours., 60 - 95 %; d) boronic acid pinacol ester (4.0 eq.), 1,2-dimethoxyethane:2M Na₂CO₃ (3:1), dichloro 1,1'-bis(diphenylphosphino)ferrocene-palladium(II)dichloride dichloromethane complex (0.025 eq.), 90 °C, 15 - 20 hours.

4.1.2. Fragment Validation Step as an Effective Method in Process of Creating Novel and Active ZTSK474 Derivatives

Through our *fragment validation step* (Figure 11) we examined which structural fragments of the known PI3K inhibitor ZSTK474 (**NCB38**) are significant for biological activity and which could serve for further chemical optimization. For this purpose, several derivatives of ZSTK474 (**NCB38**) were synthesized (Table 1, Table 2 and Table 3), and the nature of their interactions with the target protein was analyzed by different cellular assays, X-ray and *in silico* experiments. We determined the crystal structure of PI3K γ in complex with ZSTK474 (**NCB38**) (Figure 12), which has shown that the key hydrogen bonds were made through the interaction of morpholine oxygen with the backbone amide of the hinge Val-882 and fluorine of difluoromethyl group with Lys-833. The contact list with exact description of amino acids responsible for the hydrogen bond formations and for hydrophobic interactions is given in the table on a page 100.

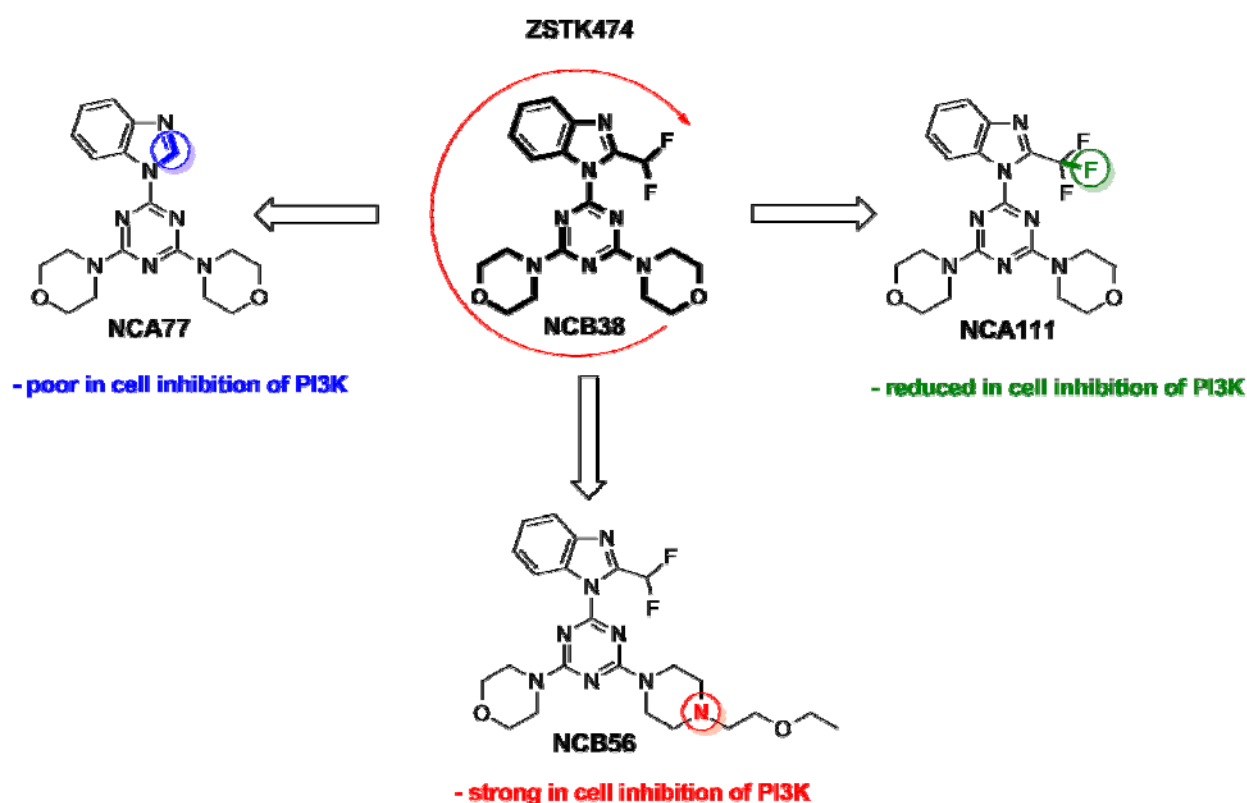


Figure 11. In the fragment validation step we examined, which structural fragments of the known PI3K inhibitor ZSTK474 (**NCB38**) are significant for biological activity, and which could serve for further chemical optimization. For this purpose, we modified all possible positions around the molecular scaffold and synthesized several analogues of the ZSTK474. Activity and the binding mode of those ZSTK474 analogues were further analyzed by different cellular assays, X-ray and *in silico* experiments.

Insertion of trifluoromethyl group instead of a difluoromethyl group leads to reduction of activity, while the absence of difluoromethyl group leads to poor in cell inhibition that can be explained by the lack of hydrogen bond with Lys-833 where the fluorine atom of the difluoromethyl group serves as an H-bond acceptor. Substitution of one morpholine with various piperazine groups did not drastically affect the biological activity, what inspired us to continue to modify one morpholine unit in order to create novel, active and more selective PI3K inhibitors.

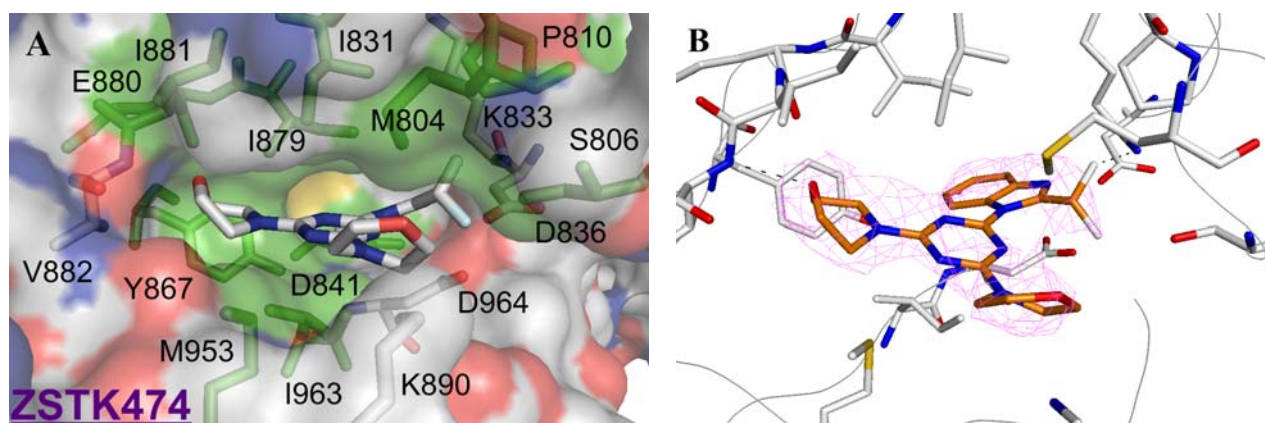


Figure 12. A) Represented is a surface diagram of X-ray elucidated ZSTK474-PI3K γ complex zoomed into the ATP binding site. Amino acids residues and the ligand are represented in stick form, coloured according to the element (C atoms in grey, N atoms in blue, O atoms in red); B) Extracted amino acids mediating PI3K/ZSTK474 interactions within the ATP-binding site; the electron density map of the compounds is presented in magenta mesh. Only hydrogen bonds that we are confident with are shown as black dashed lines.

Table 1. Inhibitor activity^a

Compound	R ¹	<i>In vitro</i> PI3K α 200 nM	A2058 cell inhibition		TSC2 ^{-/-} -MEFs cell inhibition
			pPKB/PKB 1 μ M	pS6 1 μ M	pS6 1 μ M
(NCA173) 28		65	161.65 \pm 7.46	92.88 \pm 2.95	87.95 \pm 2.80
(NCA77) 29		69	77.09 \pm 2.02	69.65 \pm 1.64	55.85 \pm 3.90
(NCA181) 30		89	129.38 \pm 2.00	91.11 \pm 2.58	92.08 \pm 6.95
(NCA152) 31		86	127.52 \pm 9.28	89.69 \pm 4.86	81.07 \pm 4.80
(NCB82) 32		92	85.79 \pm 2.40	102.32 \pm 0.54	80.18 \pm 10.39
(NCA111) 33		25	63.69 \pm 9.14	63.84 \pm 6.37	69.99 \pm 13.34

^aInhibitor efficacy and their cell permeability were measured by *in cell* Western inhibition assay on melanoma cell line A2058 and TSC2^{-/-}-MEFs cell line; *in vitro* PI3K α inhibition was measured by *Kinase Glo* assay and given numbers represent % remaining activity, the smaller the value, the stronger is the inhibition; coloured numbers represent: blue - no activity, green - low activity, red - good activity, orange - very good activity.

Table 2. Inhibitor activity^a

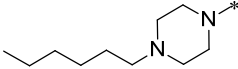
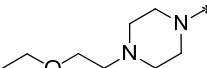
Compound	R ²	<i>In vitro</i> PI3K α 200 nM	A2058 cell inhibition		TSC2 ^{-/-} -MEFs cell inhibition
			pPKB/PKB 1 μ M	pS6 1 μ M	pS6 1 μ M
(NCB53) 34		53	16.02 \pm 1.15	65.58 \pm 1.32	91.59 \pm 0.46
(NCB94) 35		28	33.84 \pm 1.75	61.62 \pm 5.42	98.16 \pm 10.25

^aInhibitor efficacy and their cell permeability were measured by *in cell* Western inhibition assay on melanoma cell line A2058 and TSC2^{-/-}-MEFs cell line; *in vitro* PI3K α inhibition was measured by *Kinase Glo* assay and given numbers represent % remaining activity, the smaller the value, the stronger is the inhibition; coloured numbers represent: blue - no activity, green - low activity, red - good activity, orange - very good activity.

High inhibitor activity of compounds (**34**) and (**35**) (Table 2) could be explained by the concept of bioisosterism. Bioisosterism represents one approach used by the medicinal chemist for the rational modification of compounds into more effective agents. Reasons to use bioisosterism are to design new drugs by including improvement of the pharmacological activity, determination of the selectivity for an enzymatic isoform subtype, optimization of the pharmacokinetics and toxicity effects. This concept is very often used by pharmaceutical industry to discover new therapeutically innovative and commercial attractive analogs. Bioisosteres may be atoms and molecules that possess similar molecular shapes, volumes, similar distribution of electrons, physical properties and have a similar type of biological activity [47] For example, the substitution of hydrogen by fluorine is one of the more commonly bioisosteric replacements. Steric parameters of these atoms are similar; their van der Waal's radii are 1.2 (for hydrogen) and 1.35 Å (for fluorine). Their

pharmacological differences can be attributed to the influence of the electron-withdrawing effect that the fluorine substitution causes on interaction with either a biological receptor or enzyme. Bioisosteric replacement of the methyl group in compound (**34**) with the chlorine atom led to the compound (**35**). The chlorine atom is often viewed to be isosteric and isolipophilic with the methyl group. Exchange of the methyl group with the chlorine atom can increase the metabolic stability of the relevant compound [48].

Table 3. Inhibitor activity^a

Compound	R ³	<i>In vitro</i> PI3K α 200 nM	A2058 cell inhibition		TSC2 ^{-/-} - MEFs cell inhibition
			pPKB/PKB 1 μ M	pS6 1 μ M	pS6 1 μ M
(NCB55) 36		45	21.69 \pm 0.53	106.52 \pm 2.90	70.53 \pm 3.63
(NCB56) 37		42	9.07 \pm 1.49	54.20 \pm 3.91	68.85 \pm 1.08

^aInhibitor efficacy and their cell permeability were measured by *in cell* Western inhibition assay on melanoma cell line A2058 and TSC2^{-/-}-MEFs cell line; *in vitro* PI3K α inhibition was measured by *Kinase Glo* assay and given numbers represent % remaining activity, the smaller the value, the stronger is the inhibition; coloured numbers represent: blue - no activity, green - low activity, red - good activity, orange - very good activity.

4.1.3. Synthesis of Novel, Active and Selective ZSTK474 Derivatives

Structural studies showed that one of the determinants, which influence kinase inhibitor selectivity, termed as “gatekeeper” residue is placed in hydrophobic pocket of ATP binding site. Smaller gatekeepers such as threonine allow bulky substituents to enter deeper into the hydrophobic pocket in contrast to the larger gatekeeper residues such as methionine or phenylalanine which prevent access to this pocket. An example that exploits this kind of selectivity filter is Gleevec a known drug used to treat chronic myelogenous leukemia by utilizing a threonine gatekeeper in the Abl tyrosine kinase domain [49]. The analyses have shown that mutation of threonine gatekeeper residue into the larger amino acid is one of the most common mechanisms of resistance to Gleevec.

In recent docking studies and molecular modeling experiments by utilizing the available crystal structures of PI3K γ and PI3K α , Zvelebil and colleagues revealed that one of the differences between p110 α and other PI3K isoforms of class I is absence of Asp-Lys as a gatekeeper pair only in p110 α (Asp950-Lys807 in p110 γ , Asp897-Lys755 in p110 δ and Asp923-Lys782 in p110 β) (Table 4). Appropriate residues in p110 α are Ser-919 and Ala-775 respectively (Figure 13). In contrast to Asp-Lys pair, Ala-Ser pair can not create intramolecular hydrogen bond because of their large enough mutual distance, enabling affordable access to hydrophobic region of ATP pocket and more convincing binding mode [50]. Taking into account their smaller size relating to Asp-Lys pair, it is clear that Ser-Ala gatekeeper residues may allow easier and fuller access to hydrophobic ATP pocket that could lead to a simultaneous improvement in selectivity and potency of appropriate inhibitors.

K	x	M80	A80	S80	K807	K808	P810	I831	K833	D836	Y867	I879	E880	I881	V882	A885	T886	T887	a889	K890	D950	n951	M953	I963	D964	p110 γ
R	x	M772	s773	S774	a775	k776	P777	I800	K802	d806	Y836	I846	E847	V848	V849	S854	H855	T856	M858	Q859	S919	N920	m922	I932	D93	p110 α
T	x	M752	D753	S754	K755	m756	P758	I777	K779	d782	Y813	I825	E826	V827	V828	S831	D832	T833	a835	N836	D897	N898	M900	I910	D911	p110 δ
K	x	M779	d780	S781	K782	M783	P785	I803	K805	d808	Y839	I851	E852	V853	V854	S857	E858	T859	a861	D862	D923	n924	M926	I936	D937	p110 β

Table 4. Residues that have been identified by close structural inspection of each isoform to be part or near the ATP binding site. The residues framed in red colour are those that differ between the class I PI3K isoforms [50].

In aim to achieve that effect, we substituted one of two morpholine units of ZSTK474 (**38**) with bulky heterocyclic analogs with the strategy that such substitution will fill a free cavity within the hydrophobic pocket II of the ATP binding pocket in PI3K α isoforme (Figure 14).

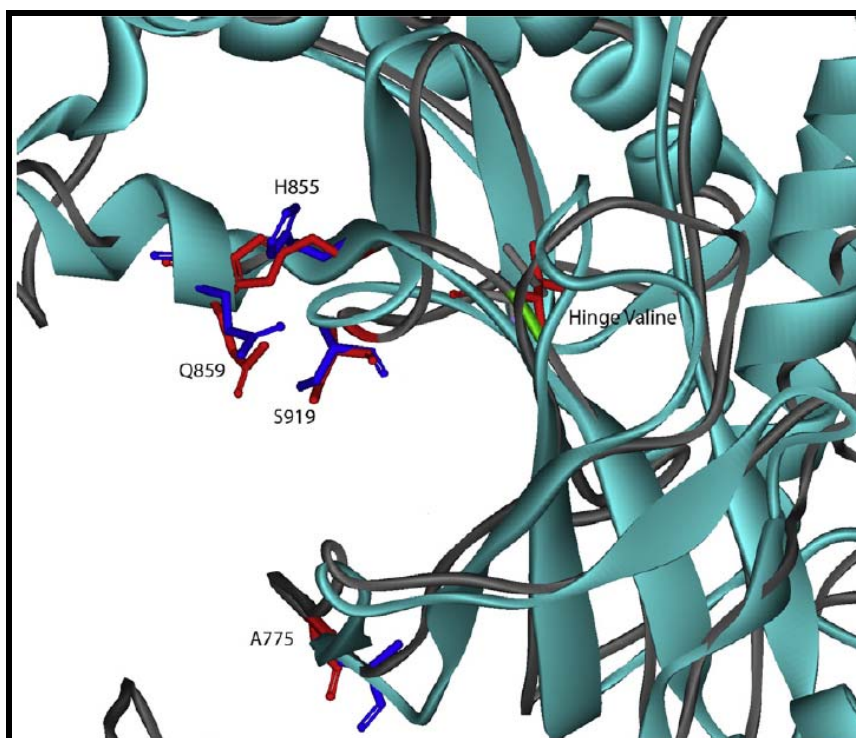


Figure 13. The ATP binding site from the X-ray structure (blue ribbon) imposed on the modelled structure (gray backbone) of p110 α . The gatekeeper residues described previously are presented as sticks and coloured blue in the X-ray structure and red in the model [50].

Docking studies assumed that this substitution would lead to greater specificity amongst the isoforms. Interestingly, comparing to ZSTK474 (**38**), introduction of diverse morpholine substituents (Scheme 5, Table 5) by amination process as: dimethyl morpholine NCB136 (**39**), homomorpholine NCB137 (**40**) and bridged morpholine NCB138 (**41**) led those derivatives to better inhibition in cellular assay, greater selectivity to mTOR and similar inhibition *in vitro* against PI3K α . In case of 1-methylhomopiperazine NCB87 (**42**) replacement, slight less activity was obtained *in vitro* experiments and *in cell* inhibition (pPKB/PKB), but significant decreasing of selectivity towards mTOR (Figure 15).

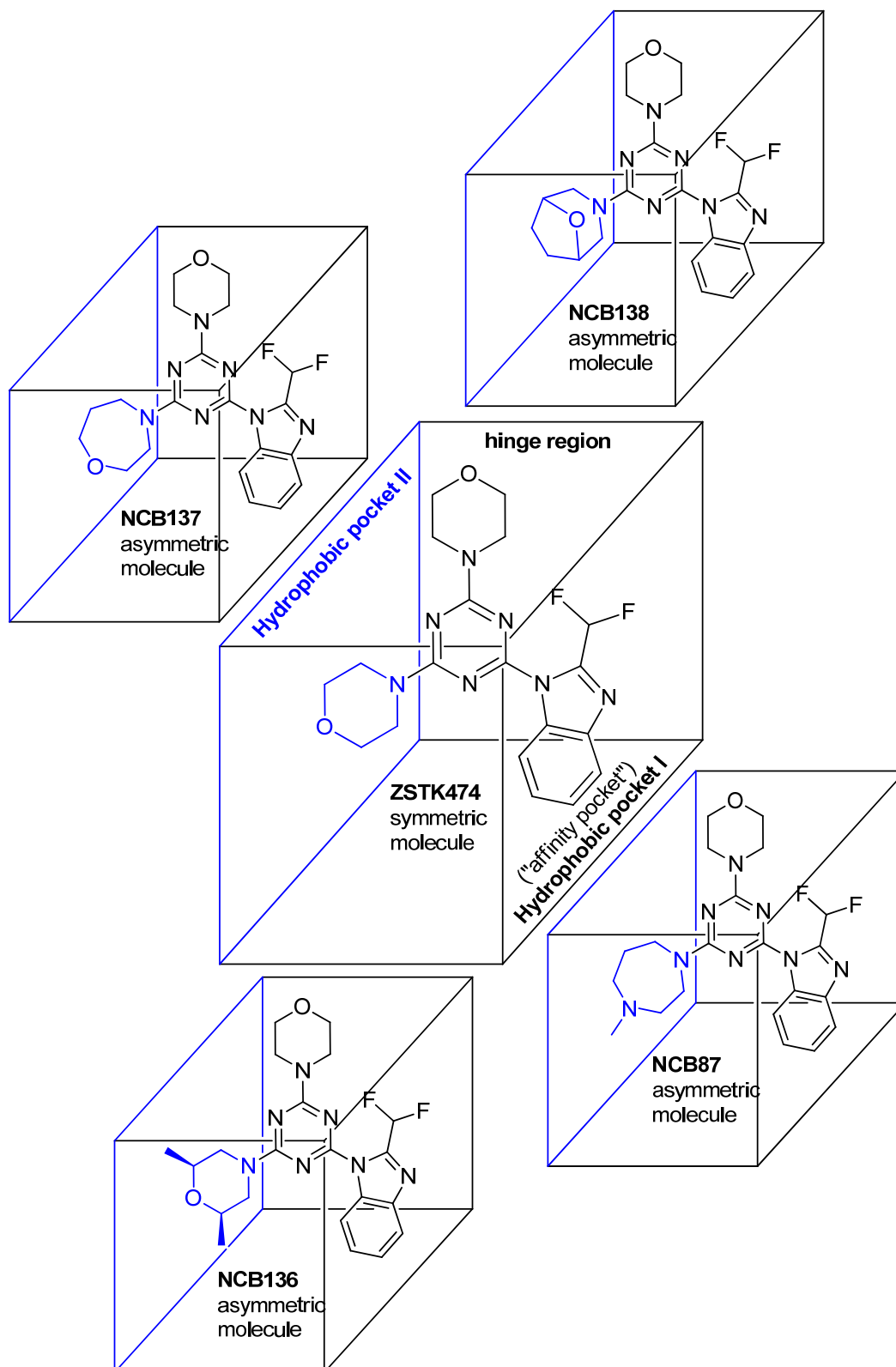
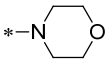
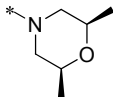
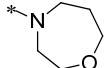
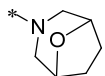
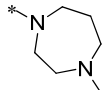


Figure 14. ZSTK474 morpholine unit (coloured in blue) is located at the entrance of the ATP binding pocket (hydrophobic pocket II) and was exchanged with bulky morpholine or piperazine analogs with the aim to fill a free cavity within hydrophobic pocket II in PI3K α isoforme.

Table 5. Inhibitor activity^a

Compound	R ⁴	<i>In vitro</i> PI3K α 200 nM	A2058 cell inhibition		TSC2 ^{-/-} -MEFs cell inhibition
			pPKB/PKB 1 μ M	pS6 1 μ M	pS6 1 μ M
(NCB38) 38		13	12.83 \pm 7.03	19.46 \pm 1.53	20.67 \pm 1.39
(NCB136) 39		16	8.31 \pm 3.56	30.09 \pm 1.21	5.60 \pm 1.49
(NCB137) 40		22	3.86 \pm 1.17	21.14 \pm 1.82	9.77 \pm 1.79
(NCB138) 41		18	2.21 \pm 4.81	34.44 \pm 4.39	10.75 \pm 0.71
(NCB87) 42		34	24.74 \pm 1.88	78.63 \pm 5.58	86.52 \pm 7.45

^aInhibitor efficacy and their cell permeability were measured by *in cell* Western inhibition assay on melanoma cell line A2058 and TSC2^{-/-}-MEFs cell line; *in vitro* PI3K α inhibition was measured by *Kinase Glo* assay and given numbers represent % remaining activity, the smaller the value, the stronger is the inhibition; coloured numbers represent: blue - no activity, green - low activity, red - good activity, orange - very good activity.

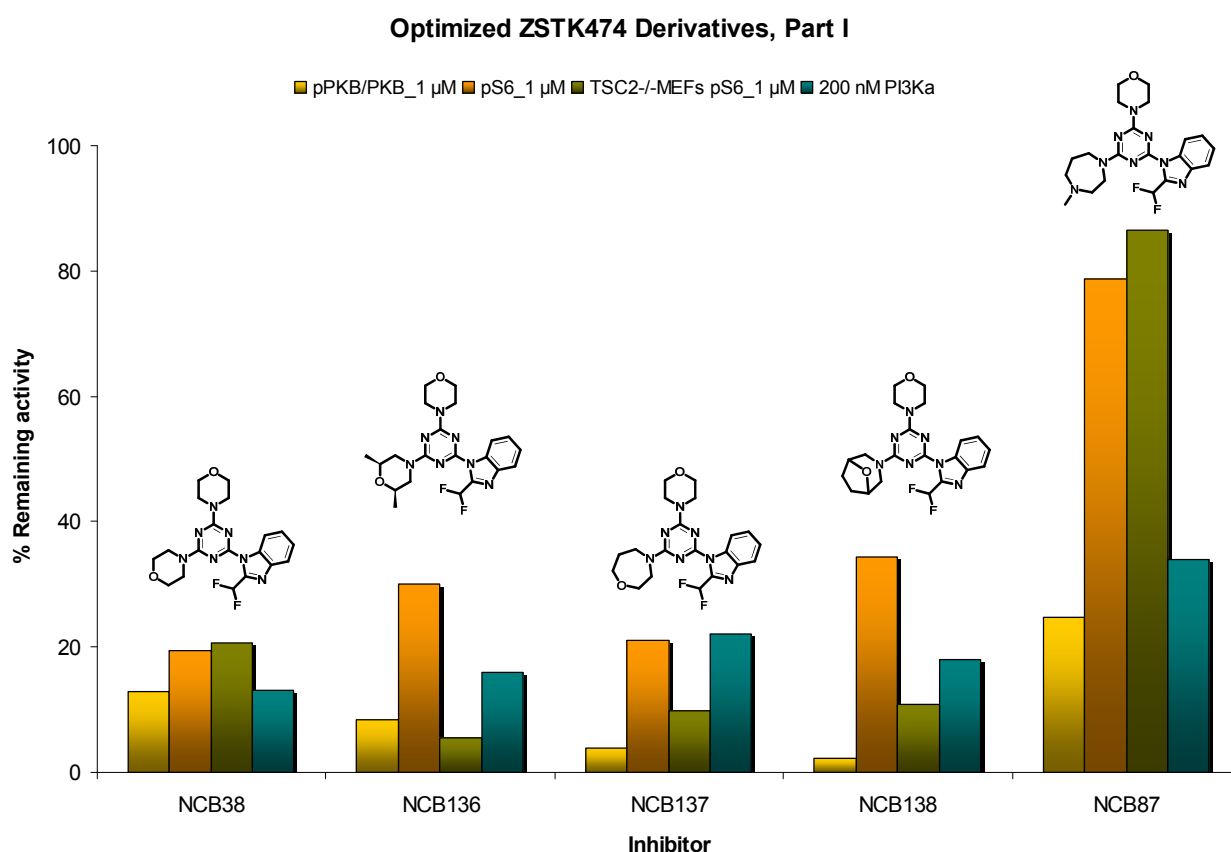


Figure 15. Presented is cellular activity (pPKB/PKB and pS6 on A2058 and pS6 on TSC2-/-MEFs) at 1 μM and *in vitro* activity against PI3K α at 200 nM; the lower the bar chart the better is the activity of the relevant compound.

The next step was the insertion of aromatic substituents by Suzuki coupling instead of morpholine (Scheme 5, Table 6). In the same time we also applied fluorine strategy in our project. As already known, introducing of fluorine in inhibitors can lead to an increase of metabolic stability, lipophilicity, binding affinity in protein-ligand complexes and regulation of physicochemical properties [51]. However, replacement of morpholine by fluorinated aromatic reagents 3,5-bis(trifluoromethyl)-phenylboronic acid NCB48 (**44**) did not lead to expected results, which can be explained by rigid and too bulky aromatic system and its inability to fit into the hydrophobic pocket. Better results *in vitro* and *in cell* inhibition are obtained in case of 2,4-difluorophenylboronic acid pinacol ester NCB51 (**43**) and 4-(4-morpholinomethyl)-phenylboronic acid pinacol ester NCB49 (**45**) replacement, compared to NCB48 (**44**) (Figure 16).

Table 6. Inhibitor activity^a

Compound	R ⁶	<i>In vitro</i> PI3K α 200 nM	A2058 cell inhibition		TSC2 ^{-/-} -MEFs cell inhibition
			pPKB/PKB 1 μ M	pS6 1 μ M	pS6 1 μ M
(NCB38) 38		13	12.83 \pm 7.03	19.46 \pm 1.53	20.67 \pm 1.39
(NCB51) 43		31	56.42 \pm 3.14	104.47 \pm 3.78	98.78 \pm 1.46
(NCB48) 44		115	88.97 \pm 13.09	112.65 \pm 1.71	110.59 \pm 2.10
(NCB49) 45		41	64.73 \pm 7.84	96.27 \pm 6.59	72.26 \pm 2.24

^aInhibitor efficacy and their cell permeability were measured by *in cell* Western inhibition assay on melanoma cell line A2058 and TSC2^{-/-}-MEFs cell line; *in vitro* PI3K α inhibition was measured by *Kinase Glo* assay and given numbers represent % remaining activity, the smaller the value, the stronger is the inhibition; coloured numbers represent: blue - no activity, green - low activity, red - good activity, orange - very good activity.

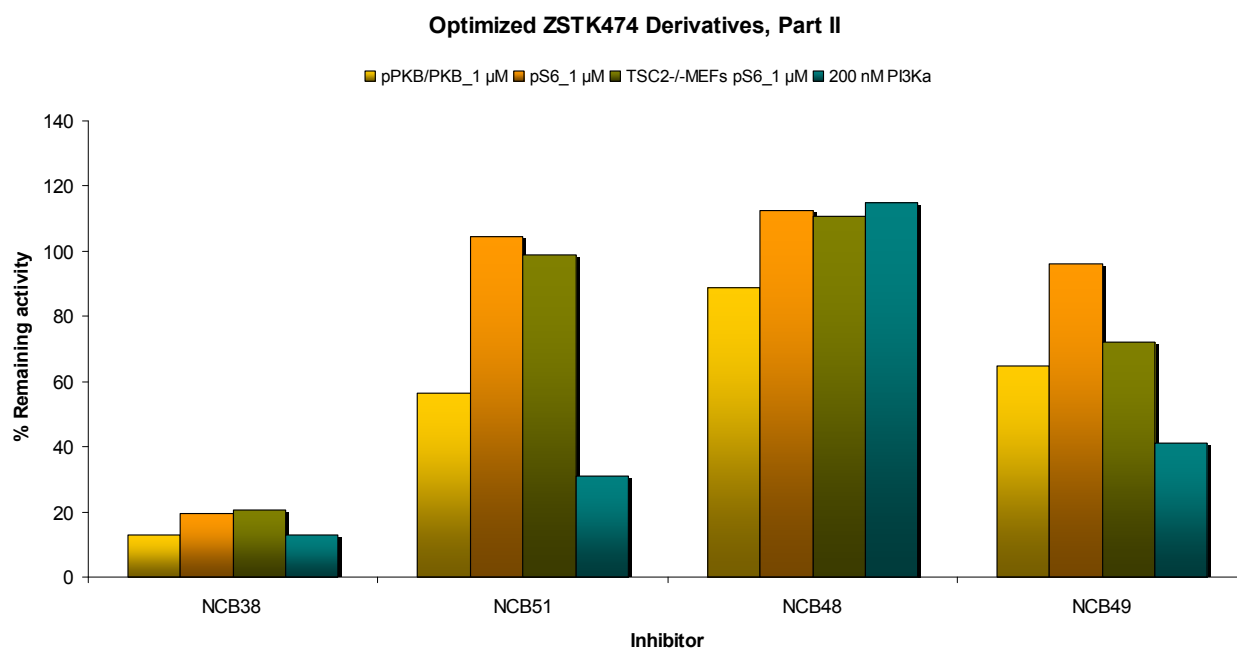


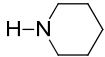
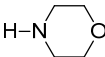
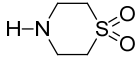
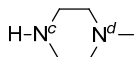
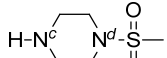
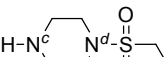
Figure 16. Presented is cellular activity (pPKB/PKB and pS6 on A2058 and pS6 on TSC2-/-MEFs) at 1 μM and *in vitro* activity against PI3K α at 200 nM; the lower the bar chart the better is the activity of the relevant compound.

The further step was the improvement of physicochemical properties of ZSTK474 (**38**) by applying a sulfone strategy (Scheme 5). Insertion of sulfone group causes reduction of lipophilicity because of its high electron withdrawing and basicity-reduced effect [52]. We observed how different fragments containing the sulfone group inserted instead of morpholine modulate the biological activity and selectivity of ZSTK474 (**38**) derivatives to PI3K and mTOR (Table 7 and Table 8).

Comparing to ZSTK474 (**38**), introducing of more basic piperidine NCB37 (**46**) instead of morpholine, caused a significant decrease in activity towards mTOR in A2058 cell line. Interestingly, inhibition of pS6 phosphorylation in TSC2-/-MEFs cell line was improved as well as inhibition of pPKB/PKB phosphorylation in A2058 (Table 8, Figure 18). Reduction in activity was noticed *in vitro* experiments against PI3K α . Replacement with more acidic and more soluble thiomorpholine 1,1-dioxide NCB91 (**47**) led to considerable reduction in biological activity both *in vitro* and *in cell* inhibition. The next thing what we explored is influence of N-methylpiperazine NCB36 (**48**) and sulphonyl containing piperazine NCB60 (**49**), NCB57 (**50**) on activity and selectivity against PI3K and mTOR. Increasing of activity against PI3K, but significant diminishing of selectivity to mTOR in TSC2-/-MEFs cell line was obtained by insertion of N-methylpiperazine NCB36 (**48**). Crystal structure of PI3K γ in complex with NCB36 (**48**) (Figure 17) explained

increment of activity by the presence of additional hydrogen bond of N21 with Asp-964. Interestingly, replacement with more acidic and more soluble 1-(methylsulfonyl)piperazine NCB60 (**49**) led to even better activity *in cell* experiments comparing to ZSTK474 (**38**). When 1-(ethanesulfonyl)piperazine NCB57 (**50**) (with similar acidity to **49**) was introduced, biological activity against PI3K was slight decreased, while activity to mTOR became notable reduced.

Table 7. Physicochemical properties^a

N ^o		pKa	LogP	LogD	Log(S)
1.		11.1 ^b	0.93 ± 0.24	-2.1 ± 1.0	-0.17
2.		8.5 ^b	-1.08 ± 0.27	-3.0 ± 1.0	1.48
3.		5.4 ^b	-1.45 ± 0.47	-1.6 ± 1.0	-0.14
4.		^c 9.65 ± 0.25 ^d 4.35 ± 0.30	-0.18 ± 0.32	-2.7 ± 1.0	0.84
5.		^c 6.38 ± 0.25 ^d -8.68 ± 0.20	-0.67 ± 0.48	-0.8 ± 1.0	-0.67
6.		^c 6.38 ± 0.25 ^d -8.69 ± 0.20	-0.14 ± 0.48	-0.2 ± 1.0	-1.04

^aPhysicochemical properties were calculated using a commercial database [53]. pKa = Amine basicity; LogP = Intrinsic lipophilicity; LogD = Logarithmic n-octanol/water distribution coefficient at pH = 7; Log(S) = Logarithm of Intrinsic solubility of the neutral base.

^bExperimental pKa values [53]. ^cpKa1; ^dpKa2.

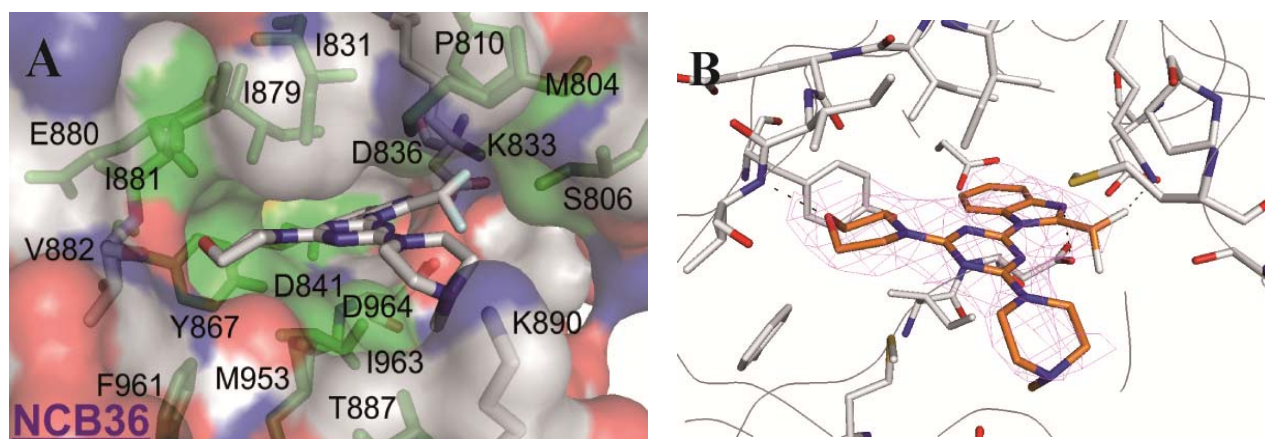
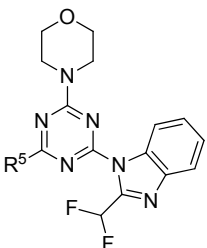
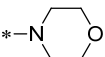
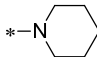
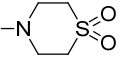
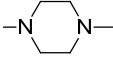
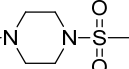
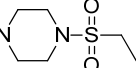


Figure 17. A) Represented is a surface diagram of X-ray elucidated NCB36-PI3K γ complex zoomed into the ATP binding site. Amino acids residues and the ligand are represented in stick form, coloured according to the element (C atoms in grey, N atoms in blue, O atoms in red); B) Extracted amino acids mediating PI3K/ZSTK474 interactions within the ATP-binding site; the electron density map of the compounds is presented in magenta mesh. Only hydrogen bonds that we are confident with are shown as black dashed lines.

According to our molecular modelling experiments, we concluded that oxygen atom of sulfonyl group has the potential to form an additional hydrogen bond with the target protein making this compound more potent. Additionally, due to the polarity of the sulfonyl group compound NCB60 (**49**) has better water solubility comparing to ZSTK474 (**38**). This could partially explain better inhibitor activity of compound NCB60 (**49**).

Table 8. Inhibitor activity^a


Compound	R ⁵	<i>In vitro</i> PI3K α 200 nM	A2058 cell inhibition		TSC2 ^{-/-} -MEFs cell inhibition
			pPKB/PKB 1 μ M	pS6 1 μ M	pS6 1 μ M
(NCB38) 38	*-N 	13	12.83 \pm 7.03	19.46 \pm 1.53	20.67 \pm 1.39
(NCB37) 46	*-N 	39	9.36 \pm 0.35	57.48 \pm 2.75	7.13 \pm 0.34
(NCB91) 47	*-N 	34	49.03 \pm 11.85	98.88 \pm 10.16	57.86 \pm 0.40
(NCB36) 48	*-N 	33	0.17 \pm 2.27	23.19 \pm 1.00	93.26 \pm 0.97
(NCB60) 49	*-N 	17	-2.03 \pm 1.80	12.79 \pm 0.31	12.14 \pm 0.11
(NCB57) 50	*-N 	35	18.27 \pm 1.13	82.15 \pm 9.79	73.72 \pm 5.61

^aInhibitor efficacy and their cell permeability were measured by *in cell* Western inhibition assay on melanoma cell line A2058 and TSC2^{-/-}-MEFs cell line; *in vitro* PI3K α inhibition was measured by *Kinase Glo* assay and given numbers represent % remaining activity, the smaller the value, the stronger is the inhibition; coloured numbers represent: blue - no activity, green - low activity, red - good activity, orange - very good activity.

Optimized ZSTK474 Derivatives, Part III

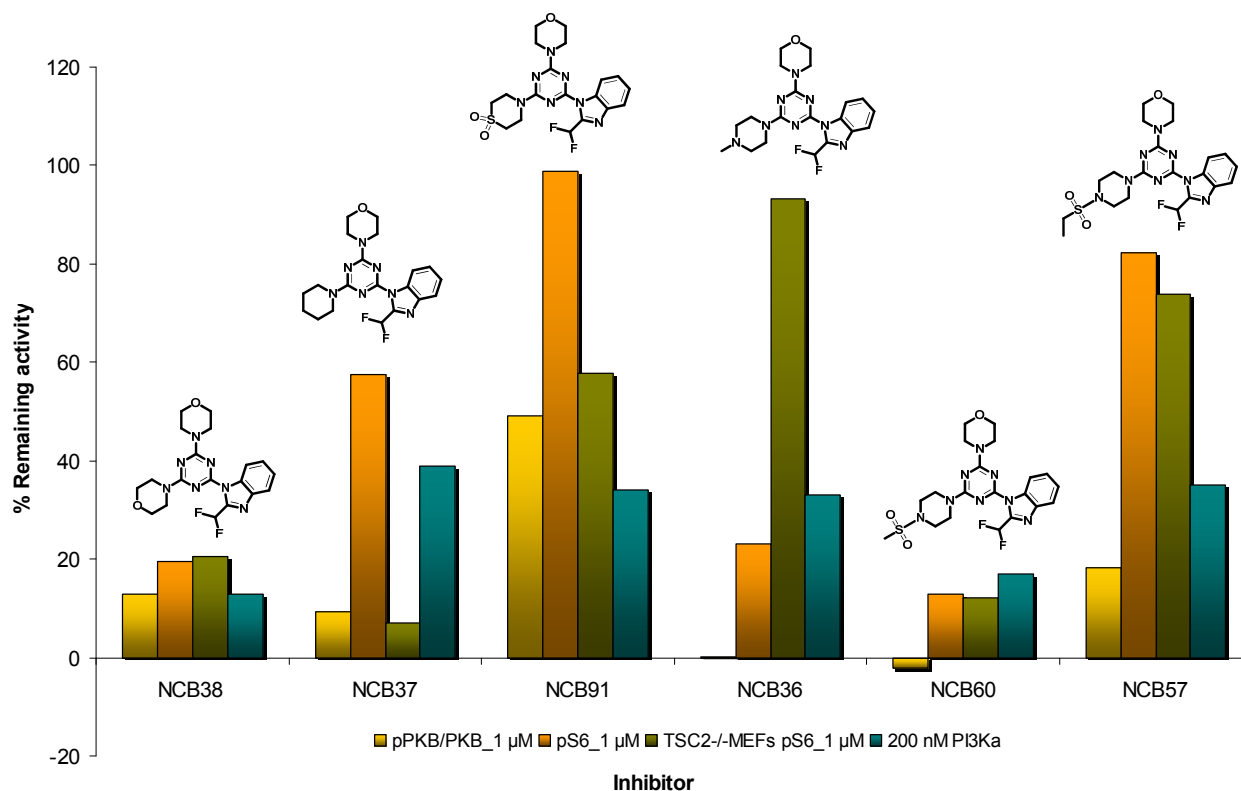


Figure 18. Optimization of ZSTK474 by applying sulfone strategy. Presented is cellular activity (pPKB/PKB and pS6 on A2058 and pS6 on TSC2-/-MEFs) at 1 μM and *in vitro* activity against PI3K α at 200 nM; the lower the bar chart the better is the activity of the relevant compound.

4.2. Structure-Based Design of Irreversible PI3K Inhibitors

Structure-based drug design relies on knowledge of the three dimensional structure of the biological target obtained through methods such as X-ray crystallography or NMR spectroscopy. If an experimental structure of a target is not available, it may be possible to create a homology model of the target based on the experimental structure of a related protein. Based on information obtained from the crystal structure of PI3K γ and PI3K δ in complex with ZSTK474 (**38**) we designed the inhibitors, which could improve their activity and selectivity through covalent interaction with enzyme or protein receptor. Known irreversible inhibitors, usually possess electrophilic functional groups such as α , β -unsaturated carbonyls or halomethyl carbonyls that covalently modify nucleophilic amino acids such as cysteine, serine, threonine or tyrosine. However, due to the higher probability of toxicity as a result of covalent binding, there has been a tendency to avoid covalent drugs. In contrast there are many effective irreversible acting drugs on the market such as aspirin, penicillin, entire class of β -lactam antibiotics and many others [54]. Advances in chemical biology and bioinformatics data analysis methods has contributed more easily identifying and predicting a level of toxicity of a covalent modification, allowing further progress in the development of covalent inhibitors.

4.2.1. Benefits of Covalent Binding Mechanism

There are several considerable advantages by targeting appropriate proteins or enzymes with small molecular weight covalent inhibitors.

- **Increased selectivity:** Due to their ability to form covalent bonds with suitable amino acids residues that are unique to disease-causing proteins, covalent drugs contribute to enhanced selectivity, which leads to better efficacy and reducing of side-effects.
- **Prolonged duration of action:** In account of such unique mode of complete binding to a protein drug target, covalent drugs effectively ‘silence’ their targets, which remain silenced until their novel cellular production. Thus, covalent drugs lead to a prolonged duration of action, in contrast to most current drugs which need to maintain high exposure, while the protein-drug interaction is temporary. The benefits of this include the potential for better efficacy, less frequent dosing and less overall drug exposure that should improve safety.

- **Mutational resistance:** Often mutation of disease-causing proteins leads to changes of proteins binding site in their shape and size, what usually prevent or decrease effective binding of conventional drugs. However, because covalent drugs only must attack the protein once in order to form a strong bond, they will not easily separate from a mutated protein and can retain efficacy. Therefore covalent drugs are particularly well-suited to the treatment of cancers.

4.2.2. Published Irreversible Kinase Inhibitors

This chapter will present a short overview about already published irreversible kinase inhibitors in last several years. Focus will be directed towards diverse protein kinases as most frequent targeted proteins by irreversible molecules. Additionally, natural PI3K inhibitor wortmannin (**1**) as irreversible PI3K inhibitor will be briefly described.

HKI-272 (**51**) is HER-2 irreversible inhibitor and was discovered by Wyeth five years ago. HER-2 belongs to the ErbB family of receptor tyrosine kinases, which has been involved in a development of various cancer diseases. Overexpression of HER-2 is found in ~ 30% of breast cancer patients, therefore blocking of its function by small molecule kinase inhibitors may lead to inhibition of growth of HER-2 positive tumors. HKI-272 (**51**) reduces HER-2 autophosphorylation in cells and affects the inactivation of downstream signal transduction events. *In vivo*, this inhibitor is also active in HER-2 depended tumor xenograft models by orally administration. HKI-272 (**51**) contains a Michael acceptor functional group, which covalently reacts with sulfhydryl group of Cysteine-805 located within the catalytic core of HER-2. In xenograft studies, HKI-272 (**51**) was well tolerated without obvious toxicity [55].

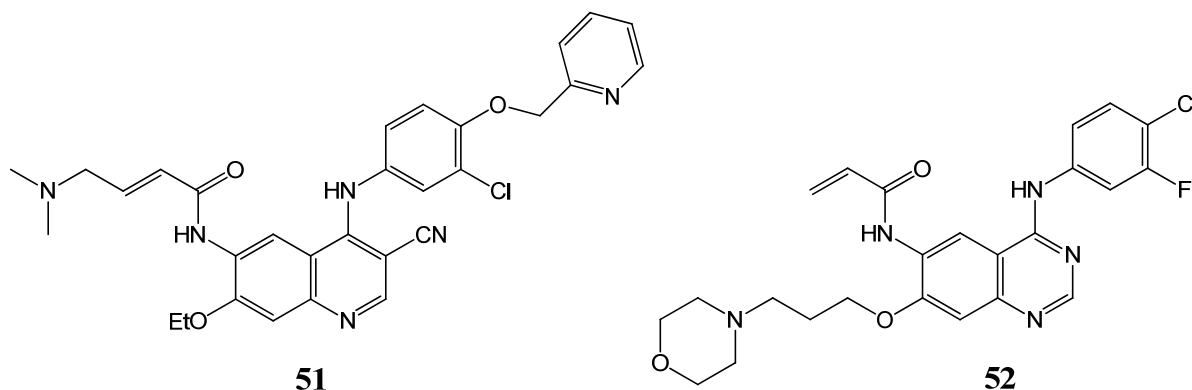


Figure 19. Chemical structures of the irreversible kinase inhibitors: HKI-272 (**51**) and Canertinib (**52**).

Canertinib (CI-1033) (**52**) is an irreversible nonselective EGFR inhibitor with an IC_{50} value at low nanomolar range. It was found that Canertinib (**52**) is active against human breast carcinomas both *in vitro* and *in vivo* tumor xenograft models. In clinical phase II Canertinib (**52**) was tested against metastatic nonsmall cell lung cancer and metastatic breast cancers. The most common side effect associated with Canertinib (**52**) were diarrhea, skin rash, nausea and stomatitis [56].

Bruton's tyrosine kinase (Btk) is a member of Tec family kinases and is a key component in the B-cell receptor signal pathway (BCR). Pyrazolo-pyrimidine containing Btk inhibitor (**53**) has an IC_{50} value in the subnanomolar range and it showed dose-dependent efficacy in a mouse arthritis model [57].

Compound (**54**) is irreversible kinase inhibitor of Wyeth-Ayerst with IC_{50} of 38.5 nM against EGFR receptor tyrosin kinase. It was developed with the aim to treat nonsmall cell lung cancer (NSCLC), colorectal neoplasia and other EGFR depended solid tumours. The reactive acryl group of compound (**54**) is able to interact through the Michael addition with the cysteine or serine residues within the binding pocket of EGFR paralogous [58].

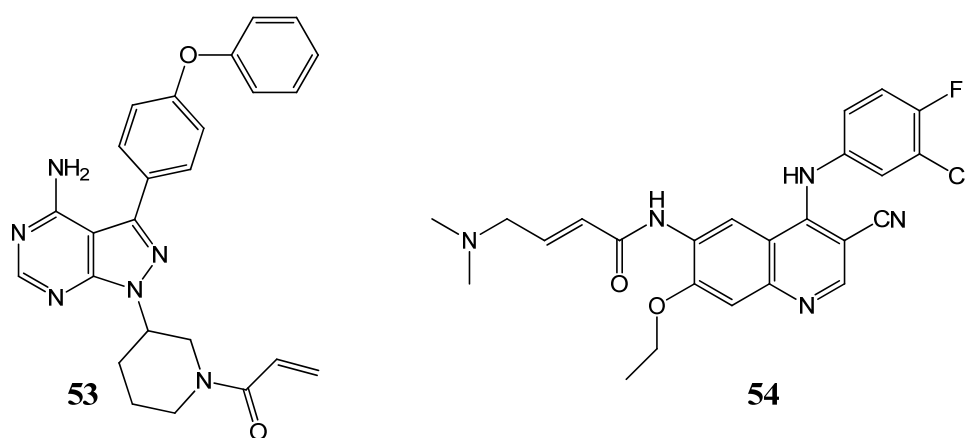


Figure 20. Chemical structures of the irreversible kinase inhibitors: compound (**53**) and (**54**).

FIIN-1 (**56**) is a first irreversible inhibitor of FGFRs with nanomolar *in vitro* IC_{50} values against FGFR1 isoforms. FIIN-1 (**56**) was created on the basis of structural information of compound PD173074 (**55**) bound to tyrosine kinase receptor FGFR1 (Figure 21). Insertion of acrylamide moiety led to formation of a covalent bond with Cysteine-486, placed in the P loop within the active site of the protein. FIIN-1 (**56**) showed high degree of selectivity against the panel of 402 kinases. The IC_{50} values were determined to be 9, 6, 12, and 189 nM against FGFR1, FGFR2, FGFR3, and FGFR4, respectively. Binding and activity assays suggest that FIIN-1 (**56**) is a selective FGFR inhibitor [59].

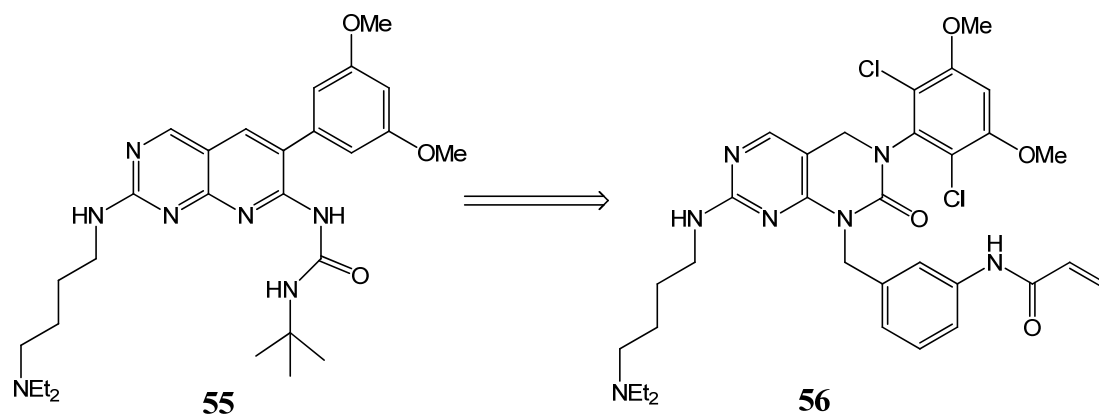
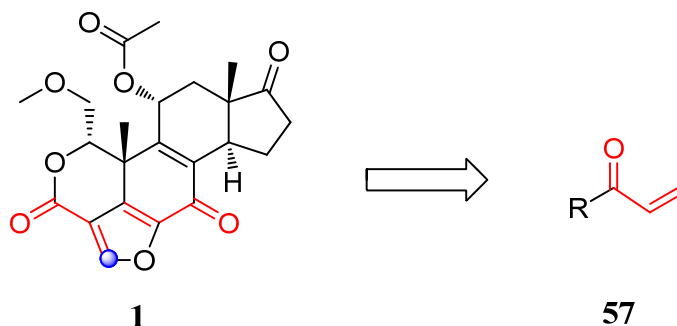


Figure 21. Chemical structures of PD173074 (**55**) and irreversible kinase inhibitor FIIN-1 (**56**).

Wortmannin (**1**) is natural and only known irreversible PI3K inhibitor. As previously described, wortmannin (**1**) covalently reacts with Lys-802 residue of PI3K α . Wymann and co-workers discovered that ϵ -amino group of Lys-802 attacks C-20 of wortmannin (**1**) which results in furan ring opening to form an enamine (Scheme 2). It is important to note that wortmannin (**1**) is a bimodal inhibitor, what means that inhibition of PI3K is established through both non-covalent interactions as well as covalent modification of lysine that leads to irreversible adduct [60].

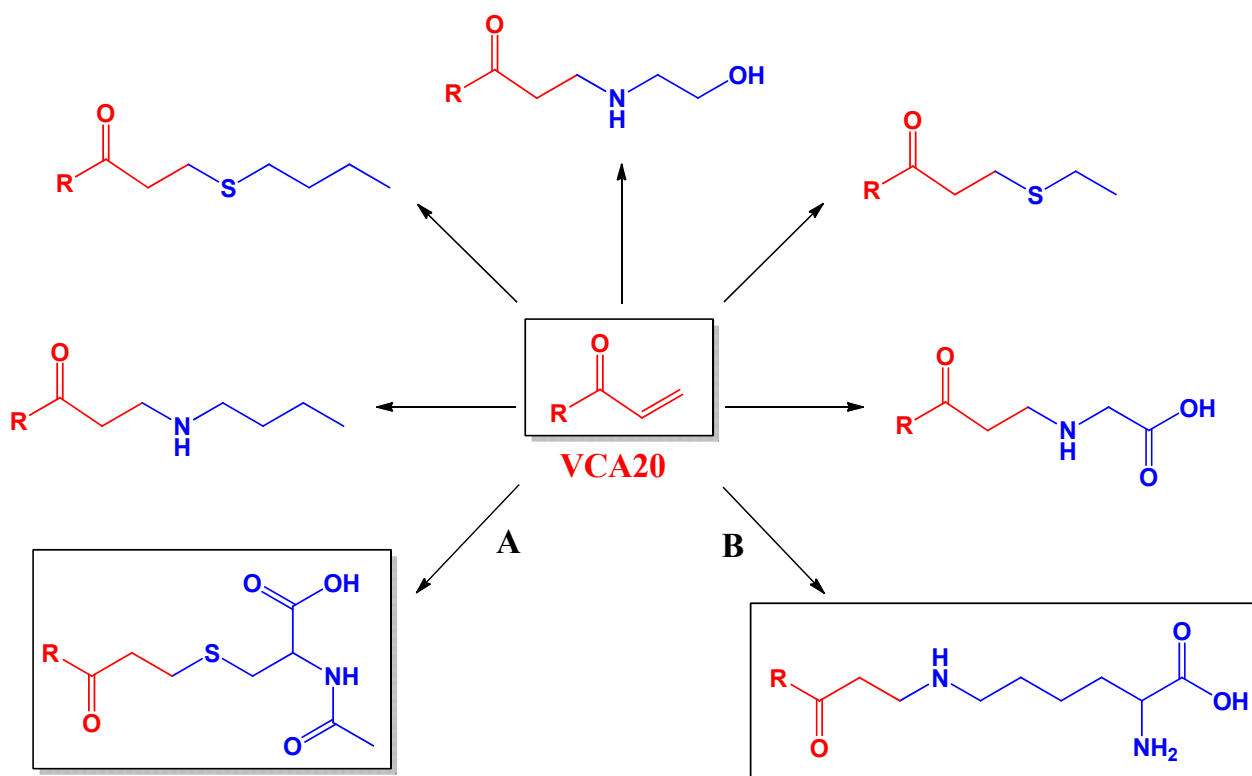
4.2.3. Michael Addition of Amine and Thiol Nucleophiles to the Acryl Containing Probe VCA20 in Water

The extensive chemistry of protein-reactive wortmannin (**1**) was a forceful inspiration for the design of synthetic irreversible PI3K inhibitors. The furan ring of natural product is double activated with two acrylic Michael systems. In order to create effective synthetic irreversible PI3K inhibitor, we inserted firstly the acrylamide group as an electrophilic group for the covalent modification of PI3K (Scheme 6).



Scheme 6. Double Michael system (red) makes wortmannin (**1**) attractive for attack of Lys-802 on C-20 position (blue); decision to use acrylamide moiety as a reactive group for creation of irreversible PI3K inhibitor.

It was suggested that free lysine residues from the proteins could react with the electrophilic acrylic group in the similar manner as the active Lys-802 with wortmannin (**1**) through the Michael addition. That assumption was proven during the master work studies of Cmiljanovic V. (data unpublished). *In vitro* proof was based on the use of butylamine as imitation of lysine site chain that was added to the acryl containing chemical probe VCA20 under physiological conditions. After ~ 50 hours of reaction at 37 °C in phosphate buffer (PBS buffer, pH 7.4), desired product was obtained in quantitative yield as the only product. After encouraging results, several different amines and thiol nucleophiles were tested with VCA20 under same conditions. In almost all cases a decrease of NMR chemical shifts for acryl amid protons was observed.



Scheme 7. Investigated nucleophiles in Michael addition to VCA20 in H₂O. Conditions: nucleophile (2.0 eq.), PBS buffer (pH 7.4), ~ 50 hours, 37 °C; A) VCA20 (1.0 eq.), Ac-Cys-OH (3.3 eq.), PBS buffer (pH 9.3), 150 h, 38 - 40 °C, 70%; B) VCA20 (1.0 eq.), lysine HCl (10 eq.), PBS buffer (pH 9.3), ~ 166 hours, 38 - 40 °C, 42% (Cmiljanovic V. master work-unpublished).

The results of reactions presented in (Scheme 7) indicated the possibility for Michael addition of both lysine as well as cysteine to the acryl containing chemical probes. Therefore, the further step was focused on reaction of VCA20 with lysine and cysteine as nucleophile reagents. Addition of those amino acids to VCA20 was followed by kinetic measurements. Due to the very slow lysine and cysteine addition to VCA20 in water by pH 7.4, the measurements were carried on pH ~ 9. The reaction **A** in (Scheme 7) with Ac-Cys-OH gave better yield (70%, after 150 hours of reaction time) in contrast to reaction **B** with lysine (42%, after 166 hours of reaction time). Motivated by these results, we attached the acrylamide group to PI3K inhibitor ZSTK474 (**38**) in order to covalently target appropriate lysine moiety in PI3K γ , located at the entrance of hydrophobic region of the ATP pocket.

4.2.4. Selectivity Filter Approach for Successful Design of Irreversible Inhibitors

In order to create more selective and potent PI3K inhibitors, we started from ZSTK474 (**38**) as a selective inhibitor for class I PI3K family. Here, it will be described a rational design of irreversible PI3K inhibitors.

On the basis of X-ray structural studies of PI3K γ in complex with ZSTK474 (**38**) as well as docking studies of the same inhibitor to the other class I PI3K isoforms (Figure 22), we identified amino acids at the entrance of the ATP-binding pocket, available only by PI3K γ and not by other isoforms. Additionally, we identified amino acids available only by PI3K α and not by other PI3K isoforms. Selective targeting of these amino acids could lead to the first isoform-selective PI3K γ and PI3K α inhibitors. By PI3K γ isoform we identified Lys-890 as a “selectivity filter” residue. According to the X-ray crystal structure of ZSTK474 (**38**) in complex with PI3K γ , Lys-890 makes hydrophobic contacts with the morpholine group of the ligand at the entrance of the hydrophobic pocket II (see page 100). By using a sequence alignment analysis of the PI3K isoforms we observed that other PI3K isoforms do not contain an appropriate lysine residue at the entrance to the hydrophobic pocket II. It was motivating us to design novel compounds for selective targeting of PI3K γ . Additionally, we identified Cys-862 in PI3K α , respectively Lys-841 in PI3K δ as selectivity filter residues (Figure 22). According to the modeling studies by PI3K α and X-ray crystal structure by PI3K δ these residues are not closely located to the ligand ZSTK474 (**38**), so by there targeting a linker strategy has been applied.

By using this structural information, we design a small library of possible irreversible PI3K inhibitors by insertion of different chemical electrophilic groups at the morpholine moiety of ZSTK474 (**38**) that could covalently bind to nucleophilic residues such as Lys-890 by PI3K γ , Cys-862 by PI3K α or Lys-841 by PI3K δ .

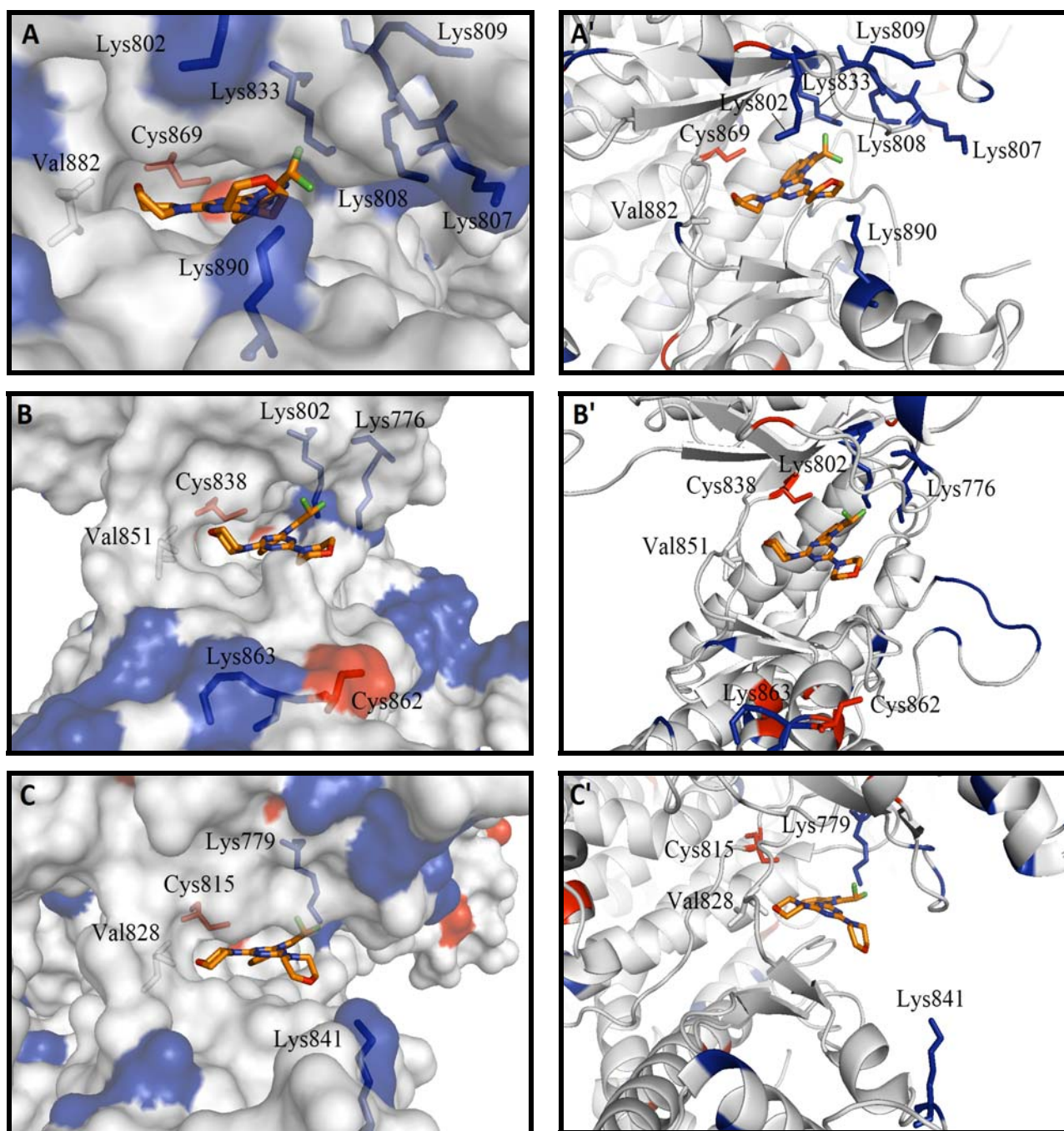
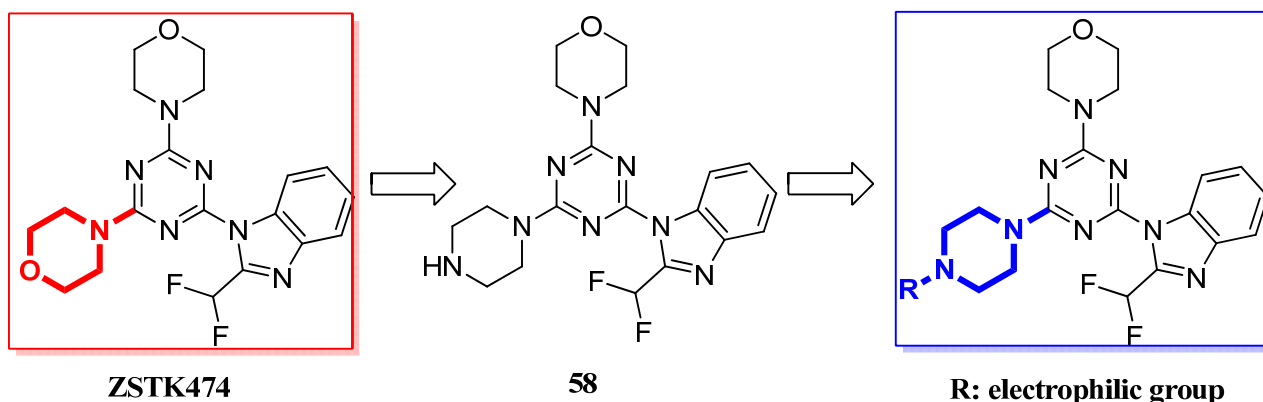


Figure 22. A) Represented is a surface diagram of X-ray elucidated ZSTK474-PI3K γ complex zoomed into the ATP binding site; B) Surface diagram of ZSTK-PI3K α complex, where ZSTK474 has been manually docked to the X-ray crystal structure of PI3K α ; C) Surface diagram of X-ray elucidated ZSTK474-PI3K δ complex. Identified nucleophilic amino acid residues as well as ligand ZSTK474 are represented in a stick form, colored according to the element (C atoms in yellow, N atoms in blue, O atoms in red, and F atoms in green). In figures A', B' and C' represented is a ribbon diagram of appropriate ligand-PI3K complex.

4.2.5. Chemistry and Biology of Irreversible ZSTK474 Derivatives

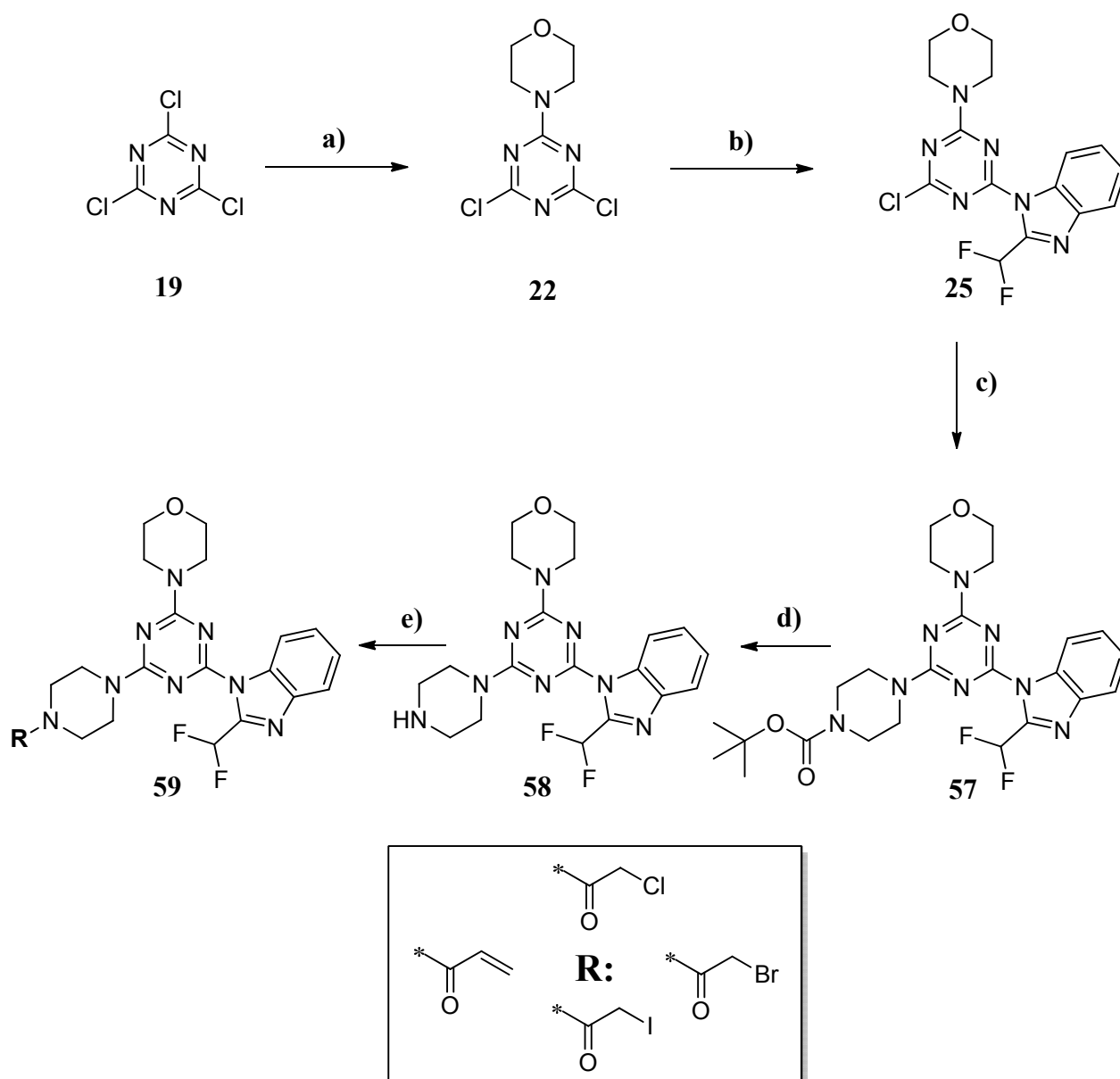
During our SAR studies we discovered that the exchange of one morpholine ring with appropriate piperidine and piperazine derivatives in ZSTK474 (**38**) does not have a considerable effect on reduction of inhibitor activity. Therefore we replaced morpholine ring with electrophilic group containing piperazine derivatives with the aim to create isoform selective irreversible PI3K inhibitors.



Scheme 8. Chemical modifications of ZSTK474 through the replacement of morpholine with piperazine and piperazine derivatives bearing an electrophilic reactive group to yield possible irreversible ZST474 analogs.

As previously described, during my PhD work we elucidated the X-ray crystal structure of ZSTK474 in complex with PI3K γ . To target the identified selectivity filter amino acid Lys-890 by PI3K γ we performed the chemistry described in (Scheme 9).

Cyanuric chloride (**19**) was substituted by morpholine in methylene chloride, at $-50\text{ }^{\circ}\text{C}$ for 20 minutes to give intermediate (**22**). Replacement of second chlorine center with 2-difluoromethyl-1H-benzimidazole in presence of K_2CO_3 in DMF, at $-5\text{ }^{\circ}\text{C}$ for 30 minutes and further stirring at room temperature for 4 hours led to the intermediate (**25**). The next step gave product (**57**) by amination with 1-boc-piperazine in presence of K_2CO_3 and DMF as a solvent at room temperature for 45 minutes. Further, compound (**58**) was obtained by Boc deprotection in HCl (dioxane solution), stirring at room temperature for 1.5 hours in methylene chloride as a solvent. Final product (**59**) was obtained by amidation with appropriate anhydride reagent, by stirring at room temperature for 1-2 hours in methylene chloride and in presence of N,N-diisopropylethylamine as a base.

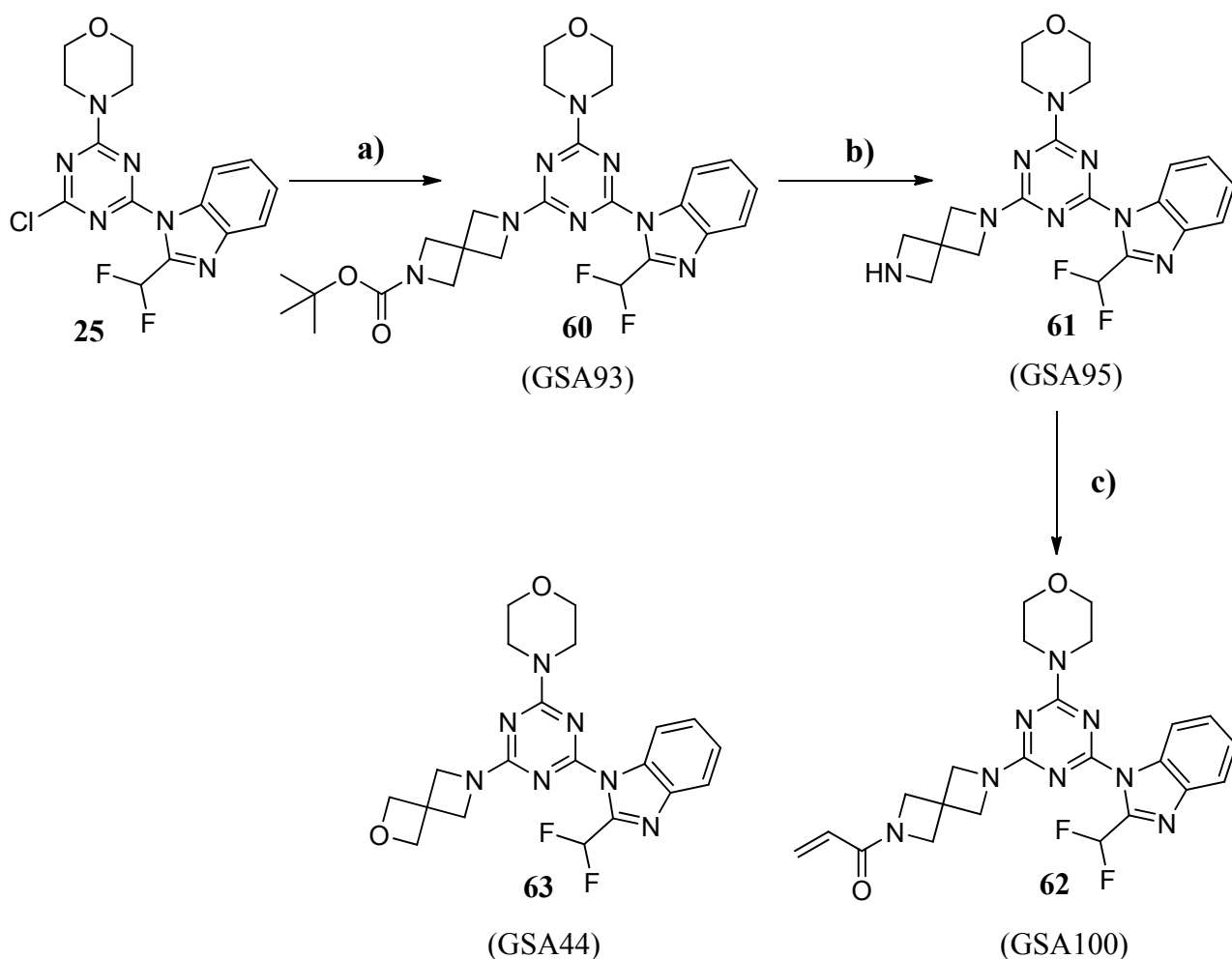


Scheme 9. Reagents and conditions: a) morpholine (1.0 eq.), CH_2Cl_2 , $-50\text{ }^\circ\text{C}$, 20 minutes, 28 %; b) K_2CO_3 , (1.44 eq.), 2-difluoromethyl-1H-benzimidazole (1.4 eq.), DMF, 30 minutes at $-5\text{ }^\circ\text{C}$, 4 hours at room temperature, 65 %; c) 1-boc-piperazine (1.2 eq.), K_2CO_3 (3.2 eq.), DMF, 1 hour at room temperature, 95 %; d) compound (57) (260 μmol , 1.0 eq.), HCl in dioxane (~2 ml), CH_2Cl_2 , 1.5 hours at room temperature, 100 %; e) N,N-diisopropylethylamine (1.1 eq.), electrophilic group (1.0 eq.), CH_2Cl_2 , 1 - 2 hours at room temperature, 37 – 88 %.

Table 9. Inhibitor activity^a

Compound	R	<i>In vitro</i> PI3K α 200nM	A2058 cell inhibition		TSC2 ^{-/-} MEFs cell inhibition
			pPKB/PKB 1 μ M	pS6 1 μ M	pS6 1 μ M
(NCB141) 80		8.1	45.26 \pm 2.98	75.84 \pm 0.86	98.78 \pm 0.73
(NCB144) 81		7.4	8.43 \pm 0.66	25.5 \pm 1.06	37.40 \pm 1.55
(NCB145) 82		3.4	12.34 \pm 1.93	24.48 \pm 1.66	94.32 \pm 2.25
(NCB147) 83		8.5	17.96 \pm 2.13	32.53 \pm 0.30	67.06 \pm 4.75

^aInhibitor efficacy and their cell permeability were measured by *in cell* Western inhibition assay on melanoma cell line A2058 and TSC2^{-/-}-MEFs cell line; *in vitro* PI3K α inhibition was measured by *Kinase Glo* assay and given numbers represent % remaining activity, the smaller the value, the stronger is the inhibition; coloured numbers represent: blue - no activity, green - low activity, red - good activity, orange - very good activity.



Scheme 10. Reagents and conditions: a) *tert*-butyl 2,6-diazaspiro[3.3]heptane-2-carboxylate (GSA79) (0.6 eq.), potassium carbonate (3.2 eq.), DMF, room temperature, 3 hours, 95%; b) trifluoroacetic acid/methylene chloride 1:2, room temperature, 2 hours, 80%; c) acrylic anhydride (1.0 eq.), DIPEA (1.1 eq.), CH₂Cl₂, room temperature, 1.5 hours, 68 %.

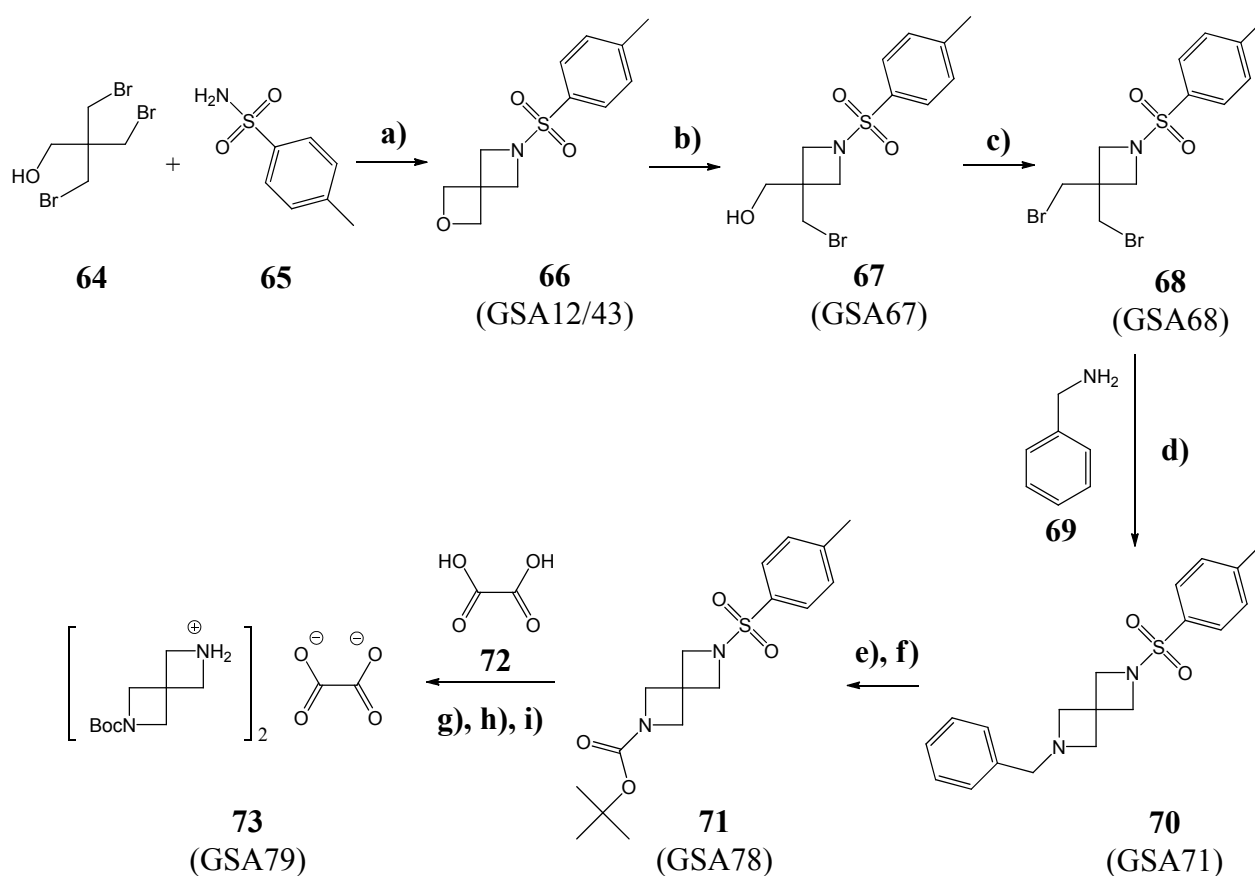
Considering the good biological activity of compound GSA44 (**63**), we decided to synthesize an acrylamid containing spiroperazine derivative (Scheme 10 and Table 10). According to (Scheme 11) produced mono *N*-boc protected spiroperazine GSA79 (**73**) was coupled onto compound (**25**). Then the Boc group of azetidine GSA93 (**60**) was cleaved by treatment with trifluoroacetic acid to give the free amine GSA95 (**61**). Final product GSA100 (**62**) was obtained by amidation with acrylic anhydride, by stirring at room temperature for 1.5 hours in methylene chloride and *N,N*-diisopropylethylamine as a base.

Table 10. Inhibitor activity^a

Compound	R ¹	<i>In vitro</i> PI3K α 200 nM	A2058 cell inhibition		TSC2-/- MEFs cell inhibition
			pPKB/PKB 1 μ M	pS6 1 μ M	pS6 1 μ M
(GSA100) 62		22	38.25 \pm 3.46	61.57 \pm 0.38	131.22 \pm 17.94

^aInhibitor efficacy and their cell permeability were measured by *in cell* Western inhibition assay on melanoma cell line A2058 and TSC2-/-MEFs cell line; *in vitro* PI3K α inhibition was measured by *Kinase Glo* assay and given numbers represent % remaining activity, the smaller the value, the stronger is the inhibition; coloured numbers represent: blue - no activity, green - low activity, red - good activity, orange - very good activity.

The synthesis of *N*-tosyl-2-oxa-6-azaspiro[3.3]heptane GSA12/43 (**66**) was investigated by the group of Prof. Carreira from ETH Zurich. Then the oxetan moiety was opened with hydrobromic acid to give bromoalcohol GSA67 (**67**) in quantitative yield. This bromoalcohol GSA67 (**67**) was transformed via an Apple reaction into di-brominated compound GSA68 (**68**), which was further reacted with benzylamine (**69**) to provide 2-benzyl-6-tosyl-2,6-diazaspiro[3.3]heptane GSA71 (**70**). Hydrogenolytic cleavage of the *N*-benzyl group and subsequent treatment with Boc₂O gave *N*-Boc protected azetidine GSA78 (**71**). The last step is again the tosylate deprotection, to give *tert*-butyl 2,6-diazaspiro[3.3]heptane-2-carboxylate GSA79 (**73**).



Scheme 11. Reagents and conditions: a) 3-bromo-2,2-bis(bromomethyl)propan-1-ol **64** (1.0 eq.), *p*-tosylamide (**65**) (1.2 eq.), potassium hydroxide (3.2 eq.), ethanol, 90 °C, 94 hours, 56-63 %; b) HBr (33 % in AcOH, 1.2 eq.), diethyl ether, 0 °C → 25 °C, 45 minutes, 98 %; c) PPh₃ (1.7 eq.), CBr₄ (1.7 eq.), DCM, 0 °C, 1.5 hours, then room temperature, 4 hours, 73 %; d) benzylamine (2.0 eq.), DIPEA (5.0 eq.), acetonitrile, 93 °C, 72 hours, 95 %; e) Pd/C (10 % on charcoal, 0.05 eq.), H₂ (balloon pressure), methanol, 45 °C, 48 hours; f) Boc₂O (1.0 eq.) methanol, room temperature, 1 hour, 73%; g) magnesium powder (8.0 eq.), methanol, ultrasonication, room temperature, 1 hour; h) sodium sulfate decahydrate (9.0 eq.), diethyl ether, room temperature, 1 hour; i) oxalic acid 50 (0.5 eq.), diethyl ether, ethanol, 70 %.

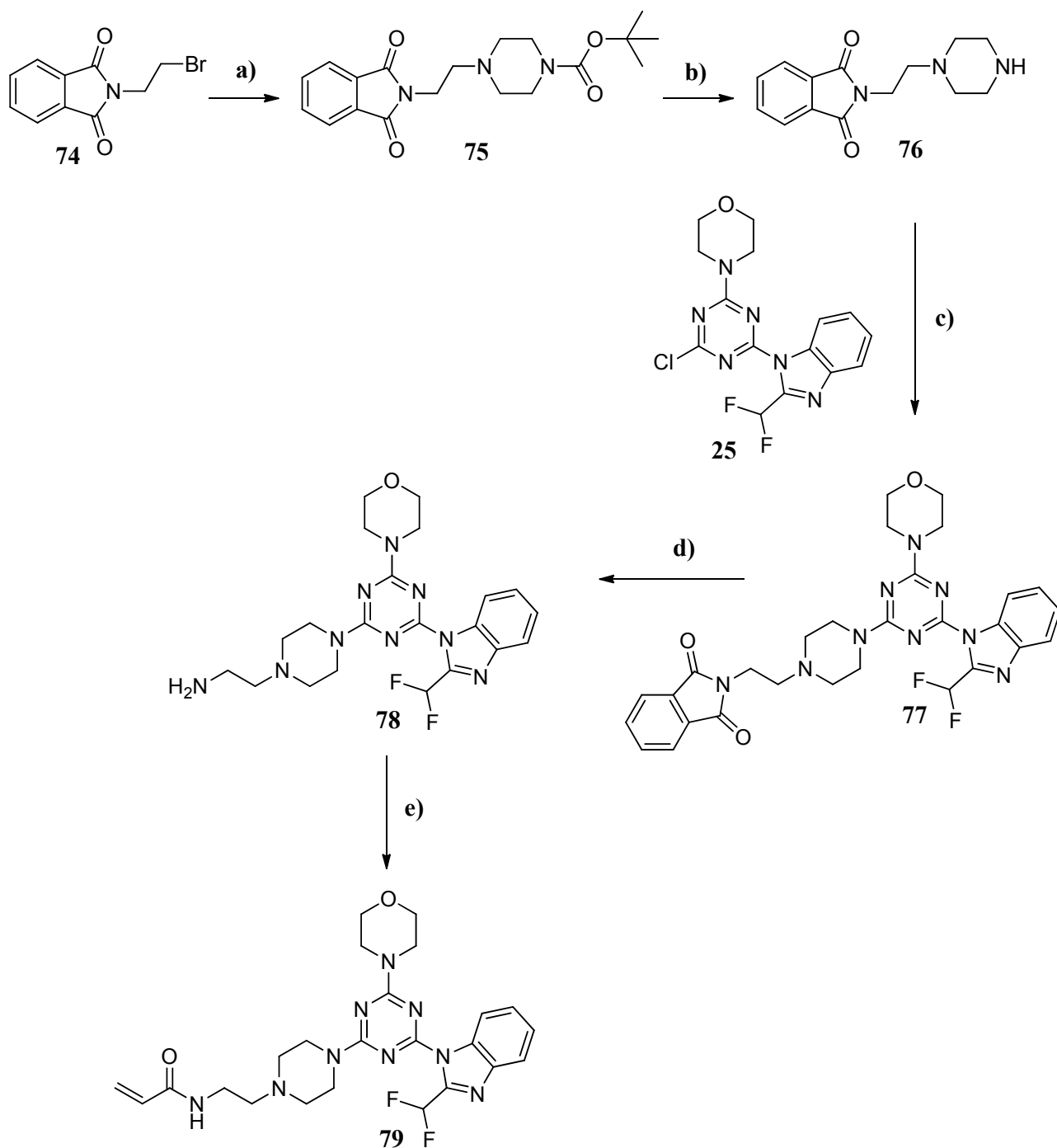
Our next strategy based on docking studies^a was design of irreversible inhibitors that may selectively target the isoform PI3K α or PI3K δ , avoiding the inhibition of PI3K γ , by introducing a linker strategy.

Amination of compound (**74**) with 1-Boc-piperazine in presence of diisopropylethylamine and anhydrous acetonitrile as a solvent under reflux at 84 °C for 22 hours gave intermediate (**75**). By Boc deprotection in trifluoroacetic acid/methylene chloride (3:2) solution at room temperature for 2 hours was obtained compound (**76**), which has been added to the compound (**25**) in presence of K₂CO₃ and DMF to yield the compound (**77**). After deprotection of the N-phthalimide with hydrazine monohydrate in ethanol by refluxing at 100 °C (Gabriel synthesis) acrylic anhydride has been added to the primary amine containing compound (**78**) to yield the final product (**79**) (Scheme 12), a possible irreversible inhibitor of PI3K α (targeting Cys-862) or PI3K δ (targeting Lys-841) or both of them (Figure 22).

Firstly the activity of these potential covalent compounds has been determined by using *in cell* Western inhibition assay and *in vitro* PI3K α Kinase Glo assay. Compounds NCB144 (**81**) and NCB145 (**82**) have been identified as highly active inhibitors in melanoma cells (Table 9). Additionally, very good cellular inhibitor activity has been noticed by compound NCB147 (**83**) (Table 9). Chloracetamid containing compound NCB141 (**80**) showed low inhibitor activity. Very good cellular inhibitor activity was also achieved by a spirocyclic compound GSA100 (**62**) (Table 10).

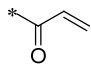
High cellular activity was accomplished by compound NCB152 (**79**) (Table 11). Also very good *in vitro* activity for PI3K α led to a conclusion that NCB152 (**79**) could be an irreversible inhibitor of PI3K α . Further cellular, chemical genetics as well as protein mass spectrometry experiments are on-going to confirm the covalent bond modification of Cys-862 by PI3K α by using the compound NCB152 (**79**).

^a Docking studies are computational techniques for the exploration of the possible binding modes of a substrate to a given receptor, enzyme or other binding site.



Scheme 12. Reagents and conditions: a) N,N-diisopropylethylamine (1.0 eq.), 1-Boc-piperazine (1.0 eq.), anhydrous CH₃CN, reflux under argon at 84 °C for 22 hours, 64 %; b) trifluoroacetic acid/methylene chloride (3:2) (25 ml), 2 hours at room temperature; c) compound (**25**) (1.0 eq.), 2-(2-(piperazin-1-yl)ethyl)isoindoline-1,3-dione (**76**) (1.7 eq.), K₂CO₃ (3.2 eq.), DMF, 2 hours at room temperature; d) hydrazine monohydrate (421 μmol, 1.1 eq.), EtOH, reflux at 100 °C for 5 hours, than conc. HCl (91.4 μl) was added and further reflux for 1 hour; e) N,N-diisopropylethylamine (1.1 eq.), acrylic anhydride (1.0 eq.), CH₂Cl₂, 2 hours at room temperature, 47 %.

Table 11. Inhibitor activity^a

Compound	R ²	<i>In vitro</i> PI3K α 200 nM	A2058 cell inhibition		TSC2-/- MEFs cell inhibition
			pPKB/PKB 1 μ M	pS6 1 μ M	pS6 1 μ M
(NCB152) 79		20	5.45 \pm 1.74	16.27 \pm 0.96	47.18 \pm 4.08

^aInhibitor efficacy and their cell permeability were measured by *in cell* Western inhibition assay on melanoma cell line A2058 and TSC2-/-MEFs cell line; *in vitro* PI3K α inhibition was measured by *Kinase Glo* assay and given numbers represent % remaining activity, the smaller the value, the stronger is the inhibition; coloured numbers represent: blue - no activity, green - low activity, red - good activity, orange - very good activity.

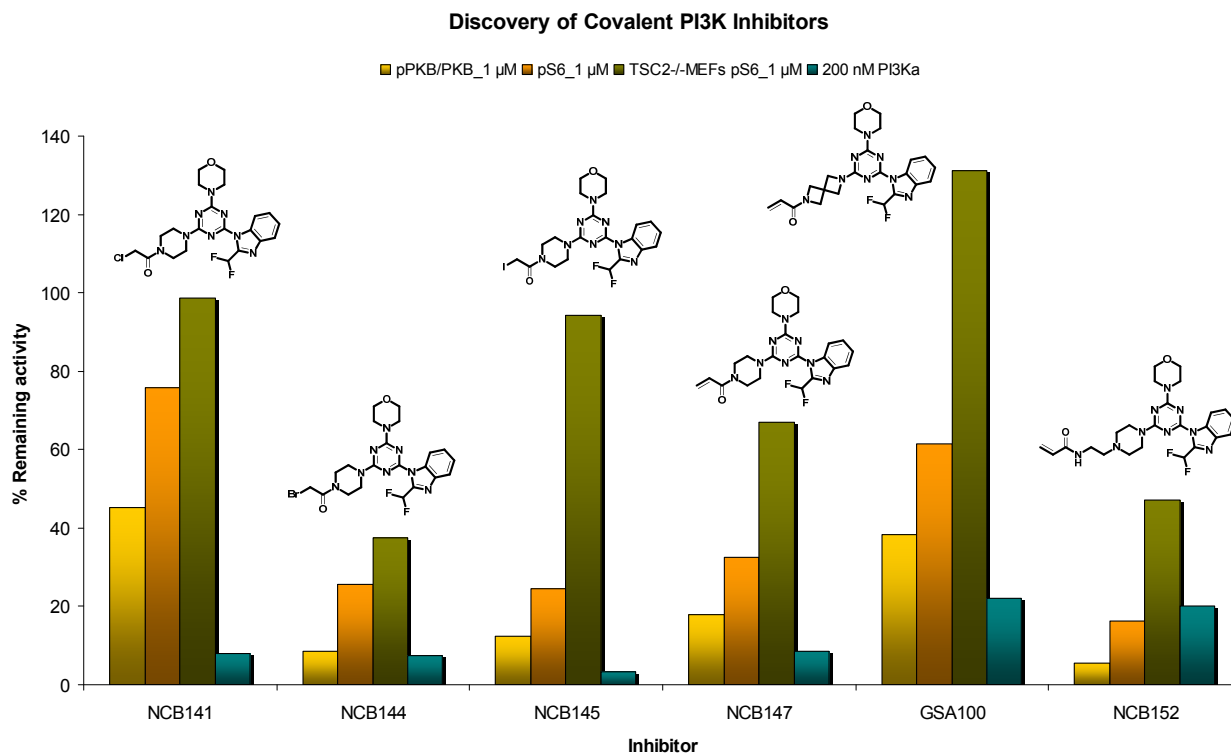


Figure 23. Presented is cellular activity (pPKB/PKB, pS6 on A2058 and pS6 on TSC2-/-MEFs) at 1 μM and *in vitro* activity against PI3K α at 200 nM; the lower the bar chart the better is the activity of the relevant compound.

Compounds (**84-87**) (Table 12) are synthesized in the same way as already presented in (Scheme 9). They showed low activity *in vitro* and *in vivo* experiments. Replacement of difluoromethyl group with methyl group led to a strong reduction in inhibitor activity due to loss of hydrogen bond formation between fluorine atom and catalytic Lys-833 in ATP pocket of PI3K γ isoform. Also, a lack of the *fluorine effect* should not be ignored. Fluorine increases the lipophilicity of a given inhibitor which leads to a better cellular permeability. The better is inhibitor permeability the higher is its concentration within the cell and therefore better inhibition of PI3K.

Table 12. Inhibitor activity^a

Compound	R ³	<i>In vitro</i> PI3K α 200 nM	A2058 cell inhibition		TSC2 ^{-/-} MEFs cell inhibition
			pPKB/PKB 1 μ M	pS6 1 μ M	pS6 1 μ M
(NCB133) 84		24	80.46 \pm 1.69	90.46 \pm 5.76	106.74 \pm 0.92
(NCB134) 85		36	68.13 \pm 0.07	80.29 \pm 4.39	120.91 \pm 0.15
(NCB130) 86		22	67.92 \pm 1.23	89.02 \pm 4.04	100.83 \pm 0.93
(NCB135) 87		45	52.61 \pm 19.06	63.14 \pm 0.03	127.59 \pm 7.51

^aInhibitor efficacy and their cell permeability were measured by *in cell* Western inhibition assay on melanoma cell line A2058 and TSC2^{-/-}-MEFs cell line; *in vitro* PI3K α inhibition was measured by *Kinase Glo* assay and given numbers represent % remaining activity, the smaller the value, the stronger is the inhibition; coloured numbers represent: blue - no activity, green - low activity, red - good activity, orange - very good activity.

Further biological examinations have also done on bone marrow derived mast cells (BMMC). It was quantificated the inhibition of Thr308 phosphorylation (in PKB) normalized to the signal of adenosine (Ade) stimulated cells without inhibitor treatment. Experiments were repeated four times for two different concentrations of inhibitors (1.0 μ M and 0.1 μ M). They indicated that our inhibitors inhibit quit well PI3K γ signalling in mast cells (Figure 24, Table 13). The next step is to

determine whether these inhibitors are highly specific for PI3K γ and whether they indeed bind covalently.

Further experiments with Wortmannin, which is a covalent ATP competitive inhibitor, confirmed that our inhibitors are capable to compete for the binding with PI3K γ (Figure 25). Then, covalent binding was tested by coupling the PI3K γ to beads, which can be recovered by sedimentation what allowed washing away of the inhibitors if they are not covalently linked to PI3K γ . If, after several washing steps of the beads, Wortmannin (which was added after the washing steps) is still unable to bind to PI3K, it is a good indication that the covalent binding of our designed inhibitors exists (Figure 25). The positive results in this experiment were obtained in case of bromoacetamid containing NCB144 (**81**) and iodoacetamid containing NCB145 (**82**).

Anyway, in order to confirm these results (covalent binding and PI3K γ specificity) more biological experiments should be done. Our next goal is to show that our potential covalent binders NCB144 (**81**) and NCB145 (**82**) for PI3K γ do not bind covalently to others PI3Ks so we could significantly reduce inhibitor concentration in long time treatments of the cells.

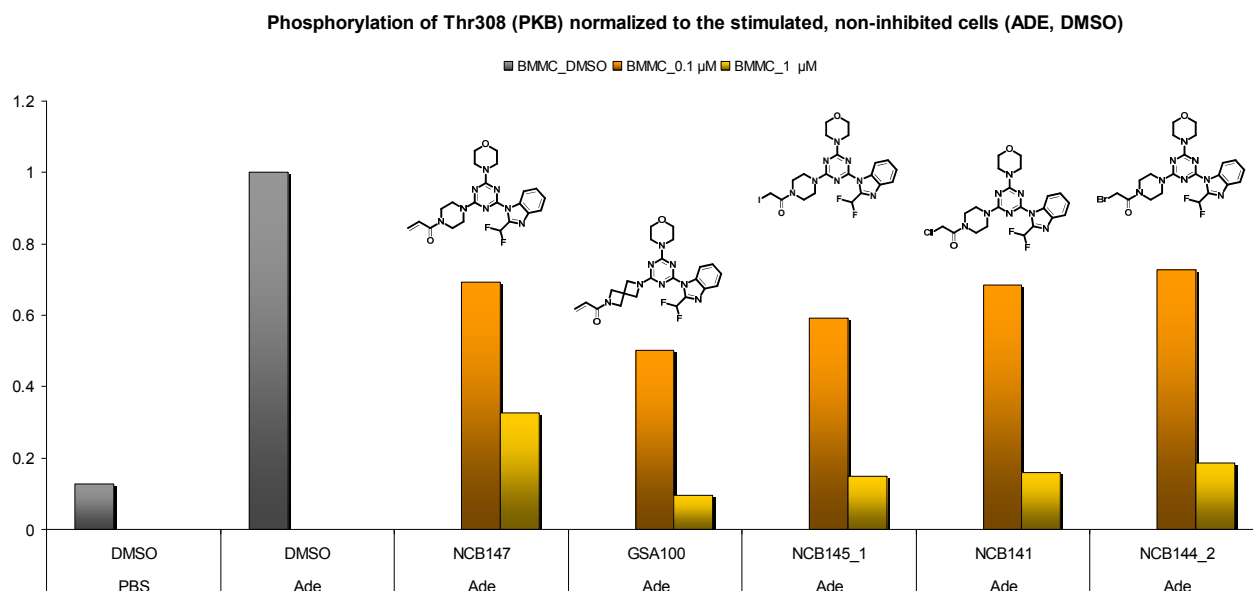
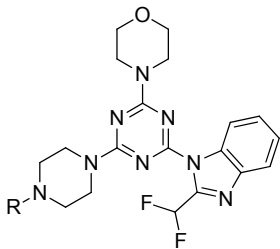
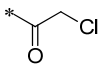
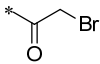
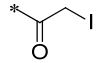
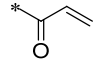
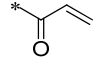


Figure 24. Presented is cellular activity against PI3K γ in bone marrow derived mast cells (BMMC) at 1.0 and 0.1 μ M; the lower the bar chart the better is activity of the relevant compound.

Table 13. Inhibitor activity^a

Compound	R	Stimulus	BMMC inhibition	
			1 μ M	0.1 μ M
				
			GSA100	
DMSO		PBS	0.13	
DMSO		Ade	1.00	
(NCB141) 80		Ade	0.16	0.68
(NCB144) 81		Ade	0.18	0.73
(NCB145) 82		Ade	0.15	0.59
(NCB147) 83		Ade	0.33	0.69
(GSA100) 62		Ade	0.09	0.50

^aInhibitor efficacy was measured by *in cell* Western inhibition assay on bone marrow derived mast cells (BMMC) at two concentration 1.0 and 0.1 μ M; the smaller the value, the stronger is the inhibition.

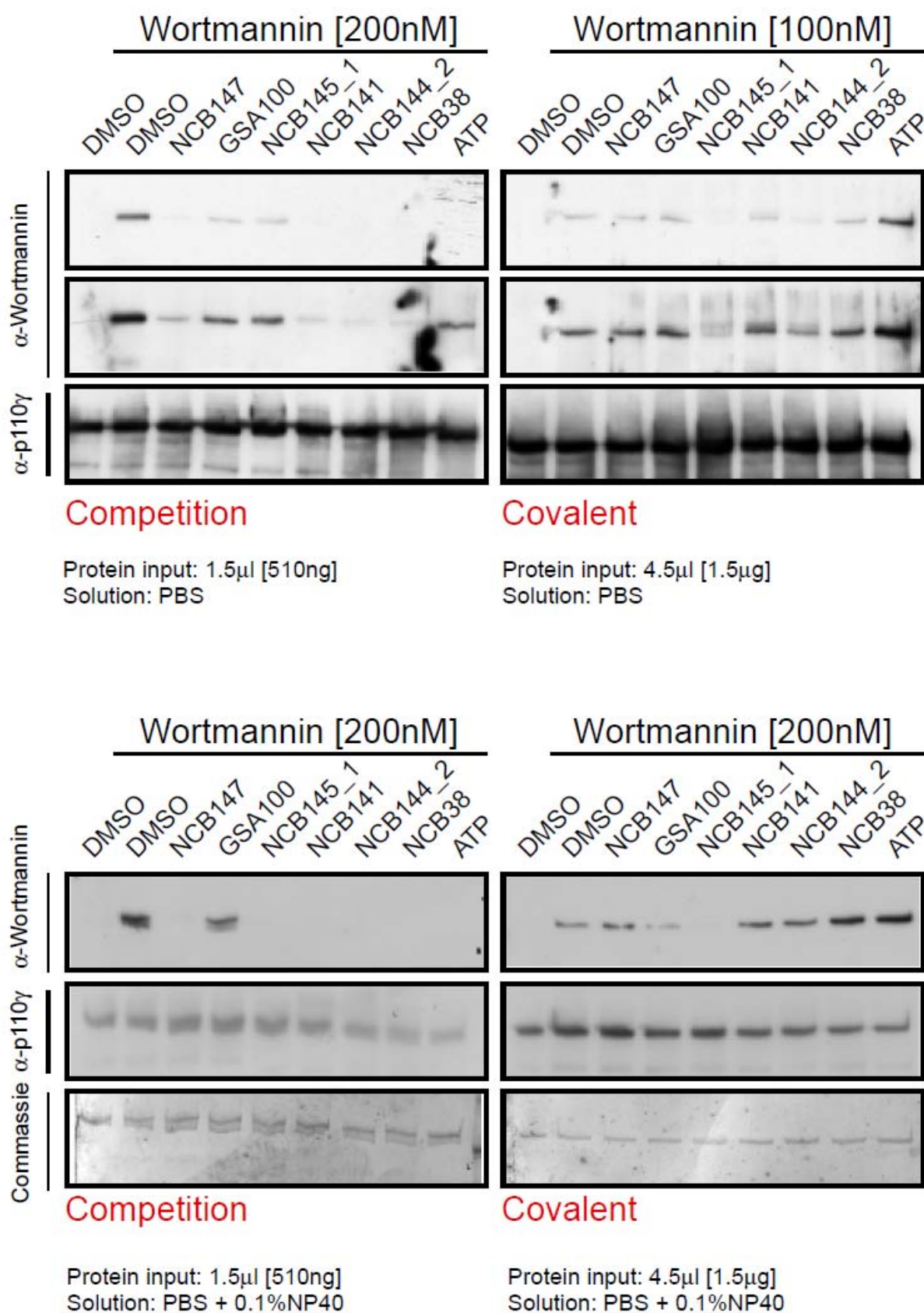


Figure 25. Competition and Covalent binding assay present weather the inhibitors compete with wortmannin for binding to the catalytic center of PI3K γ and weather they bind covalent to the PI3K γ . The weaker the signal for wortmannin the better is inhibitor. Experiments were done two times with different concentration of wortmannin of 100 nM and 200 nM. The covalent binding can be noticed by compounds NCB144 (**81**) and NCB145 (**82**).

4.3. PI3K Inhibitor Activity against Human Glioblastoma

Glioblastoma multiforme (GBM) is the most common and most malignant of the primary brain tumors and usually spreads quickly to other parts of the brain. For this reason, these kinds of tumors are difficult to treat and it is not uncommon for them to recur after initial treatment. Unfortunately, prognosis for patients with high-grade gliomas is generally poor, less than 12 months survival after diagnoses. The care of GBM is usually multidisciplinary and involves chemotherapy, radiation, radiosurgery, antiangiogenic therapy, and surgery [61]. Difficult treatment of glioblastoma is due to several complicating factors such as [62]:

- The tumor cells are very resistant to other conventional therapies
- The brain is susceptible to damage due to conventional therapy
- The brain has a very limited capacity to repair itself
- Many drugs can not cross the blood-brain barrier to act on the tumor (A physiological mechanism that alters the permeability of brain capillaries, so that some substances, such as certain drugs, are prevented from entering brain tissue, while other substances are allowed to enter freely).

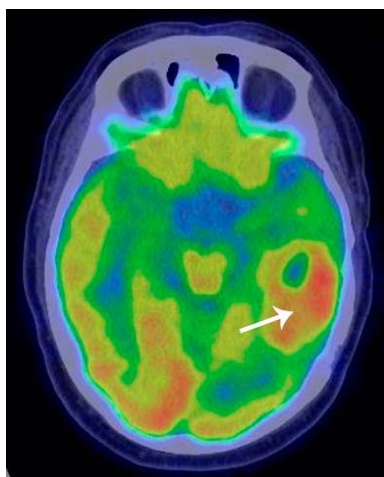


Figure 26. Positron emission tomographies (PET) scan of glioblastoma multiforme [61].

Therefore there is a need for novel and improved approaches that will be more efficient than conventional therapies. Since GBM tumors have developed the mechanisms of treatment resistance, monotherapy would not be the most effective method to treat these kinds of tumors [63].

One of the promising targets for such an approach is the PI3K/Akt^b pathway. Deregulation in PI3K-mediated signaling network plays a central role in formation of variety of tumors, including GBM [65]. PI3K and Akt are also involved in the activation of mTOR, which plays important role in regulating protein synthesis and cell growth. According to important role of this pathway, glioma cell lines were treated against of differ PI3K inhibitors, showing that inhibition of p110 α is effective in blocking of proliferation. Even better results were obtained in case of dual inhibition of PI3K and mTOR as well [66]. It was also shown that inhibition of PI3K sensitizes GBM to chemotherapy and to death receptor-induced apoptosis^c [67].

A dual PI3K/mTOR inhibitor PI-103 (**11**) was considered as promising candidate for treatment of GBM, because of its ability to selectively block p110 α and mTOR at nanomolar concentrations [35]. PI-103 (**11**) has an anti-proliferative effect on GBM cells and efficiently sensitizes them for chemotherapy induced apoptosis. It was also concluded that PI-103 (**11**) in concurrent treatment with chemotherapeutic drugs had better effect on increasing of apoptosis and reducing of colony formation^d compared with chemotherapy treatment alone. These results suggested that PI3K inhibitors used together with traditional therapies that have been insufficient to treat GBM, can restore cell's ability to undergo apoptosis [68].

^bThe serine/threonine protein kinase Akt, also known as protein kinase B (PKB) or RAC-PK, was initially identified as one of the downstream targets of phosphatidylinositol-3 kinase (PI3K). Akt kinase pathway is one of the most actively studied pathways in drug development research. Activated Akt plays important role in mediating signals for cell growth, cell survival, cell-cycle progression, differentiation, transcription, translation, and glucose metabolism.

^cApoptosis or programmed cell death is defined as a mechanism of cellular suicide which occurs after sufficient cellular damage. The end result of apoptosis is cell death without inflammation of the surrounding tissue.

^dA colony is population of a single type of microorganism that is growing on a solid or semi-solid surface. Bacteria, yeast, fungi, and molds are capable of forming colonies. Indeed, when a surface is available, these microbes prefer the colonial mode of growth rather than remaining in solution. On a colonized solid surface, such as the various growth media used to culture microorganisms, each colony arises from a single microorganism. The cell that initially adheres to the surface divides to form a daughter cell. Both cells subsequently undergo another round of growth and division. This cycle is continually repeated. After sufficient time, the result is millions of cells piled up in close association with each other. This pile, now large enough to be easily visible to the unaided eye, represents a colony.

Recently, it was reported that high cellular and *in vivo* activity of a novel PI3K inhibitor, PX-866 (**88**), against human glioblastoma. PX-866 (**88**) is irreversible, biologically stable synthetic viridinin derivative (structure related to wortmannin **1**). Inhibition is based as by wortmannin (**1**) on covalent binding to Lys-802 in PI3K α (more potent than wortmannin **1**) and Lys-883 in PI3K γ . Also, PX-866 (**88**) inhibits PI3K δ isoform and is weak inhibitor of PI3K β . Investigation of this inhibitor in glioblastoma cell lines after treatment of 72 hours resulted in dose-dependent growth inhibition. It was concluded that PX-866 (**88**) is directly involved in inhibition of invasion and angiogenic^e potential of glioblastoma cells and also was found its therapeutic activity in human tumor xenograft models [69].

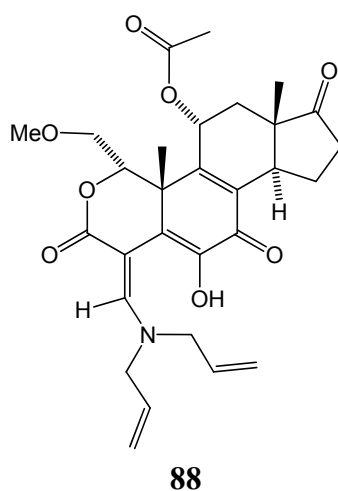


Figure 27. Chemical structure of PI3K inhibitor: PX-866 (**88**) [70].

As understanding of glioma biology has progressed, there is a hope that further efforts will lead to more effective, less toxic and rationally conceived therapeutics that target specific genes or proteins and that in combination with radio or chemo therapy will overcome various obstacles so far present. Since recent studies have implicated PI3K/Akt and mTOR pathway in pathogenesis of glioblastoma as well as other types of gliomas cancers, we tested our most active PI3K/mTOR inhibitors against human glioblastoma cell lines. Experimental results will be described in the following chapter.

^e Angiogenesis is a physiological process involving the growth of new blood vessels from pre-existing vessels. Angiogenesis is a normal and vital process in growth and development, as well as in wound healing. However, it is also a fundamental step in the transition of tumors from a dormant state to a malignant one, by supplying them with oxygen and nutrients required for their growth and expansion into the surrounding tissue.

4.3.1. PI3K Inhibitor Efficacy in Colony Formation Assay on Malignant Glioma Cell Lines

The effect of PI3K inhibition in the glioma cell lines LN18, LN215 and U343 was analyzed using colony formation assay. In a colony formation assay, both the number and size of colonies formed after 14 days of drug treatment were measured. Among the first group of tested PI3K inhibitors (Figure 28 and Table 14), ZSTK474 (**38**) and its pyrimidine derivative NCB35 (**90**) significantly reduced colony formation in GBM cell lines tested compared with the untreated control. Quite well reduction was also noticed by triazine derivative NCB5 (**89**). Therefore, the next round of testing was focused on further ZSTK474 derivatives. Unfortunately, these experimental results are not finished until the submission date of my thesis.

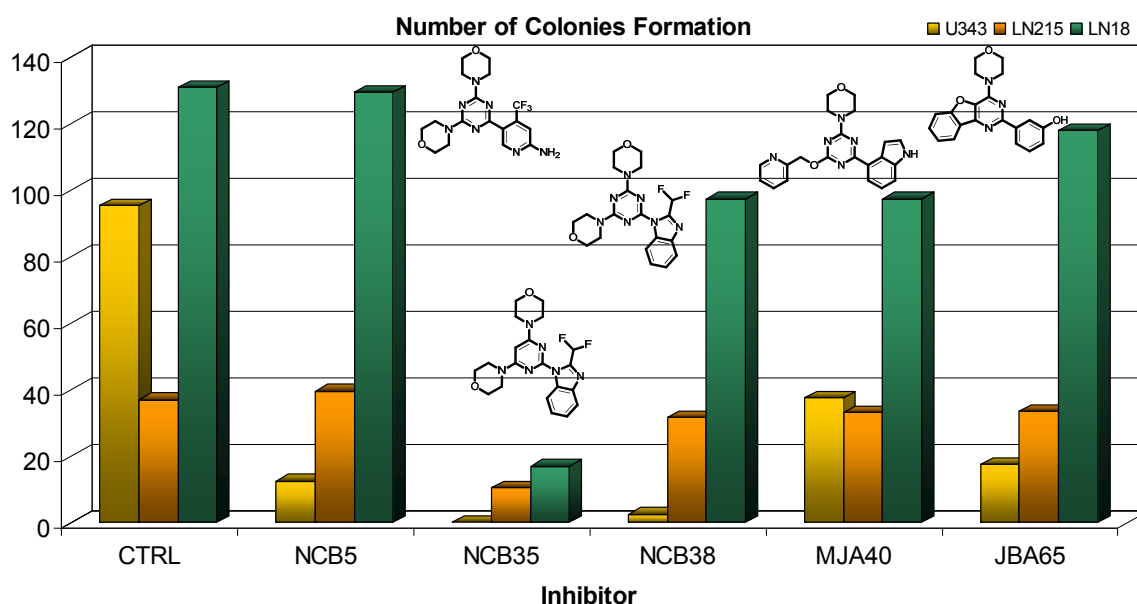
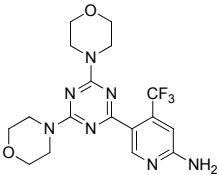
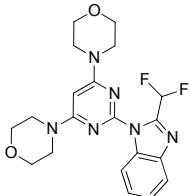
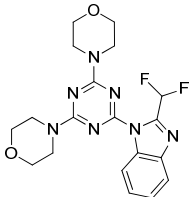
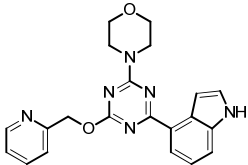
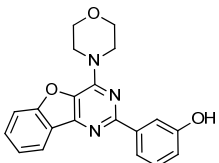


Figure 28. Presented is PI3K inhibition with various PI3K/mTOR inhibitors by reducing the colony formations of LN18, LN215 and U343 malignant glioma cell lines; the smaller the chart bar the better is inhibition.

Table 14. Inhibitor activity^a

Compound	Structure	LN18 Cell line	LN215 Cell line	U343 Cell line
		1 μ M	1 μ M	1 μ M
CTRL	DMSO	131.0 \pm 21.2	37.0 \pm 0.0	95.5 \pm 4.9
(NCB5) 89		129.5 \pm 21.9	39.5 \pm 0.7	12.5 \pm 3.5
(NCB35) 90		17.0 \pm 7.1	10.5 \pm 6.4	0.0 \pm 0.0
(NCB38) 38		97.5 \pm 0.7	31.5 \pm 9.2	2.5 \pm 3.5
(MJA40) 91		97.5 \pm 60.1	33.0 \pm 5.6	37.5 \pm 3.5
(JBA65) 92		118.0 \pm 2.8	33.5 \pm 6.4	17.5 \pm 3.5

^aInhibitor efficacy was measured by in Colony formation assay on malignant glioma cell lines LN18, LN215, U343; the smaller the value, the stronger is the inhibition.

4.4. Triazine and Pyrimidine Derivatives

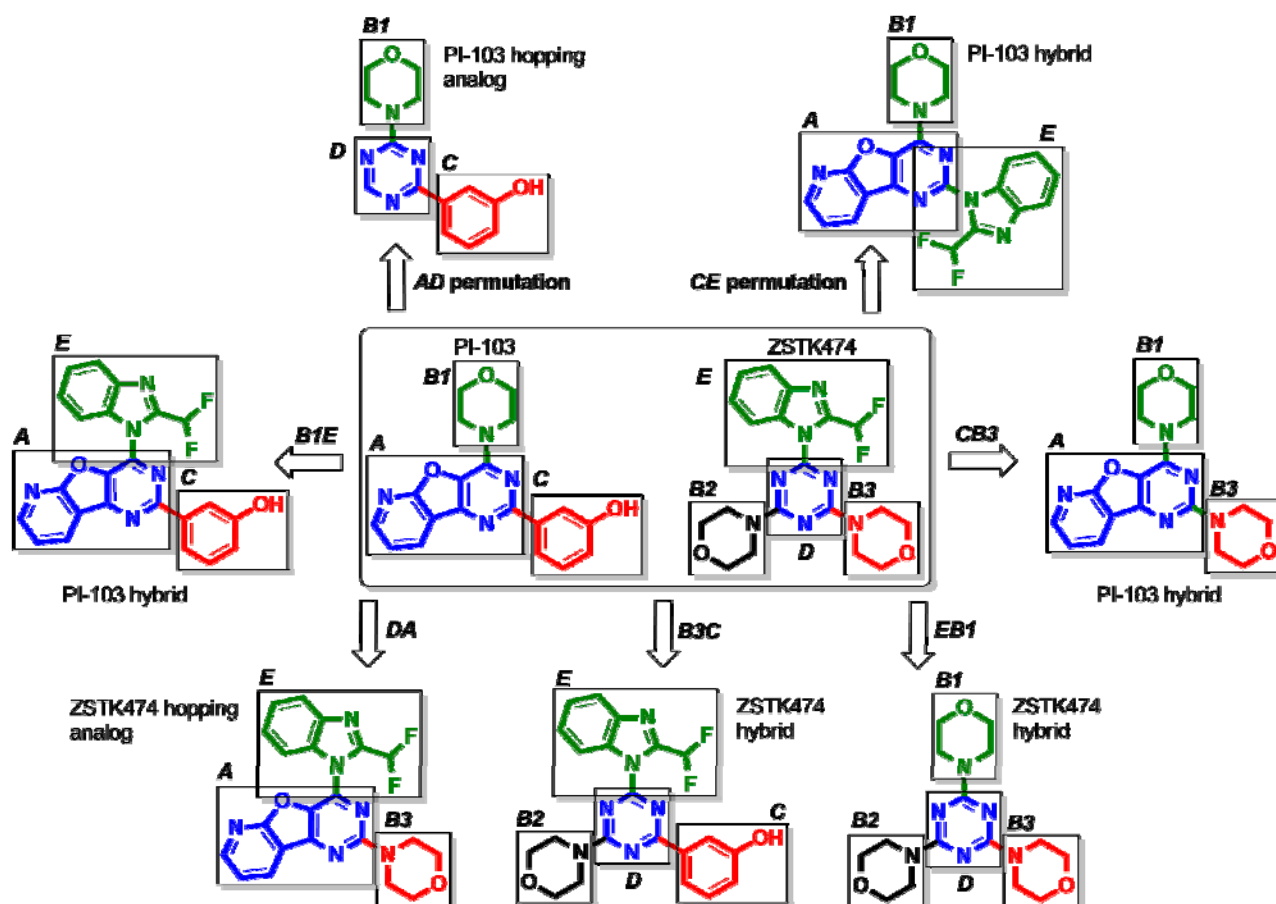
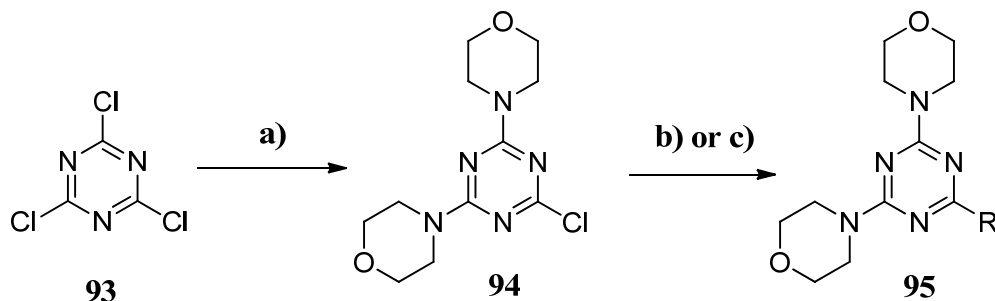


Figure 29. Presented is a strategy where the fragments of the known biologically active chemical compounds are crossed between each other, with the aim to obtain novel so-called hybrid-molecules. This offers the potential to modify existing leads in terms of selectivity, pharmacokinetic properties or side-effect profile. Novel hybrid molecules can be crossed with compounds obtained by crossing of two other PI3K inhibitors, with the aim to gain second generation hybrid molecules. In this example the chemical space of molecules PI-103 and ZSTK474 was rationally extended by applying scaffold hybridizing and scaffold hopping strategies at the same time to provide novel molecules that are not covered by pharmaceutical industry and for which interesting biological properties were obtained. In comparison with the medicinal chemistry examples from the literature, where whether hybridizing or hopping was obtained on a certain single scaffold, we obtained both strategies in a combinatorial way on several different scaffolds

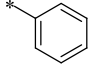
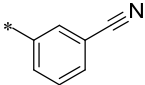
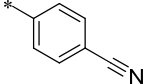
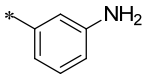
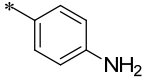
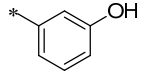
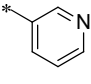
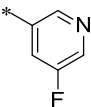
Due to ZSTK474 (**38**) excellent anti tumour activity with low toxicity, triazine scaffolds are of great interest in PI3K research. In order to extend chemical space of ZSTK474 (**38**) in rational way we applied scaffold hybridizing and scaffold hopping strategies at the same time to provide novel molecules that are not covered by pharmaceutical industry with interesting biological properties (Cmiljanovic V. unpublished).

4.4.1. Chemistry and Biology of Di-Morpholine-Containing Triazine and Pyrimidine Derivatives



Scheme 13. Reagents and conditions: a) cyanuric chloride (1.0 eq.), morpholine (4.5 eq.), DMF, 0 °C, 20 minutes, 56%; b) boronic acid pinacol ester (4.0 eq.), 1,2-dimethoxyethane:2M Na₂CO₃ (3:1), dichloro 1,1'-bis(diphenylphosphino)ferrocene-palladium(II)dichloride dichloromethane complex (0.025 eq.), 90 °C, 15 – 20 hours; c) amine (1.1 eq.), DMF, NaH (60% in mineral oil, 1.5 eq.) added at 0 °C, 30 minutes at room temperature, than reflux at 153 °C for 3.5 – 5.5 hours, 13–77 %.

Table 15. Inhibitor activity^a

Compound	R	<i>In vitro</i> PI3K α 200 nM	A2058 cell inhibition		TSC2 ^{-/-} -MEFs cell inhibition
			pPKB/PKB 1 μ M	pS6 1 μ M	pS6 1 μ M
(GSA10) 96		77	61.63 \pm 5.22	115.25 \pm 15.90	106.64 \pm 0.21
(NCA197) 97		68	119.87 \pm 18.25	112.51 \pm 3.16	102.17 \pm 0.89
(NCA201) 98		87	119.10 \pm 6.51	132.37 \pm 7.62	85.45 \pm 0.18
(NCA193) 99		82	121.19 \pm 19.07	74.42 \pm 0.95	88.29 \pm 0.37
(NCA189) 100		76	111.31 \pm 2.12	77.41 \pm 4.32	61.35 \pm 2.29
(NCA183) 101		26	41.11 \pm 5.37	24.12 \pm 2.12	65.29 \pm 4.95
(NCA205) 102		60	84.14 \pm 1.28	109.92 \pm 3.33	79.70 \pm 1.48
(NCB9) 103		97	99.13 \pm 9.83	102.43 \pm 3.00	127.46 \pm 2.04

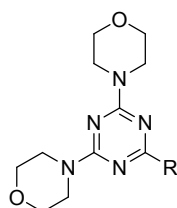


Table 15. Continued

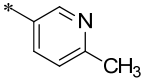
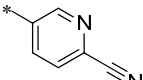
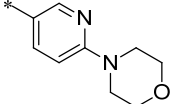
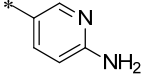
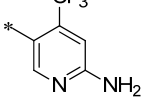
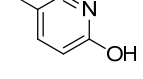
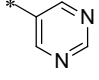
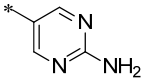
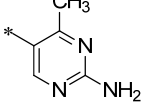
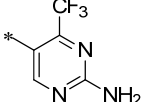
Compound	R	<i>In vitro</i> PI3K α 200nM	A2058 cell inhibition		TSC2-/-MEFs cell inhibition
			pPKB/PKB 1 μ M	pS6 1 μ M	pS6 1 μ M
(NCB90) 104		77	76.90 \pm 4.15	78.29 \pm 8.00	71.30 \pm 2.63
(NCB89) 105		99	84.40 \pm 7.90	105.60 \pm 1.18	107.76 \pm 3.36
(NCA215) 106		97	128.77 \pm 13.96	126.85 \pm 7.06	79.24 \pm 0.46
(NCA163) 107		67	90.95 \pm 21.64	30.03 \pm 1.51	11.71 \pm 2.32
(NCB5/NCB63) 89		20	8.31 \pm 3.13	25.75 \pm 5.92	17.57 \pm 0.95
(MJA47) 108		121	96.82 \pm 5.81	74.93 \pm 1.30	101.63 \pm 6.10
(NCB78) 109		72	78.19 \pm 2.92	105.67 \pm 10.89	86.69 \pm 8.52
(NCB15) 111		11	23.08 \pm 3.07	20.71 \pm 1.06	11.56 \pm 2.81
(NCB86) 112		8	16.29 \pm 7.72	42.32 \pm 4.07	39.77 \pm 3.51
(NCB127) 113		5	2.87 \pm 10.60	26.42 \pm 2.29	42.42 \pm 2.38

Table 15. Continued

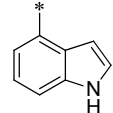
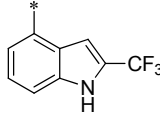
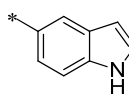
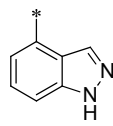
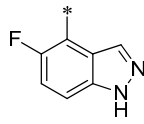
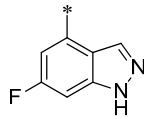
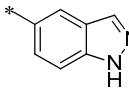
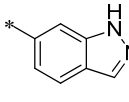
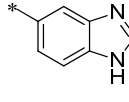
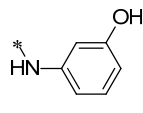
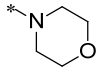
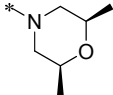
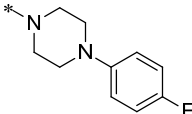
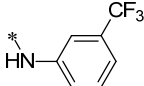
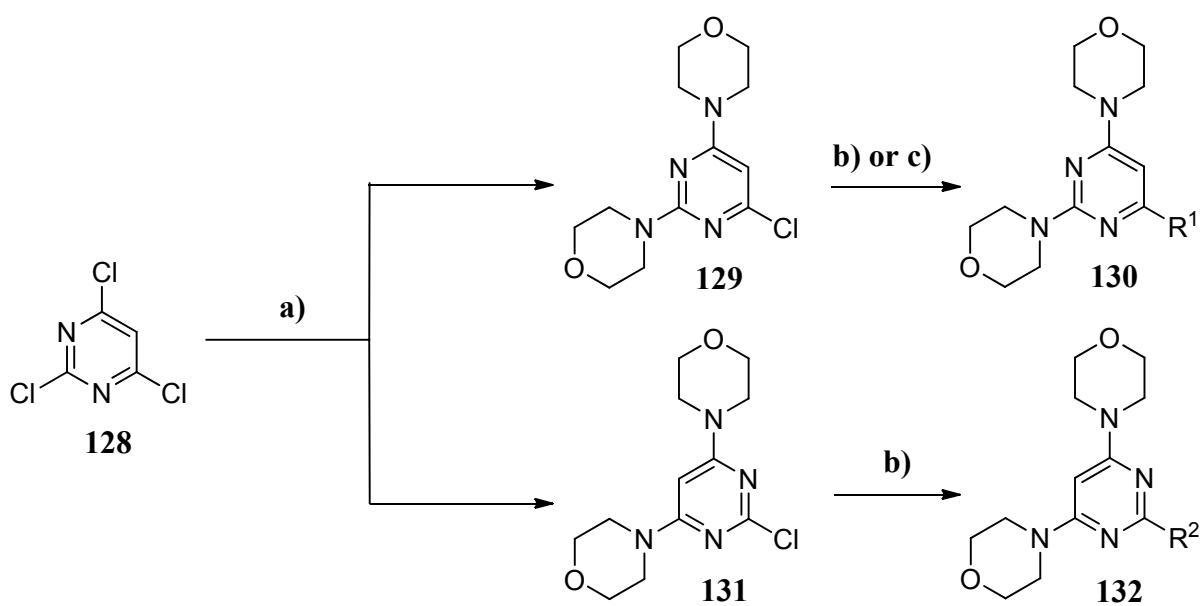
Compound	R	<i>In vitro</i> PI3K α 200nM	A2058 cell inhibition		TSC2 ^{-/-} -MEFs cell inhibition
			pPKB/PKB 1 μ M	pS6 1 μ M	pS6 1 μ M
(MJA7) 114		79	36.99 \pm 1.59	34.15 \pm 4.37	14.14 \pm 3.75
(VVA81) 115		100	90.63 \pm 0.66	137.00 \pm 4.78	73.79 \pm 1.92
(MJA6) 116		110	73.21 \pm 5.03	65.29 \pm 5.79	91.55 \pm 1.48
(MJA46) 117		38	44.13 \pm 2.32	72.60 \pm 2.31	53.40 \pm 6.74
(VVA103) 118		37	91.12 \pm 11.38	168.23 \pm 6.46	88.09 \pm 6.42
(VVA97) 119		26	45.77 \pm 2.00	142.64 \pm 19.21	70.19 \pm 0.77
(NCB22) 120		111	68.71 \pm 6.61	86.46 \pm 3.36	97.61 \pm 0.42
(MJA14) 121		119	93.33 \pm 6.38	59.95 \pm 2.66	99.16 \pm 0.38
(MJA44) 122		61	57.72 \pm 3.91	77.53 \pm 0.32	78.99 \pm 3.86
(BAS01056850) 123		77	64.41 \pm 4.01	103.79 \pm 0.13	85.27 \pm 2.54

Table 15. Continued

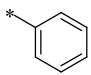
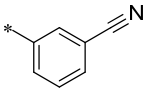
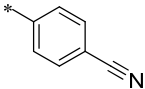
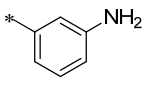
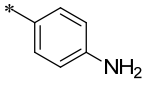
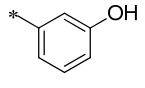
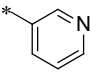
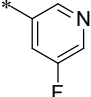
Compound	R	<i>In vitro</i> PI3K α 200nM	A2058 cell inhibition		TSC2 ^{-/-} -MEFs cell inhibition
			pPKB/PKB 1 μ M	pS6 1 μ M	pS6 1 μ M
(MJA12) 124		116	107.02 \pm 1.20	88.20 \pm 4.84	97.58 \pm 2.59
(MJA32) 125		126	96.59 \pm 9.01	125.71 \pm 4.19	95.15 \pm 0.30
(ASN09891537) 126		128	95.69 \pm 4.21	102.09 \pm 4.09	104.33 \pm 0.38
(BAS07354380) 127		103	65.32 \pm 7.97	98.41 \pm 5.85	ND

^aInhibitor efficacy and their cell permeability were measured by *in cell* Western inhibition assay on melanoma cell line A2058 and TSC2^{-/-}-MEFs cell line; *in vitro* PI3K α inhibition was measured by *Kinase Glo* assay and given numbers represent % remaining activity, the smaller the value, the stronger is the inhibition; coloured numbers represent: blue – no activity, green – low activity, red – good activity, orange – very good activity.



Scheme 14. Reagents and conditions: a) morpholine (2.5 eq.), N,N-diisopropylethylamine (3.0 eq.), ethanol, 0 °C to room temperature, 16 hours, mixture of (**129**) and (**131**) (7:1); b) dichloro 1,1'-bis(diphenylphosphino)ferrocene-palladium(II)dichloride dichloromethane complex (0.025 eq.), 90 °C, 15 – 20 hours; c) amine (1.1 eq.), NaH (1.5 eq.), DMF, 153 °C, 4 - 5 hours.

Table 16. Inhibitor activity^a

Compound	R ¹	<i>In vitro</i> PI3K α 200 nM	A2058 cell inhibition		TSC2 ^{-/-} -MEFs cell inhibition
			pPKB/PKB 1 μ M	pS6 1 μ M	pS6 1 μ M
(GSA20) 133		78	74.04 \pm 14.02	107.14 \pm 2.02	96.57 \pm 3.71
(NCA195) 134		85	157.28 \pm 13.05	143.66 \pm 6.36	88.98 \pm 3.51
(NCA199) 135		97	146.71 \pm 36.93	120.45 \pm 1.13	107.80 \pm 5.29
(NCA191) 136		73	143.05 \pm 0.53	95.23 \pm 0.98	95.69 \pm 0.48
(NCA187) 137		87	126.68 \pm 13.33	71.21 \pm 4.76	77.90 \pm 11.04
(NCA185) 138		57	90.82 \pm 16.12	56.23 \pm 1.99	56.53 \pm 4.28
(NCA203) 139		75	109.10 \pm 26.09	97.56 \pm 6.74	97.23 \pm 7.99
(NCB11) 140		117	87.88 \pm 6.55	105.63 \pm 3.28	109.70 \pm 0.28

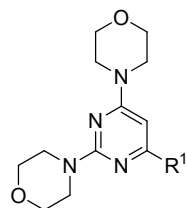


Table 16. Continued

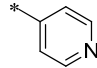
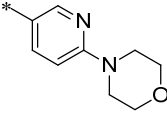
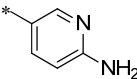
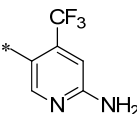
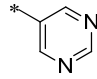
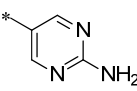
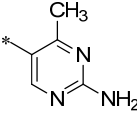
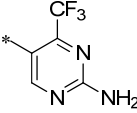
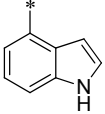
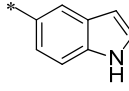
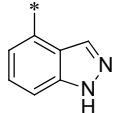
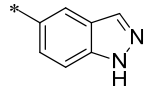
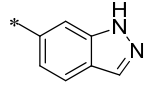
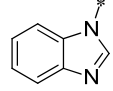
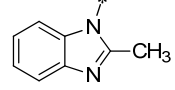
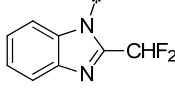
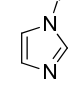
Compound	R ¹	<i>In vitro</i> PI3K α 200 nM	A2058 cell inhibition		TSC2 ^{-/-} MEFs cell inhibition
			pPKB/PKB 1 μ M	pS6 1 μ M	pS6 1 μ M
(NCA207) 141		93	117.11 \pm 10.86	98.41 \pm 7.24	94.96 \pm 7.48
(ASA89) 142		123	97.76 \pm 1.58	91.09 \pm 1.10	99.26 \pm 5.61
(NCA165) 143		51	132.28 \pm 1.49	38.33 \pm 0.60	41.10 \pm 4.80
(NCA235) 144		15	23.74 \pm 7.03	67.78 \pm 9.09	32.31 \pm 7.20
(GSA28) 145		60	74.78 \pm 30.58	115.15 \pm 5.44	120.74 \pm 9.79
(NCB16) 146		18	33.68 \pm 1.06	41.78 \pm 0.60	7.84 \pm 2.31
(NCB115) 147		30	14.34 \pm 7.90	76.72 \pm 16.53	83.58 \pm 0.80
(ND) 148		ND	ND	ND	ND
(NCB20) 149		86	49.07 \pm 1.46	67.19 \pm 1.39	96.16 \pm 3.56
(NCB19) 150		105	70.50 \pm 3.42	57.22 \pm 10.09	47.11 \pm 1.58

Table 16. Continued

Compound	R ¹	<i>In vitro</i> PI3K α 200 nM	A2058 cell inhibition		TSC2 ^{-/-} -MEFs cell inhibition
			pPKB/PKB 1 μ M	pS6 1 μ M	pS6 1 μ M
(GSA21) 151		46	57.25 \pm 5.63	96.08 \pm 4.21	85.71 \pm 1.83
(ASA87) 152		105	80.54 \pm 5.08	88.73 \pm 1.84	99.14 \pm 1.08
(ASA88) 153		114	71.55 \pm 1.31	90.95 \pm 0.45	104.60 \pm 6.17
(NCA169) 146		63	87.15 \pm 7.02	67.68 \pm 5.36	103.83 \pm 2.08
(GSA29) 154		64	106.20 \pm 7.66	107.60 \pm 5.97	87.78 \pm 0.77
(ND) 155		ND	ND	ND	ND
(NCA171) 156		66	137.28 \pm 3.46	74.66 \pm 3.65	93.03 \pm 0.46

^aInhibitor efficacy and their cell permeability were measured by *in cell* Western inhibition assay on melanoma cell line A2058 and TSC2^{-/-}-MEFs cell line; *in vitro* PI3K α inhibition was measured by *Kinase Glo* assay and given numbers represent % remaining activity, the smaller the value, the stronger is the inhibition; coloured numbers represent: blue - no activity, green - low activity, red - good activity, orange - very good activity.

Table 17. Inhibitor activity^a

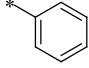
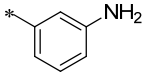
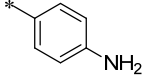
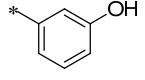
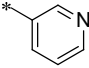
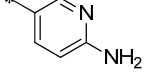
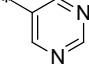
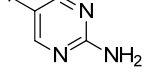
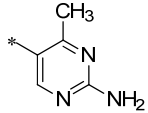
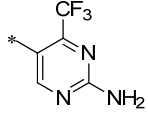
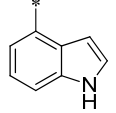
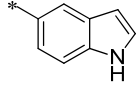
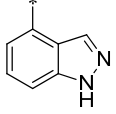
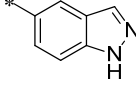
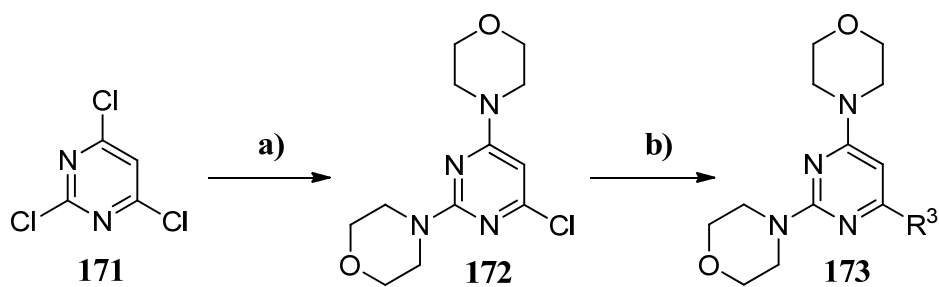
Compound	R ²	<i>In vitro</i> PI3K α 200 nM	A2058 cell inhibition		TSC2-/-MEFs cell inhibition
			pPKB/PKB 1 μ M	pS6 1 μ M	pS6 1 μ M
(GSA22) 157		87	130.19 \pm 11.15	116.52 \pm 3.59	122.11 \pm 8.76
(GSA23) 158		93	111.26 \pm 7.47	108.52 \pm 3.62	87.94 \pm 0.50
(GSA24) 159		84	104.40 \pm 6.52	111.28 \pm 5.70	98.18 \pm 4.37
(VVA105) 160		30	62.15 \pm 2.97	112.42 \pm 0.01	51.94 \pm 7.30
(VVA107) 161		81	65.41 \pm 14.93	63.24 \pm 2.78	113.79 \pm 2.88
(VVA111) 162		63	35.61 \pm 2.61	22.08 \pm 2.06	13.09 \pm 1.49
(VVA109) 163		72	39.15 \pm 1.22	66.39 \pm 4.68	98.66 \pm 2.06
(VVA113) 164		49	29.78 \pm 0.07	63.10 \pm 0.99	62.24 \pm 4.64

Table 17. Continued

Compound	R ²	<i>In vitro</i> PI3K α 200 nM	A2058 cell inhibition		TSC2 ^{-/-} -MEFs cell inhibition
			pPKB/PKB 1 μ M	pS6 1 μ M	pS6 1 μ M
(VVA131) 165		24	33.21 \pm 0.94	24.81 \pm 10.44	112.90 \pm 7.47
(ND) 166		ND	ND	ND	ND
(VVA119) 167		98	41.78 \pm 6.61	15.40 \pm 2.62	37.47 \pm 2.39
(VVA123) 168		91	45.83 \pm 8.24	19.33 \pm 13.69	59.35 \pm 3.33
(VVA117) 169		42	36.31 \pm 0.81	24.14 \pm 6.68	75.14 \pm 4.77
(VVA115) 170		97	54.17 \pm 2.69	34.29 \pm 6.07	85.89 \pm 12.86

^aInhibitor efficacy and their cell permeability were measured by *in cell* Western inhibition assay on melanoma cell line A2058 and TSC2^{-/-}-MEFs cell line; *in vitro* PI3K α inhibition was measured by *Kinase Glo* assay and given numbers represent % remaining activity, the smaller the value, the stronger is the inhibition; coloured numbers represent: blue - no activity, green - low activity, red - good activity, orange - very good activity.

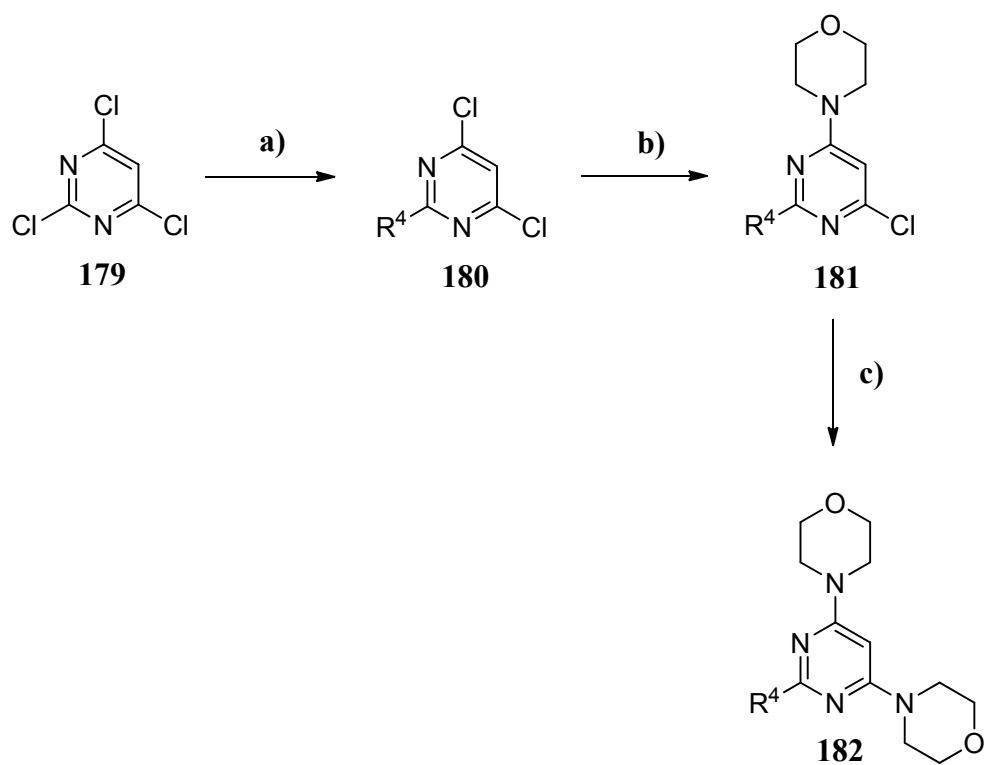


Scheme 15. Reagents and conditions: a) morpholine (2.5 eq.), N,N-diisopropylethylamine (3.0 eq.), ethanol, 0 °C to room temperature, 16 hours; b) amine (28.3 eq.), 80 °C – 120 °C, for 1–21 hours.

Table 18. Inhibitor activity^a

Compound	R ³	<i>In vitro</i> PI3K α 200 nM	A2058 cell inhibition		TSC2 ^{-/-} -MEFs cell inhibition
			pPKB/PKB 1 μ M	pS6 1 μ M	pS6 1 μ M
(ASA102) 174		107	64.82 \pm 1.28	120.92 \pm 2.02	120.21 \pm 8.34
(ASA108) 175		107	58.52 \pm 0.16	113.26 \pm 2.75	111.69 \pm 2.48
(ASA110) 176		123	102.52 \pm 8.91	127.21 \pm 4.04	75.22 \pm 0.26
(ASA109) 177		117	98.77 \pm 3.45	124.52 \pm 2.41	97.40 \pm 5.23
(ASA111) 178		134	95.64 \pm 5.21	119.60 \pm 2.53	129.61 \pm 5.28

^aInhibitor efficacy and their cell permeability were measured by *in cell* Western inhibition assay on melanoma cell line A2058 and TSC2^{-/-}-MEFs cell line; *in vitro* PI3K α inhibition was measured by *Kinase Glo* assay and given numbers represent % remaining activity, the smaller the value, the stronger is the inhibition; coloured numbers represent: blue - no activity, green - low activity, red - good activity, orange - very good activity.



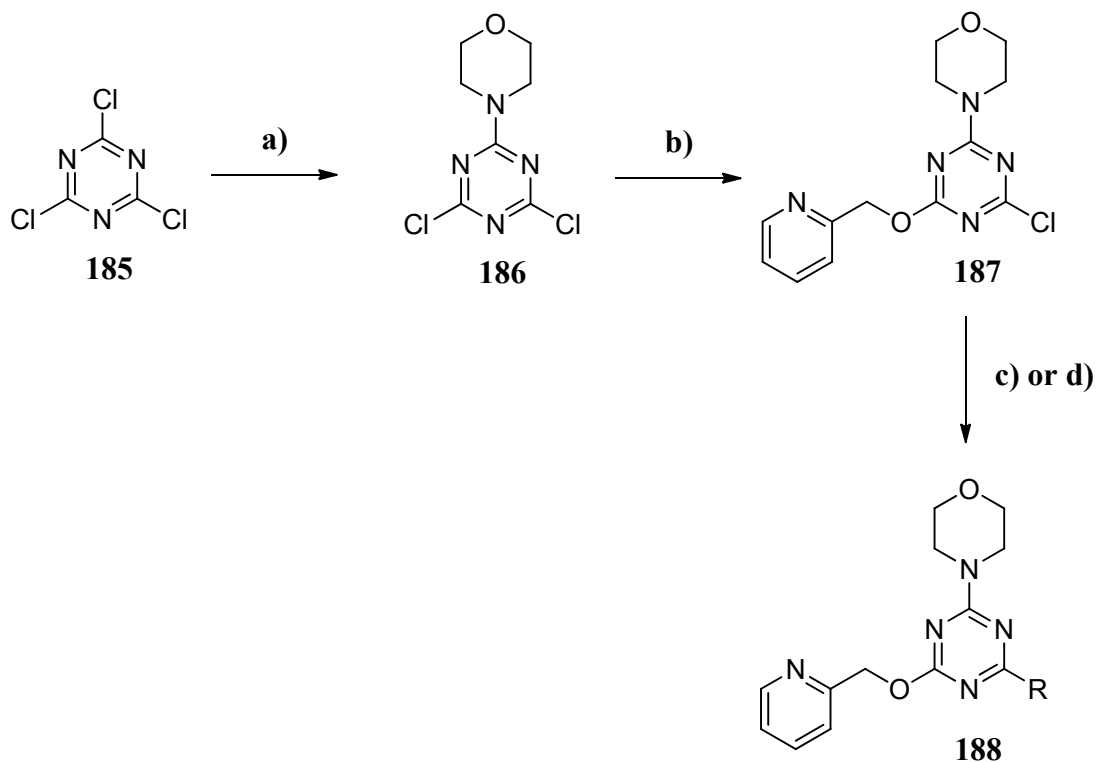
Scheme 16. Reagents and conditions: a) K_2CO_3 (1.74 eq.) and amine (0.9 eq.) added at $-5\text{ }^\circ\text{C}$ in solution of 2,4,6-trichloropyrimidine (**179**) (1.0 eq.) in DMF, stirred for 30 minutes at same temperature and then over night at room temperature; b) K_2CO_3 (2.8 eq.) and morpholine (1.0 eq.) added at $-5\text{ }^\circ\text{C}$ in solution of intermediate (**181**), stirred for 30 minutes at same temperature and then over night at room temperature; c) morpholine (28.3 eq.), $80\text{ }^\circ\text{C}$, 1 - 1.5 hours.

Table 19. Inhibitor activity^a

Compound	R ⁴	<i>In vitro</i> PI3K α 200 nM	A2058 cell inhibition		TSC2 ^{-/-} MEFs cell inhibition
			pPKB/PKB 1 μ M	pS6 1 μ M	pS6 1 μ M
(NCB106) 183		53	38.44 \pm 8.11	99.63 \pm 11.79	80.29 \pm 3.79
(NCB35) 90		11	8.23 \pm 0.85	13.23 \pm 0.37	22.81 \pm 3.31
(NCB34) 184		36	33.26 \pm 2.81	82.25 \pm 4.21	77.55 \pm 5.87

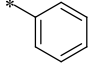
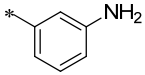
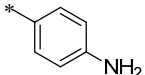
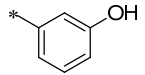
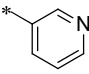
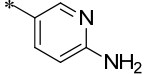
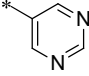
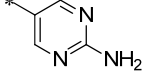
^aInhibitor efficacy and their cell permeability were measured by *in cell* Western inhibition assay on melanoma cell line A2058 and TSC2^{-/-}-MEFs cell line; *in vitro* PI3K α inhibition was measured by *Kinase Glo* assay and given numbers represent % remaining activity, the smaller the value, the stronger is the inhibition; coloured numbers represent: blue - no activity, green - low activity, red - good activity, orange - very good activity.

4.4.2. Chemistry and Biology of Linked Triazine and Pyrimidine Derivatives



Scheme 17. Reagents and conditions: a) morpholine (1.0 eq.), CH_2Cl_2 , $-50\text{ }^\circ\text{C}$, 20 minutes, 28%; b) 2-pyridylcarbinol (1.4 eq.), NaH (1.0 eq.), THF, room temperature, 2 hours; c) dichloro 1,1'-bis(diphenylphosphino)ferrocene-palladium(II)dichloride dichloromethane complex (0.025 eq.), $90\text{ }^\circ\text{C}$, 15 - 20 hours; d) amine (1.1 eq.), NaH (1.5 eq.), DMF, $153\text{ }^\circ\text{C}$, 4 - 5 hours.

Table 20. Inhibitor activity^a

Compound	R	<i>In vitro</i> PI3K α 200 nM	A2058 cell inhibition		TSC2 ^{-/-} -MEFs cell inhibition
			pPKB/PKB 1 μ M	pS6 1 μ M	pS6 1 μ M
(NCB107) 189		86	138.07 \pm 12.35	113.19 \pm 5.13	106.66 \pm 2.10
(NCB108) 190		87	55.36 \pm 12.57	116.60 \pm 15.21	97.90 \pm 5.21
(NCB109) 191		88	100.19 \pm 12.24	94.74 \pm 4.59	87.17 \pm 10.53
(MJA43) 192		51	43.86 \pm 0.45	74.76 \pm 1.49	104.80 \pm 1.00
(MJA39) 193		91	57.14 \pm 0.79	92.21 \pm 0.59	105.93 \pm 1.67
(MJA38) 194		76	56.74 \pm 4.59	104.50 \pm 7.80	103.98 \pm 5.17
(GSA33) (HGA1) 195		89	74.21 \pm 20.31	107.08 \pm 9.85	106.68 \pm 1.64
(MJA37) 196		45	75.02 \pm 5.61	84.14 \pm 4.08	84.29 \pm 9.41

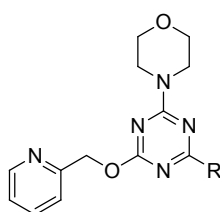
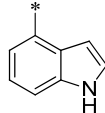
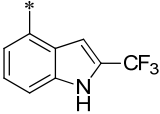
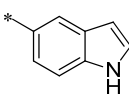
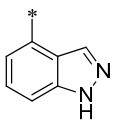
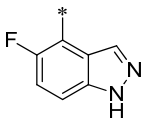
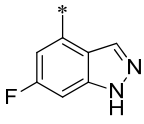
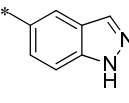
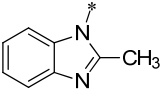
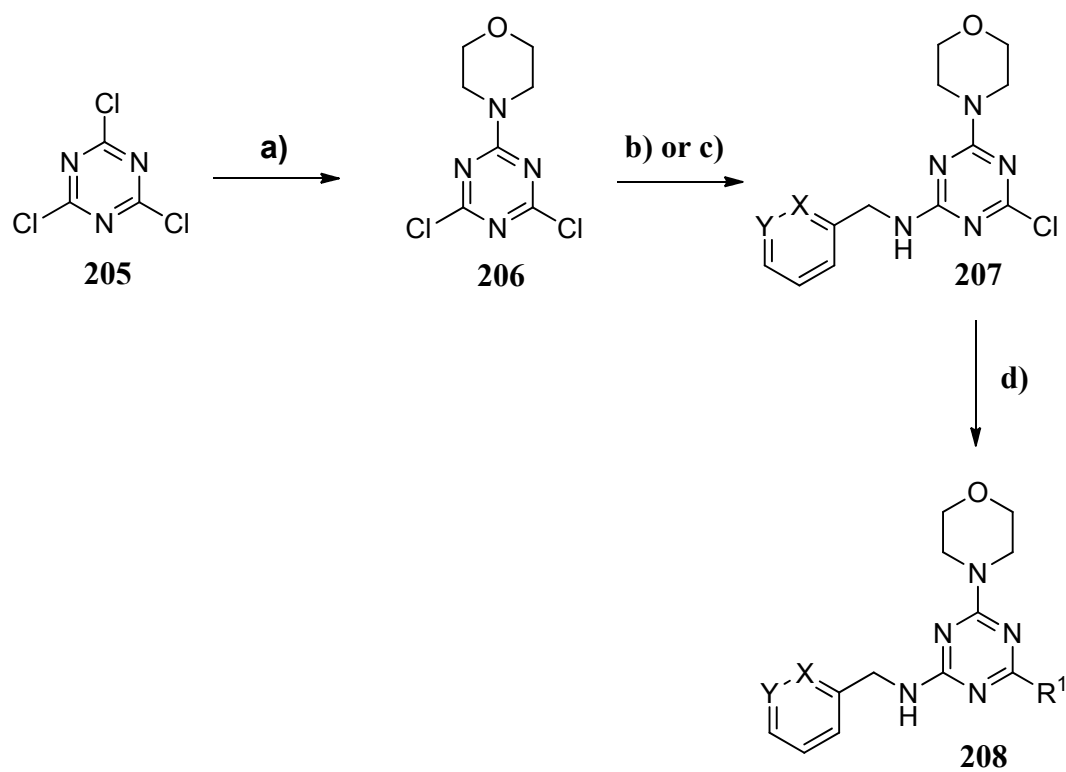


Table 20. Continued

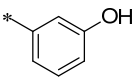
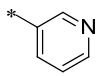
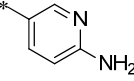
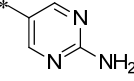
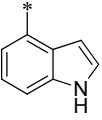
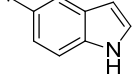
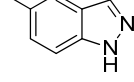
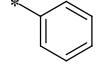
Compound	R	<i>In vitro</i> PI3K α 200 nM	A2058 cell inhibition		TSC2 ^{-/-} -MEFs cell inhibition
			pPKB/PKB 1 μ M	pS6 1 μ M	pS6 1 μ M
(MJA40) 197		65	11.79 \pm 0.10	44.81 \pm 1.23	20.69 \pm 2.06
(VVA77) 198		99	91.18 \pm 4.68	151.85 \pm 5.02	82.12 \pm 1.06
(MJA42) 199		107	68.70 \pm 3.80	77.08 \pm 8.16	64.88 \pm 0.78
(MJA60) 200		84	96.71 \pm 5.30	73.21 \pm 15.57	115.24 \pm 1.64
(VVA101) 201		103	112.93 \pm 3.16	166.84 \pm 13.02	73.96 \pm 5.92
(VVA95) 202		100	109.80 \pm 4.55	159.73 \pm 15.04	86.48 \pm 2.31
(MJA41) 203		100	64.07 \pm 0.51	87.51 \pm 3.84	96.01 \pm 2.41
(GSA31) (HGA2) 204		90	111.22 \pm 0.53	46.84 \pm 2.06	44.42 \pm 13.60

^aInhibitor efficacy and their cell permeability were measured by *in cell* Western inhibition assay on melanoma cell line A2058 and TSC2^{-/-}-MEFs cell line; *in vitro* PI3K α inhibition was measured by *Kinase Glo* assay and given numbers represent % remaining activity, the smaller the value, the stronger is the inhibition; coloured numbers represent: blue - no activity, green - low activity, red - good activity, orange - very good activity.



Scheme 18. Reagents and conditions: a) morpholine (1.0 eq.), CH_2Cl_2 , $-50\text{ }^\circ\text{C}$, 20 minutes; 28 %; b) 2-picolylamine (1.1 eq.), CH_2Cl_2 , room temperature, 21 hours; c) 3-picolylamine (1.5 eq.), CH_2Cl_2 , $-5\text{ }^\circ\text{C}$, 16 hours; d) dichloro 1,1'-bis(diphenylphosphino)ferrocene-palladium(II)dichloride dichloromethane complex (0.025 eq.), $90\text{ }^\circ\text{C}$, 15 - 20 hours.

Table 21. Inhibitor activity^a

Compound	R ¹	X	Y	<i>In vitro</i> PI3K α 200nM	A2058 cell inhibition		TSC2-/- MEFs cell inhibition
					pPKB/PKB 1 μ M	pS6 1 μ M	pS6 1 μ M
(MJA25) 209		N	C	66	67.88 \pm 4.06	118.21 \pm 5.83	117.05 \pm 2.25
(MJA29) 210		N	C	123	96.93 \pm 1.08	151.32 \pm 8.00	83.13 \pm 4.17
(MJA30) 211		N	C	71	79.64 \pm 1.53	140.29 \pm 5.92	75.74 \pm 5.17
(MJA31) 212		N	C	40	76.44 \pm 1.14	62.76 \pm 1.67	79.32 \pm 16.15
(MJA28) 213		N	C	104	74.61 \pm 0.57	142.57 \pm 8.80	76.63 \pm 0.04
(MJA26) 214		N	C	123	90.19 \pm 0.74	129.13 \pm 3.29	77.38 \pm 0.76
(MJA27) 215		N	C	125	97.83 \pm 0.33	148.24 \pm 10.02	73.45 \pm 7.96
(GSA59) (HGA13) 216		C	N	98	99.92 \pm 3.62	120.50 \pm 13.46	94.71 \pm 4.22

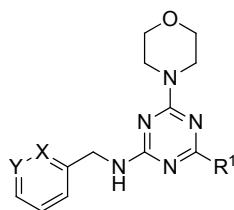
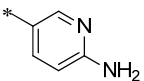
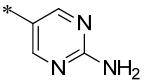
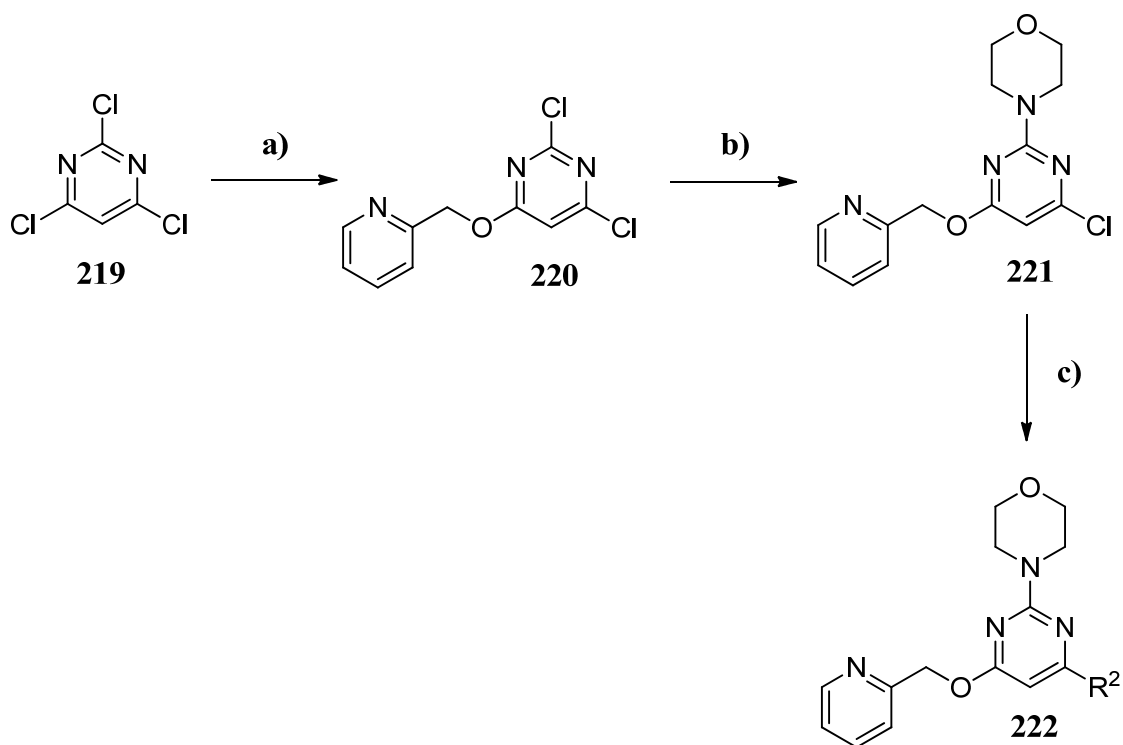


Table 21. Continued

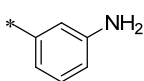
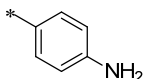
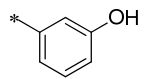
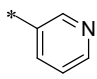
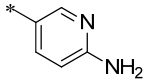
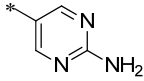
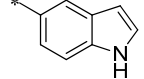
Compound	R ¹	X	Y	<i>In vitro</i> PI3K α 200nM	A2058 cell inhibition		TSC2-/- MEFs cell inhibition
					pPKB/PKB 1 μ M	pS6 1 μ M	pS6 1 μ M
(HGA14) 217		C	N	67	105.56 \pm 15.25	119.55 \pm 20.19	99.75 \pm 2.11
(HGA15) 218		C	N	19	80.92 \pm 7.78	117.41 \pm 4.39	91.39 \pm 0.61

^aInhibitor efficacy and their cell permeability were measured by *in cell* Western inhibition assay on melanoma cell line A2058 and TSC2-/-MEFs cell line; *in vitro* PI3K α inhibition was measured by *Kinase Glo* assay and given numbers represent % remaining activity, the smaller the value, the stronger is the inhibition; coloured numbers represent: blue - no activity, green - low activity, red - good activity, orange - very good activity.

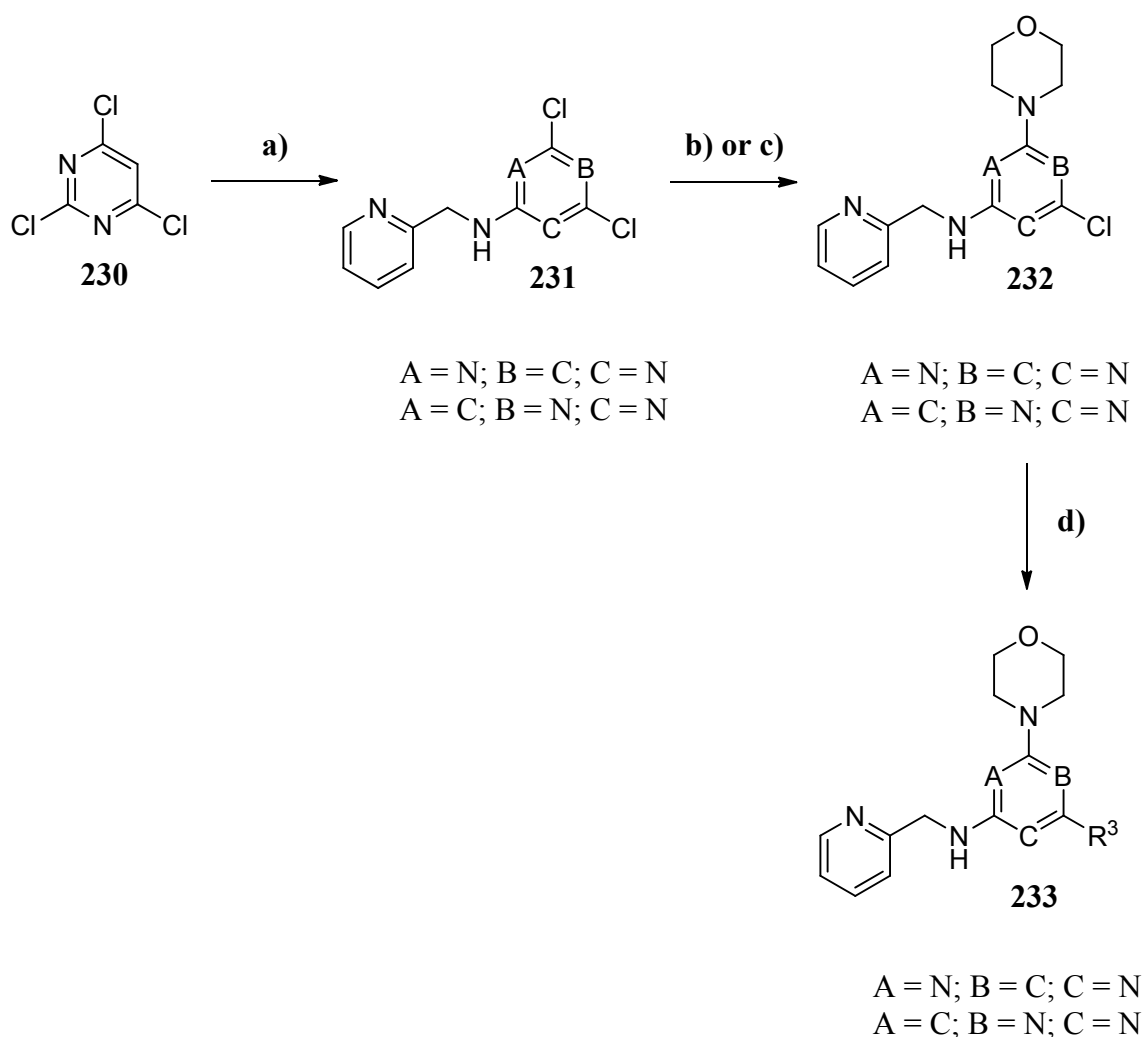


Scheme 19. Reagents and conditions: a) 2-pyridinemethanol (1.0 eq.), NaH (1.0 eq.), THF, room temperature 3 hours; b) morpholine (1.5 eq.), N,N-diisopropylethylamine (1.5 eq.), dioxane, room temperature, 2 hours, c) dichloro 1,1'-bis(diphenylphosphino)ferrocene-palladium(II)dichloride dichloromethane complex (0.025 eq.), 90 °C, 15 - 20 hours.

Table 22. Inhibitor activity^a

Compound	R ²	<i>In vitro</i> PI3K α 200 nM	A2058 cell inhibition		TSC2 ^{-/-} -MEFs cell inhibition
			pPKB/PKB 1 μ M	pS6 1 μ M	pS6 1 μ M
(JBA155) 223		124	92.46 \pm 7.84	93.57 \pm 12.43	111.78 \pm 0.90
(JBA153) 224		127	92.10 \pm 15.18	74.02 \pm 1.70	99.96 \pm 1.22
(JBA139) 225		31	54.80 \pm 3.93	84.43 \pm 1.35	104.26 \pm 3.51
(JBA157) 226		109	104.73 \pm 0.22	80.52 \pm 0.15	104.67 \pm 0.76
(JBA151) 227		66	75.40 \pm 8.44	93.72 \pm 3.60	92.87 \pm 2.84
(JBA149) 228		19	64.73 \pm 14.65	64.75 \pm 2.99	108.29 \pm 9.43
(NCB21) 229		84	83.90 \pm 3.86	71.67 \pm 7.66	85.98 \pm 1.42

^aInhibitor efficacy and their cell permeability were measured by *in cell* Western inhibition assay on melanoma cell line A2058 and TSC2^{-/-}MEFs cell line; *in vitro* PI3K α inhibition was measured by *Kinase Glo* assay and given numbers represent % remaining activity, the smaller the value, the stronger is the inhibition; coloured numbers represent: blue - no activity, green - low activity, red - good activity, orange - very good activity.



Scheme 20. Reagents and conditions: a) 1-aminomethylpyridine (1.1 eq.), N,N-diisopropylethylamine (1.1 eq.), dioxane, room temperature, 2 hours, mixture of JBA113A and JBA113B (2:1); b) JBA113A (1.0 eq.), morpholine (1.8 eq.), N,N-diisopropylethylamine (1.5 eq.), reflux, 5 hours; c) JBA113B (1.0 eq.), morpholine (1.5 eq.), N,N-diisopropylethylamine (1.5 eq.), dioxane, room temperature, 2 hours; d) dichloro 1,1'-bis(diphenylphosphino)ferrocene-palladium(II)dichloride dichloromethane complex (0.025 eq.), 90 °C, 15 - 20 hours.

Table 23. Inhibitor activity^a

Compound	R ³	A	B	C	<i>In vitro</i> PI3K α 200nM	A2058 cell inhibition		TSC2 ^{-/-} -MEFs cell inhibition
						pPKB/PKB 1 μ M	pS6 1 μ M	pS6 1 μ M
(JBA129) 234		C	N	N	103	97.72 \pm 5.43	95.73 \pm 0.37	98.49 \pm 5.99
(JBA141) 235		C	N	N	62	67.50 \pm 6.68	47.41 \pm 1.99	85.89 \pm 0.69
(JBA131) 236		N	C	N	88	101.11 \pm 22.60	68.84 \pm 0.63	109.03 \pm 1.23
(JBA143) 237		N	C	N	123	97.95 \pm 1.12	110.22 \pm 6.70	99.36 \pm 2.53

^aInhibitor efficacy and their cell permeability were measured by *in cell* Western inhibition assay on melanoma cell line A2058 and TSC2^{-/-}-MEFs cell line; *in vitro* PI3K α inhibition was measured by *Kinase Glo* assay and given numbers represent % remaining activity, the smaller the value, the stronger is the inhibition; coloured numbers represent: blue - no activity, green - low activity, red - good activity, orange - very good activity.

4.5. Graphical Overview of the Best Di-Morpholine-Containing and Linked Triazine and Pyrimidine Derivatives

In Cell Western Inhibition and *In Vitro* Inhibition for PI3K α

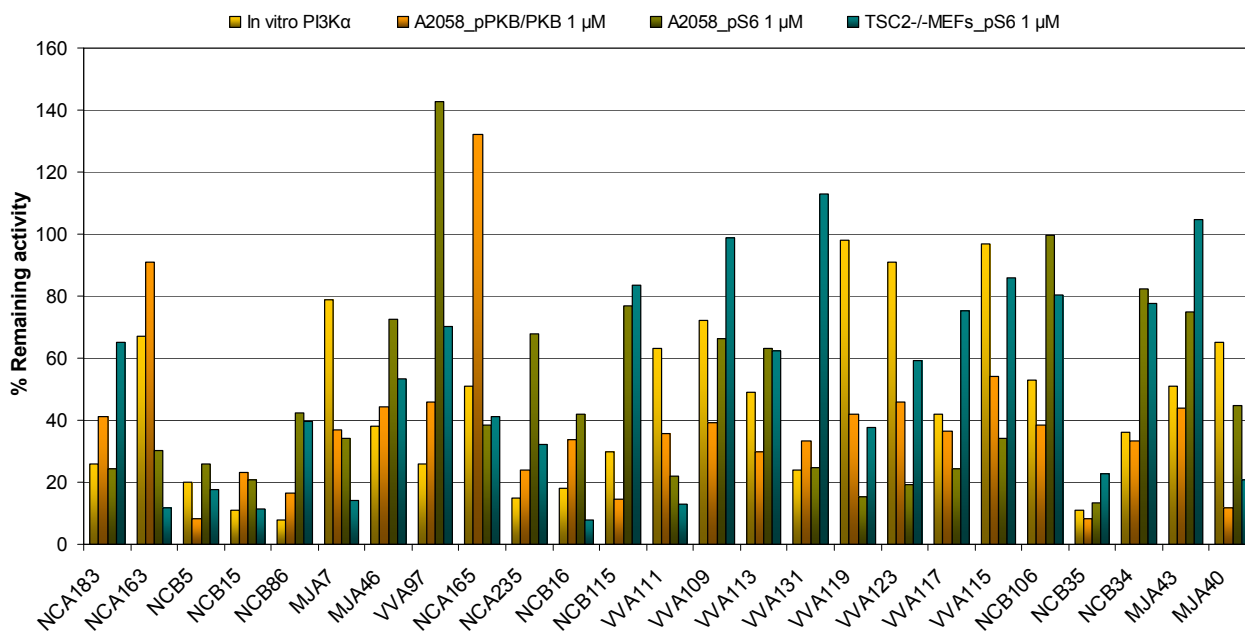


Figure 30. Presented is cellular activity (pPKB/PKB, pS6 on A2058 and pS6 on TSC2-/MEFs) at 1 μ M and *in vitro* activity against PI3K α at 200 nM; the lower the bar chart the better is the activity of the relevant compound.

In Cell Western Inhibition

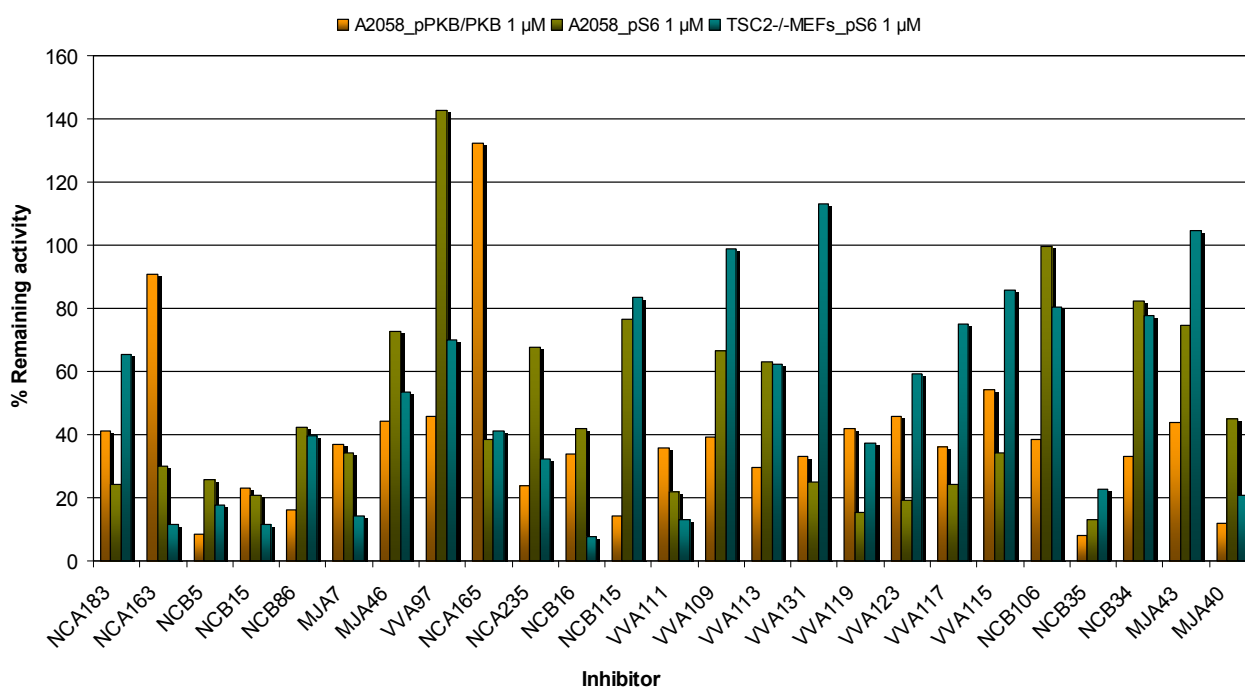


Figure 31. Presented is cellular activity (pPKB/PKB, pS6 on A2058 and pS6 on TSC2-/MEFs) at 1 μ M; the lower the bar chart the better is the activity of the relevant compound.

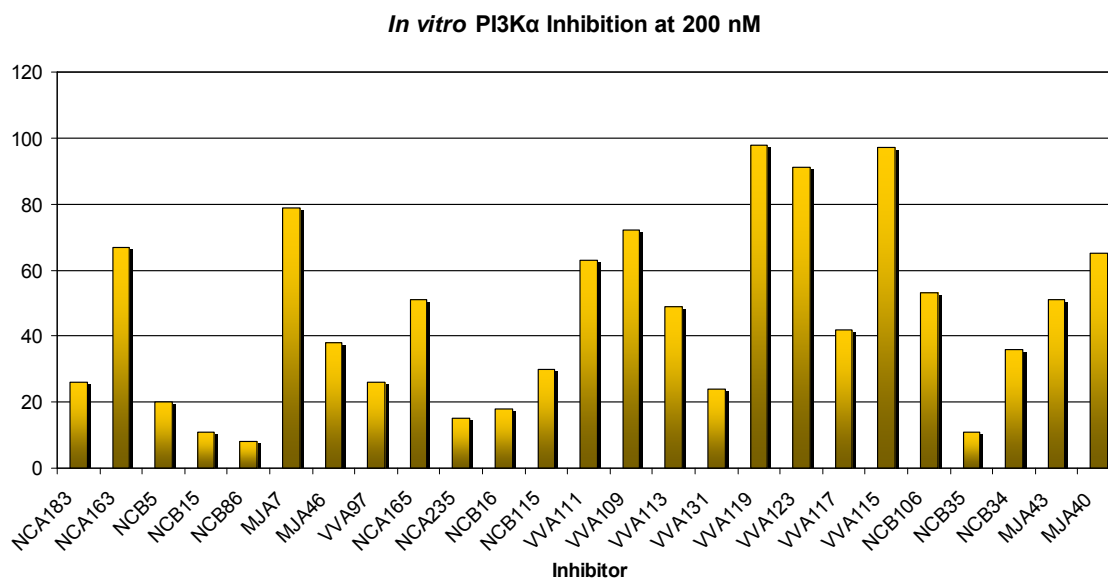


Figure 32. Presented is *in vitro* activity against PI3K α at 200 nM; the lower the bar chart the better is the activity of the relevant compound.

4.6. Crystal Structures of PI3K/mTOR Inhibitors

We have determined the crystal structures of PI3K γ in complex with inhibitors ZSTK474 (**38**), NCB36 (**48**), NCB15 (**111**), NCB5 (**89**), MJA40 (**91**) and ASA76 (for its biological and chemical information see the PhD thesis of Dr. Vladimir Cmiljanovic) (Figure 33). All of the compounds made the key hydrogen bond through the interaction of morpholine oxygen with the backbone amide of the hinge Val-882. The contact list with exact description of amino acids responsible for hydrogen bond formations and for hydrophobic interactions is given in table (see page 100).

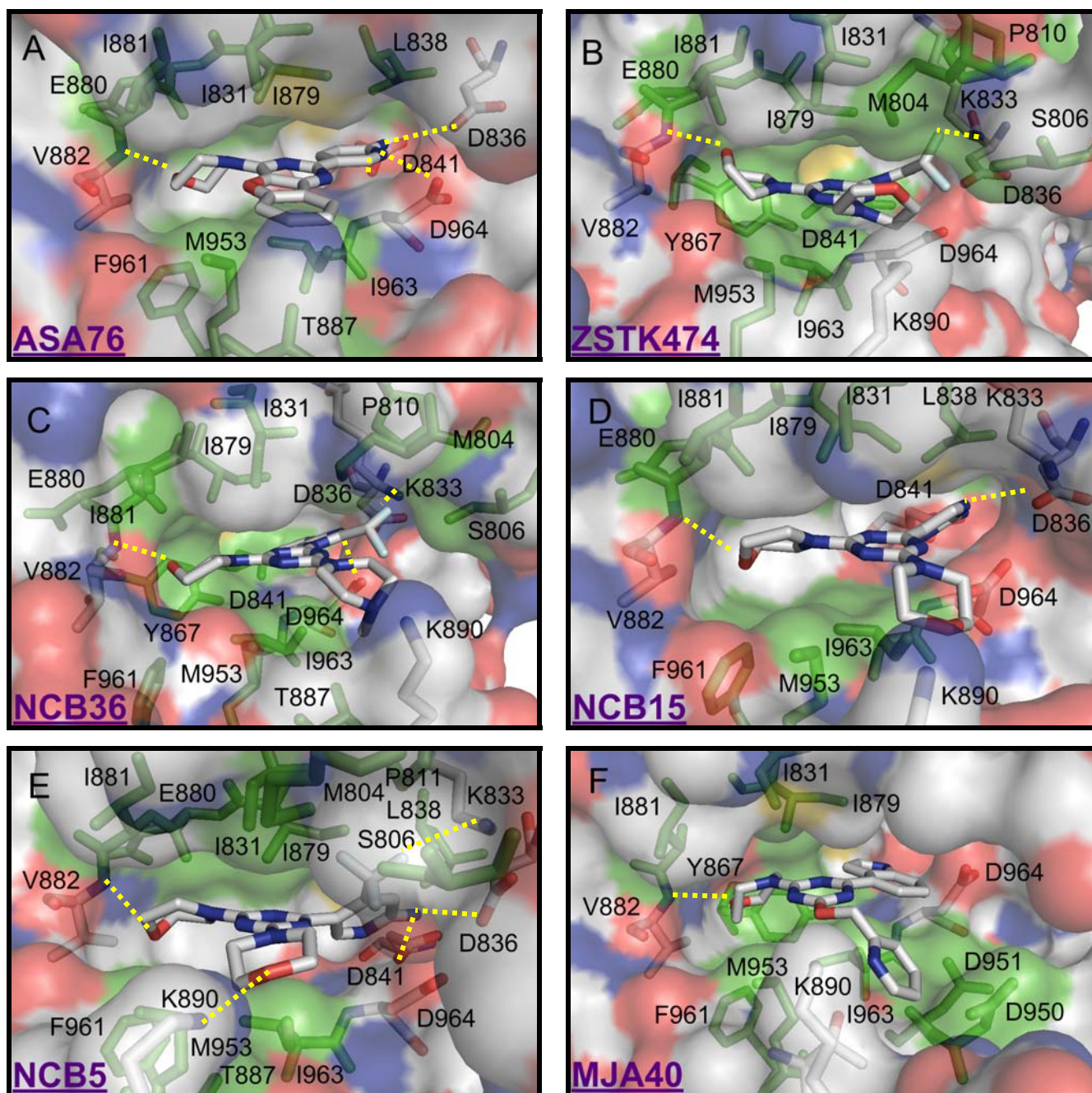


Figure 33. Targeting phosphoinositide 3-kinase (PI3K) with small molecule ATP-competitive inhibitors. (A-F) Surface diagram of ATP-PI3K γ crystal structures zoomed into the ATP-binding site. Amino acids residues and the ligands are represented in stick form, colored according to the element (C atoms in grey, N atoms in blue, O atoms in red and S atoms in yellow). Numbers denote highlighted, prominent side chains mediating PI3K/ligand interactions; in green are colored amino acids for which hydrophobic contacts with the ligand could be obtained. For amino acids such as Asp-836, Asp-841, Glu-880, Val-882, Asp-964, Lys-833, and Lys-890 both hydrophobic contacts and H-bridge formations could be obtained. Only hydrogen bonds that we are confident with are shown as yellow dashed lines. These correspond to the contact list on page 100. For MJA40 there is only density for the morpholino group in contact with Val-882 leading us to the conclusion that MJA40 is not able to reach the binding pocket of PI3K γ ; this observation was comparable with the experimental *in vitro* data and with the *in silico* data by docking MJA40 into PI3K γ .

	isoform			compounds					
mTOR	p110a	p110b	p110d	p110g	NCB5	ASA76	NCB15	NCB36	ZSTK474
Ile2163	Met772	Met779	Met752	Met804	✓			✓	✓
Ser2165	Ser774	Ser781	Ser754	Ser806	✓			✓	✓
Pro2169	Pro778	Pro785	Pro758	Pro810	✓			✓	✓
Leu2185	Ile800	Ile803	Ile777	Ile831	✓	✓	✓	✓	✓
Lys2187	Lys802	Lys805	Lys779	Lys833	✓	H-bond F29	✓	✓	H-bond F30
Glu2190	Asp805	Asp808	Asp782	Asp836	✓	H-bond N21	✓	✓	✓
Leu2192	Leu807	Leu810	Leu784	Leu838	✓	✓	✓	✓	✓
Asp2195	Asp810	Asp813	Asp787	Asp841	✓	H-bond N21	✓	✓	✓
Tyr2225	Tyr836	Tyr839	Tyr813	Tyr867				✓	✓
Ile2237	Ile948	Ile851	Ile825	Ile879	✓	✓	✓	✓	✓
Gly2238	Glu849	Glu852	Glu826	Glu880	✓	✓	✓	✓	✓
Trp2239	Val850	Val853	Val827	Ile881	✓	✓	✓	✓	✓
Val2240	Val851	Val854	Val828	Val882	✓	H-bond O12	✓	✓	H-bond O17
Thr2245	Thr856	Thr859	Thr833	Thr887	✓	✓	✓	✓	✓
Ala2248	Gln859	Asp862	Asn836	Lys890	✓	H-bond O17			✓
Ser2342	Ser919	Asp923	Asp897	Asp950					
Asn2343	Asn920	Asn924	Asn898	Asn951					
Met2345	Met922	Met926	Met900	Met953	✓	✓	✓	✓	✓
Leu2354	Phe930	Phe934	Phe908	Phe961	✓	✓	✓	✓	✓
Ile2356	Ile932	Ile936	Ile910	Ile963	✓	✓	✓	✓	✓
Asp2357	Asp933	Asp937	Asp911	Asp964	✓	✓	✓	✓	✓

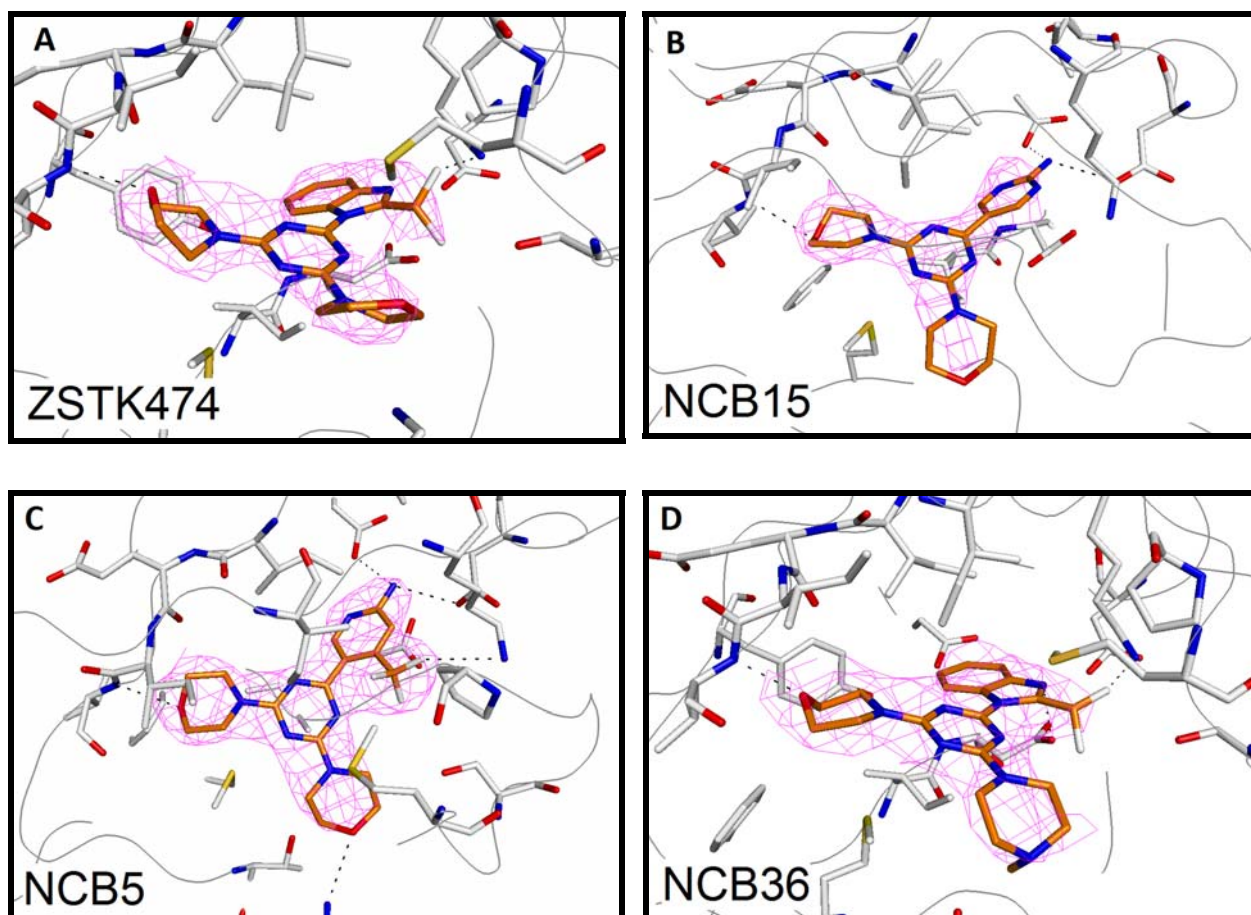


Figure 34. Targeting phosphoinositide 3-kinase (PI3K) with small molecule ATP-competitive inhibitors. (A-D) Extracted amino acids mediating PI3K/ligand interactions within the ATP-binding site; the electron density map of the compounds is presented in magenta mesh. Only hydrogen bonds that we are confident with are shown as black dashed lines.

The available crystal structures of PI3K γ and PI3K α from the Protein Data Bank were used for molecular modelling experiments. Three dimensional model of mTOR was created based upon the crystal structure of p110 γ . The models were constructed as outlined by Pirola et al. [71]. For the docking studies, we used the genetic algorithm application GOLD [72]. Compounds were docked into the crystal structures and homology model by optimizing conformational and non-bonded contacts. The default scoring functions in GOLD are GoldScore and ChemScore; after an initial examination of LY294002 to compare the docked compound in p110 γ to its X-ray structure, we elected to use GoldScore to dock the compounds, which produced nominally better results. Compound orientations using GOLD and GoldScore were generated and saved, and the highest-scoring orientation that also formed plausible hydrogen bond interactions was selected. The docked ligand and receptor structures were subsequently subjected to minimization and dynamics using the program *Yasara* and the *Yamber* forcefield. This was conducted mainly to relieve close contacts

within the protein to the ligand, and to determine whether any of the docked compounds would be “ejected” from the pocket. Minimization and dynamics cycles were performed until the conformations of both the ligand and protein remained unchanged, and none of the docked compounds were “ejected”.

5. Summary and Outlook

By reason of phosphatidylinositol-3-kinase (PI3K) signaling pathway implication in multiple aspects of tumor genesis as well as other diseases, significant efforts have been invested towards developing agents which may inhibit that pathway. These agents (chemical inhibitors) have been extremely helpful tools in verifying PI3Ks as therapeutic targets as well as in understanding the role of PI3K enzymes in signal transduction and downstream physiological and pathological processes.

Physicochemical properties such as solubility, pharmacokinetic and pharmacodynamic are very important alongside potency and selectivity in developing process of a drug candidate suitable for clinical estimation. However, great challenges are present in the creation of specific PI3K inhibitors due to the sequence and structural similarities of the ATP sites in class I PI3K isoforms. Despite these challenges, new inhibitors with surprising selectivity profiles are appearing and helping in revealing of structural determinants that control selectivity across the PI3Ks. At the beginning of PI3K inhibitor development there was a concern that those inhibitors due to their properties might lead to unwanted toxic effects in patients. That was denied by appearance and use of second generation of inhibitors in preclinical and clinical examination. Third generation inhibitors have been already starting to explore the advantages of isoform selectivity, therefore chemical biology and structure-based design approaches should continue to deliver a variety of isoform-specific or pan-selective profiles in order to reduce gaps of knowledge about the specific function of different PI3K isoforms.

6. Experimental Part

6.1. General Work Conditions

All reactions were stirred magnetically in oven-dried glassware and when air-sensitive substances were used, the reaction was performed under inert gas atmosphere. Anhydrous solvents were transferred via syringe or cannula. Acetonitrile, dichloromethane, *N,N*-diisopropylethylamine, dimethoxyethane, dimethylformamide, dioxane, ethanol, methanol, tetrahydrofuran were purchased from Fluka or Aldrich in septum sealed bottles. Diethyl ether was used from the solvent system in Lab. 023a. Technical grade solvents used for extraction and column chromatography were distilled prior to use. Deuterated solvents were purchases from Cambridge Isotope Laboratories and other materials and reagents from Fluka, Acros, Aldrich, Anthem Pharmaceutical Research, Boc Sciences, Boron Molecular, ChemCollect, Fluorochem, Frontier Scientific, Matrix Scientific, Princeton Bio, Strem, Synthonix, TCI Europe or Trylead Chemicals in the highest available grade and used without further purification. Analytical thin layer chromatography (TLC) plates from Merck were used for reaction control (silica gel 60 on aluminium sheets) and chromatographic analyses (silica gel 60 on glass). Silica gel 60 (Fluka) was used for silica gel flash column chromatography.

6.2. Conditions of Measurements

Proton nuclear magnetic resonance (¹H NMR) spectra and **Carbon-13 nuclear magnetic resonance (¹³C NMR)** spectra were recorded on Bruker spectrometers (Avance400: 400 MHz for ¹H and 100 MHz for ¹³C; Avance DRX500: 500 MHz for ¹H and 125 MHz for ¹³C; Avance DRX600: 600 MHz for ¹H and 150 MHz for ¹³C) at ambient temperature in the solvents indicated, and referenced to the residual solvent signal: CDCl₃ (7.26), DMSO-*d*₆ (2.50) or CD₃OD (3.31) for ¹H chemical shifts and CDCl₃ (77.0), DMSO-*d*₆ (39.0) or CD₃OD (49.0) for ¹³C chemical shifts. Chemical shifts are reported in δ (ppm). Coupling constants are reported in Hertz (Hz). The following abbreviations are used: s (singlet), s, br (broad singlet), d (doublet), t (triplet), q (quartet) and m (multiplet). ¹³C NMR spectra were routinely run with broadband decoupling.

Mass Spectrometry Electron Ionization (MS-EI) and **Fast Atom Bombardment (MS-FAB)** spectra were recorded on a VG70-250 (EI) and a MAT 312, using 3-nitrobenzyl alcohol as a matrix (FAB). **Mass Spectrometry Electron Spray Ionisation (MS-ESI)** spectra were recorded in

methanol on a Finnigan MAT LCQ spectrometer. **High Resolution Mass Spectrometry (HR-MS)** was performed by the mass service at the University of Fribourg (CH). Mass signals are given in mass units per charge. The fragments and intensities are given in brackets.

Elemental Analysis (EA) was carried out on a Leco CHN-900 device. The values are given in mass percent.

X-ray analysis of intermediate compounds **NCA131** and **NCA79** are presented by (Figure 35 and 36).

Figure 35. X-ray images of NCA131

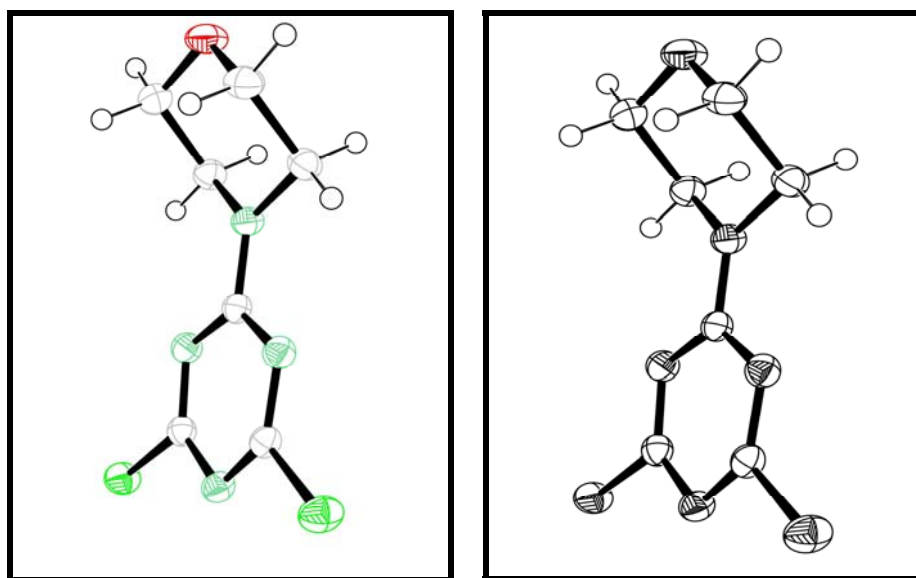
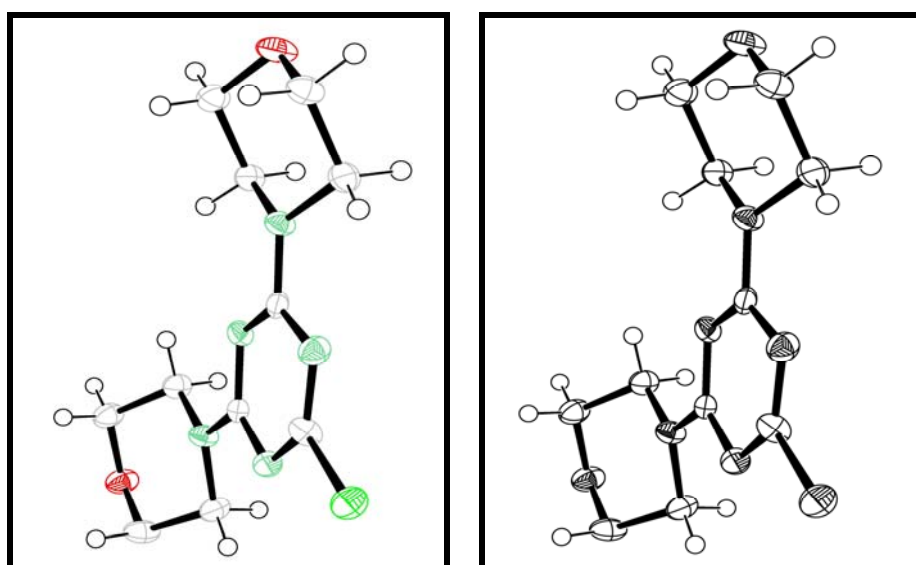


Figure 36. X-ray images of NCA79



6.3. Biological Methods and Parameters

6.3.1. In Cell Western High Throughput Screening Assay

In every part the biological results from *in cell* Western-inhibition high throughput screening assay are given in tables with classifications for PI3K and mTOR inhibition activity. Both activities are listed with inhibitor concentrations of 1 μM and 10 μM . To determine the inhibition activity, cells are incubated with the synthesized inhibitors (dissolved in DMSO). This leads to an inhibition of PI3Ks, so that phosphate group transfer to downstream effectors (e.g. PKB or S6) is reduced or blocked. Inhibition of PI3K results in non phosphorylated downstream effector PKB and inhibition of mTOR in non phosphorylated S6 downstream effector. Specific first antibodies recognize and bind selectively to phosphorylated downstream effectors pPKB (Ser473) or pS6 (Ser235/236). Then fluorescent labeled secondary antibodies (IRDye800 green) bind specifically to the first ones and the emitted fluorescence of these secondary antibodies can be measured. The stronger the fluorescence, the higher the concentration of binded first antibodies to phosphorylated downstream effectors and the weaker the activity of the inhibitor.

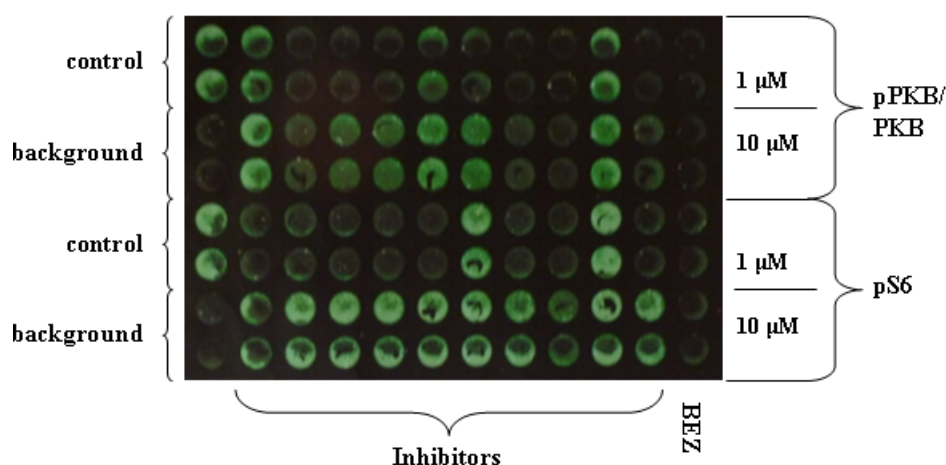


Figure 37: The 96-well-View Plate seen through 800nm wavelength with cells and synthesized inhibitors, which were incubated with the secondary antibody IRDye800 (green) for pPKB and pS6 amount. The pPKB/PKB and pS6 control windows are an assembly of cells, specific first antibodies and fluorescent labelled secondary antibodies (IRDye800). Therefore these control windows are giving the highest possible fluorescent intensity and this measured value is normalized to 1. The background windows are only composed of cells and secondary antibodies for pPKB and pS6, while no primary antibodies are in the background windows. These windows show undesirable fluorescent signals of secondary antibodies reacting directly with the cell. This resulting value is subtracted from the measured values. The

first two columns give the fluorescent intensity with a 1 μ M concentration of the synthesized inhibitor, the third and fourth column give the fluorescent light intensity for a 10 μ M concentration of the same inhibitor. From these two values the mean value is formed. In the same concentrations are divided the last four columns for pS6. Compound BEZ235 (Novartis) is an excellent PI3K inhibitor and is used as a reference inhibitor. For more accurate results, an additional secondary inhibitor for PKB (IRDye680) (red) is used. Through scanning at 600 nm the amount of PKB in cells can also be measured and by forming the ratio of pPKB and PKB values, variability due to cell amount can be eliminated. For pS6 there no corresponding method found and just the amount of pS6 is measured.

Protocol for Phospho-PKB/PKB Detection on A2058 Melanoma

Inhibitor efficacy was measured by a cell assay employing the following protocol:

Cells were plated in black 96 well view plates (Packard) 24 hours prior to the experiment. Inhibitor or DMSO as control were added to the medium (each sample as duplicates) and incubated for 3 hours. Para-formaldehyde, 4%, was applied for 20 minutes at room temperature to fix the cells. After washing with PBS/ 0.1% Triton/X-100, blocking with 10% goat serum in PBS was done for 1 hour. On a shaker, antibodies diluted in PBS against pPKB Ser473 (Cell Signalling) and PKB (gift from E. Hirsch) or pS6 Ser 235/236 (Cell Signalling) were incubated overnight at 4°C. After washing with PBS, secondary antibodies (LI-COR) diluted in PBS were applied at room temperature in the dark. Plates were washed with PBS prior to scanning on an Odyssey reader.

Day 0

1. Plate 80'000 cells /well in a black Packard 96 well ViewPlate.
2. Pipette with the multi channel pipette 200 μ l of cell suspension per well.
3. Check under the microscope the homogeneity of the plating.
4. Incubate cells 24 hours

Day 1

1. Carefully throw away the medium and refill the wells with 100 μ l of medium.
Check under the microscope for cell loss.
2. Add 1 μ l of 100x concentrated DMSO or Inhibitor.
3. Incubate for 3 hours at 37°.
4. Add 60 μ l para-formaldehyde 10% (final 4%) and incubate at room temperature for 20 minutes.
5. Wash 3 times 5 minutes with (200 μ l) PBS/ 0.1% Triton/X-100.
6. Block 60 minutes with (100 μ l) of 10%FCS in PBS at room temperature.
7. Incubate over night with 50 μ l pPKB Ser473 (1:500) and PKB (1:500) or pS6 Ser 235/236 (1:500) in PBS at 4°C on a shaker.

Day 2

1. Wash 3 times 5 minutes with PBS.
2. Incubate 60 minutes with 50 µl secondary antibody anti-rabbit IRDye800 (1:800) and anti-mouse IRDye680 (1:500) in PBS at room temperature in the dark on a shaker.
3. Wash 3 times 5 minutes with PBS.
4. Read the plate on an Odyssey reader.

Reagents

- Packard ViewPlate (black) #6005225
- Anti-Phospho PKB Ser 473 (Cell Signaling cat. 4058)
- Anti-PKB (gift from E. Hirsch, Torino)
- Anti-pS6 Ser235/236 (Cell Signaling cat. 4856)
- Goat anti-Rabbit-IRDye 800 CW (LI-COR cat. 926-32211)
- Goat anti Mouse- IRDye 680 (LI-COR cat. 926-32220)

The higher the phosphorylation in PKB as measured with the Odyssey scan, the higher the pPKB/PKB values were indicating lower strength of inhibition of signalling. Assessment of compound permeability was indirectly extrapolated by using this assay. The compounds were applied to the apical surface of cell monolayers and compound permeation into the cellular compartment could be extrapolated by measuring the inhibition of PI3Ks.

6.3.2. Kinase Glo Luminescent Assay**Reagents and Solutions****Kinase Buffer**

For 20ml:

200 µl 1 M Tris HCl pH 7.5 (10 mM final concentration)

60 µl 1 M MgCl₂ (3 mM final concentration)

500 µl 2 M NaCl (50 mM final concentration)

100 µl 10% CHAPS in H₂O (0.05% final concentration) (prepare the day before)

200 µl 100 mM DTT in H₂O (1 mM final concentration)

18.94 ml H₂O

Phosphatidylinositol Solution (PI) (2x PI=20 µg/ml)

L-alpha-phosphatidylinositol (from liver bovine) stock 1 mg/ml in CHCl₃ from Sigma Cat# P-2517 200 µl 1 mg/ml PI are dried with nitrogen gas in glass tube (clean and dry with EtOH before adding PI) and resuspended in 200 µl 3% Octylglucoside (prepared in H₂O the day before!). Then 9.8 ml of kinase buffer is added. The lipids are stored in a glass tube at 4 °C for 2-3 weeks. Final concentration per well 10 µg/ml.

ATP Solution (2x ATP=2 µM)

6.7 µl 3 mM ATP (from Roche cat# 10519979001) in H₂O are resuspended in 10 ml of kinase buffer. Final concentration per well 1 µM.

PI3K Solution

PI3K α EMV BV1075, MW=138kDa, conc. 12,3 µM / 0.32 mg/ml

PI3K δ EMV BV1060.1698, MW=134.5kDa, conc. 35.1 µM / 4.72 mg/ml

Dilute the kinases in PI solution at the following concentrations:

20 nM PI3K α , final concentration per well 10 nM

5 nM PI3K δ , final concentration per well 2.5 nM

Kinase Glo from Promega

10x10 ml cat# V6712

Procedure

Pipet 25 µl of the desired PI3K solution in each well of a 96 well plate (white microplate). In 2 wells add only 25 ml buffer. Add 1 ml of the inhibitors at the following concentrations: 51.2 mM (final 2.048 mM), 6.4 mM (final 256 nM), 1.6 mM (final 64 nM), 400 nM (final 16 nM), 100 nM (final 4 nM) and 25 nM (final 1nM). Carefully tap at the plate to mix and incubate the plate at room temperature for 30 minutes.

Add 25 µl of the ATP solution per well to start the kinase reaction. Carefully tap at the plate to mix and incubate it at room temperature for 30 minutes.

Then add of 50 µl kinase Glo to start the luciferase reaction. Incubate 10 minutes at room temperature and then read the plate with the Syngery 4.

6.3.3. *In cell* Western Inhibition Assay on Bone Marrow Derived Mast Cells

Bone marrow derived mast cells (BMMC) were serum-starved and IL-3 depleted for 3 hours (this is to eliminate any pPKB signals in the unstimulated cells) and kept in 24 wells of a 24 well plate (37 °C, 5% CO₂). After 2 hours the inhibitors or DMSO were added to the wells, mixed and incubated for another hour. Subsequently cells were stimulated with PBS (first lane) or with Adenosine (highly PI3Kgamma specific, for 2 min., 37 °C). Stimulation was stopped on ice, the cells collected, washed in PBS and lysed for SDS-PAGE. Proteins were separated by SDS-PAGE, blotted onto PVDF membranes. Proteins were then detected by immunological detection. pThr308 reflects PI3K activity PKB (total) confirms equal loading of protein in each sample.

6.3.4. Covalent PI3Kγ Inhibitors

Material

- Recombinant PI3Kgamma-[His₆] , 340 ng/ml (from Romy), remove only from -20°C immediately before taking the aliquots, freeze immediately again
- DMSO
- Inhibitors dissolved in DMSO (1mM and 0.1mM in DMSO of NCB147, GSA100, NCB145_1, NCB141, NCB144_2, NCB38)
- 100mM ATP in H₂O
- 200μM and 20μM Wortmannin in DMSO
- 1x PBS throughout Experiment 1 or 1x PBS + 0.1% NP-40 throughout the Experiment 2
- 2x and 5x Sample buffer

Experimental Procedure

- Thaw inhibitors and ATP solution
- Prepare and label all eppendorf tubes required
- Adjust Thermoblock to 37°C
- Fill ice bucket

Competition Assay

1. Pipette inhibitors (0.5 μ l) or ATP (1 μ l) into the labeled 1.5 ml eppendorf tubes and add to 2 tubes DMSO.
2. Transfer 500 μ l PBS (\pm 0.1% NP40).
3. Add 15 μ l recombinant, mix.
4. Distribute 50 μ l into the tubes, containing DMSO, inhibitors or ATP, mix.
5. Lock tubes and place on the Thermoblock, shake for 30 minutes at 37 $^{\circ}$ C.
6. Place tubes on ice.
7. Add to one tube with DMSO only 0.5 μ l DMSO (no Wortmannin, required as control).
8. Add to all the others 0.5 μ l Wortmannin (20 μ M).
9. Incubate for 15 minutes on ice and mix every 2 minutes by snipping with the fingers.
10. Add 10 μ l 5x sample buffer and heat to 95 $^{\circ}$ C for 7 minutes.
11. Store at -20 $^{\circ}$ C, or directly perform SDS-PAGE, WB.

Covalent Binding Assay

1. Wash 90 μ l Ni-NTA beads (Qiagen) in 1 ml PBS (\pm 0.1% NP40) for each reaction (thus 9 x 1.5 ml eppendorf tubes are required).
2. Pellet Ni-NTA beads by centrifugation (4 $^{\circ}$ C, 3 minutes, 1000g).
3. Aspirate supernatant.
4. Repeat washing step once.
5. Add 1 ml PBS to the beads.
6. Add 4.5 μ l recombinant PI3K γ -[His₆] to the tubes.
7. Pipette inhibitors (10 μ l) or ATP (20 μ l) into the labeled 1.5 ml eppendorf tubes. Add to 2 tubes DMSO.
8. Mix by inverting several times, so that the beads are equally distributed.
9. Lock tubes and place on the Thermoblock, shake (1200 rpm) for 45 minutes at 37 $^{\circ}$ C, remove tubes regularly and invert repeatedly to redistribute the beads (avoid sedimentation).
10. Pellet Ni-NTA beads and the coupled PI3K γ -[His₆] by centrifugation (4 $^{\circ}$ C, 3 minutes, 1000g).
11. Aspirate supernatant.
12. Add 1 ml PBS, and invert the tubes several tubes.
13. Shake for 5 minutes on the Thermoblock (1200 rpm, while Thermoblock cools to 4 $^{\circ}$ C).

14. Repeat these steps (starting from the centrifugation) 3x.
15. Place tubes on ice.
16. Add 1 ml PBS to the tubes.
17. Add to one tube with DMSO only 1 μ l DMSO (no Wortmannin).
18. Add to all the others 1 μ l Wortmannin (200 μ M).
19. Incubate for 15 minutes on the Thermoblock (now 4 °C, 1200 rpm) and invert tubes regularly as before.
20. Pellet Ni-NTA beads and the coupled PI3K γ -[His₆] by centrifugation (4 °C, 3 minutes, 1000g).
21. Aspirate supernatant.
22. Add 60 μ l 2x Sample buffer.
23. Heat to 95 °C for 7 minutes.

SDS-PAGE, WESTERN BLOTTING, IMMUNOLOGICAL DETECTION

Usage of Antibodies

Anti-Wortmannin (Waldi), 1:2000 in 5% skim milk TBST, 1h, RT

Goat anti Rabbit- HRP coupled, 1:5000 in 5% skim milk TBST, 1h, RT

- CUTTING OF THE GEL OR THE MEMBRANE BELOW THE 94 kDA MARKER STRONGLY REDUCES THE BACKGROUND SIGNAL DUE ELIMINATION OF KERATIN BANDS
- LONG WASHING INTERVALLS ARE HELPFUL FOR NICE FILMS

6.3.5. Colony Formation Assay

For each cell line, 500 cells were plated in duplicates into 25-cm² cell culture flasks containing 10 ml of culture medium with 10% FCS with or without different PI3K inhibitors. Cells were grown for 14 days at 37°C and 5% CO₂. The medium was renewed at day 7. Cells were then fixed with 4% formaldehyde in 1x PBS and stained with crystal violet.

Reagents

- Cell culture media: DMEM (Invitrogen), supplemented with 10% FCS (LabForce)
- Nunc Flasks Nunclon™ Δ with Vent/Close Cap. Cat no: 163371

6.4. Crystallization and Inhibitor Soaks

Δ ABDp110 γ crystals were obtained by the sitting-drop vapour diffusion method at 17°C in the presence of 16% PEG 4000, 250mM (NH₄)₂SO₄ and 100mM Tris pH7.5. The crystals reached their maximum size (0.2 mm × 0.1mm × 0.1mm) in about 10 days.

The inhibitors NCB5, NCB15 and NCB36 were prepared in DMSO and diluted in cryoprotectant containing 25% PEG 4000, 15% glycerol, 250mM (NH₄)₂SO₄ and 100mM Tris pH7.5 to a final concentration of 1mM. The inhibitor MJA40 was prepared in DMSO and diluted in cryoprotectant consisting of 20% PEG 4000, 20% DMSO, 250mM (NH₄)₂SO₄ and 100mM Tris pH7.5 to a final concentration of 1mM. The inhibitor in cryoprotectant solution was added to the drop containing the crystals in a stepwise manner. The crystals were soaked in the final 1mM inhibitor solution for 3 hours (MJA40), 4 hours (NCB15, NCB5, NCB36) or 16 hours (ZSTK474). Crystals were then transferred to fresh inhibitor in cryoprotectant solution for 30 seconds and flash frozen in liquid nitrogen.

6.4.1. Data Collection and Structure Determination

Diffraction datasets were collected at the ESRF beamlines ID23-1 and ID29. Images were processed using Mosflm [73] or XDS [74] and scaled with SCALA [75].

The crystal structure of Δ ABDp110 γ /NCB5 complex was solved by molecular replacement using Phaser [76] with the previously published human Δ ABDp110 γ as the search model (PDB entry 1E8Y) and subsequently refined using Refmac [77]. Coot was used to manually build inhibitors in the unaccounted Fo-Fc difference electron density within the active site of the map [78]. Initial models of the inhibitors were generated using the PRODRG server (<http://davapc1.bioch.dundee.ac.uk/prodrg>) [79]. Refmac refinement was iterated with manual rebuilding using Coot until the structure converged.

Compound	NCB5	ASA76	MJA40	NCB15	NCB36	ZSTK474
PDB entry	****	****	****	****	****	****
Data Collection						
Wavelength (Å)	1.0072	0.9395	0.9395	1.0000	1.0000	0.9395
Spacegroup	C2	C2	C2	C2	C2	C2
Unit cell dimensions						
a, b, c (Å)	139.03, 67.22, 103.24	143.28, 67.29, 106.47	143.70, 67.47, 106.59	140.35, 66.96, 103.09	141.24, 67.11, 104.83	144.31, 67.73, 107.31
α, β, γ (°)	90.00, 96.94, 90.00	90.00, 95.74, 90.00	90.00, 95.73, 90.00	90.00, 96.40, 90.00	90.00, 96.21, 90.00	90.00, 95.03, 90.00
Resolution (Å)	60.44-2.66	40.83-2.70	35.62-2.43	61.20-2.90	61.43-3.20	71.88-2.69
% completeness (last shell)	98.3(97.2)	97.6(99.0)	99.4(100.0)	99.6(99.4)	99.4(99.3)	89.7(93.8)
R_{merge} (last shell)	0.065(0.468)	0.073(0.780)	0.096(1.51)	0.068(0.37)	0.077(0.368)	0.066(0.412)
$\langle I/\sigma \rangle$ (last shell)	11.9(2.5)	12.0(1.7)	11.6(1.4)	11.6(2.4)	12.7(3.8)	10.1(2.6)
Multiplicity (last shell)	3.5(3.5)	3.7(3.8)	7.2(7.5)	3.5(3.5)	3.5(3.6)	3.7(3.8)
Refinement						
Resolution (Å)	60.43-2.70	35.52-2.70	35.35-2.43	60.74-2.90	61.43-3.20	57.36-2.69
No. reflections	24861	26283	36862	20860	15623	24903
$R_{\text{int}}/R_{\text{free}}$	0.206/0.280	0.221/0.305	0.227/0.291	0.211/0.290	0.202/0.278	0.285/0.222
No. atoms						
Protein	6740	6791	6787	6729	6744	6735
Ligand	29	26	29	25	31	30
Water	35	39	33	13	24	16
Average B-factor (Wilson)	89.4(56.125)	89(72.66)	73.4(73.72)	79.3(74.7)	100.3(91.6)	92.5(83.8)
r.m.s. deviation from ideality						
Bond Lengths (Å)	0.015	0.015	0.017	0.014	0.015	0.019
Bond angles (°)	1.67	1.63	1.71	1.53	1.51	1.6
Dihedrals (°)	6.73	7.05	6.86	6.48	6.47	6.47
R.M.S.D.B for bonded main (side) chain atoms	0.70(1.93)	0.61(1.73)	0.78(2.21)	0.56(1.07)	0.49(1.24)	0.56(1.42)

7. References

1. Somberg, J.C., *The Evolving Drug Discovery and Drug Development Process: Increasing Efficiency and Cost Effectiveness*, eds. Welling, P. G., Lasagna, L., Banakar, U. V., Marcel Dekker, New York. 1996.
2. <http://www.uga-cdd.org/index.php>.
3. http://www.ppd.com/about_ppd/.
4. <http://www.novartis.com/index.shtml>.
5. <http://info.cancerresearchuk.org/index.htm>.
6. Marone, R., et al., *Targeting phosphoinositide 3-kinase—Moving towards therapy*. *Biochimica et Biophysica Acta*, 2007. **1784**(1): p. 159-185.
7. Walker, E.H., et al., *Structural insights into phosphoinositide 3-kinase catalysis and signalling*. *Nature*, 1999. **402**(6759): p. 313-320.
8. Rommel, C., M. Camps, and H. Ji, *PI3K[delta] and PI3K[gamma]: partners in crime in inflammation in rheumatoid arthritis and beyond?* *Nat Rev Immunol*, 2007. **7**(3): p. 191-201.
9. Hennessy, B.T., et al., *Exploiting the PI3K/AKT Pathway for Cancer Drug Discovery*. *Nat Rev Drug Discov*, 2005. **4**(12): p. 988-1004.
10. Folkes, A.J., et al., *The Identification of 2-(1H-Indazol-4-yl)-6-(4-methanesulfonyl-piperazin-1-ylmethyl)-4-morpholin-4-yl-thieno[3,2-d]pyrimidine (GDC-0941) as a Potent, Selective, Orally Bioavailable Inhibitor of Class I PI3 Kinase for the Treatment of Cancer*. *Journal of Medicinal Chemistry*, 2008. **51**(18): p. 5522-5532.
11. Hawkins, P.T., et al., *Signalling through class I PI3Ks in mammalian cells*. *Biochemical Society Transactions*, 2006. **34**: p. 647-662.
12. Wymann, M.P. and R. Marone, *Phosphoinositide 3-kinase in disease: timing, location, and scaffolding* *Current Opinion in Cell Biology*, 2005. **17**(2): p. 141-149.
13. Cully, M., et al., *Beyond PTEN mutations: the PI3K pathway as an integrator of multiple inputs during tumorigenesis*. *Nature Reviews Cancer*, 2006. **6**(3): p. 184-192.
14. Vivanco, I. and C.L. Sawyers, *The phosphatidylinositol 3-Kinase-AKT pathway in human cancer*. *Nat Rev Cancer*, 2002. **2**(7): p. 489-501.
15. Brian, P.W., et al., *Wortmannin, an antibiotic produced by Penicillium Wortmanni*. *Trans. Br. Mycol. Soc.*, 1957. **40**: p. 365-368.

16. Petcher, T.J., H.P. Weber, and Z. Kis, *Crystal-Structure and Absolute Configuration of Wortmannin and of Wortmannin Para Bromobenzoate*. Journal of the Chemical Society-Chemical Communications, 1972(19): p. 1061-1062.
17. Arcaro, A. and M.P. Wymann, *Wortmannin is a potent phosphatidylinositol 3-kinase inhibitor: the role of phosphatidylinositol 3,4,5-trisphosphate in neutrophil responses*. Biochem J., 1993. **296 (Pt 2)**: p. 297-301.
18. Wymann, M.P., et al., *Wortmannin inactivates phosphoinositide 3-kinase by covalent modification of Lys-802, a residue involved in the phosphate transfer reaction*. Mol. Cell. Biol., 1996. **16(4)**: p. 1722-1733.
19. Dexin, K. and Y. Takao, *Phosphatidylinositol 3-kinase inhibitors: promising drug candidates for cancer therapy*. Cancer Science, 2008. **99(9)**: p. 1734-1740.
20. Woscholski, R., et al., *A Comparison of Demethoxyviridin and Wortmannin as Inhibitors of Phosphatidylinositol 3-Kinase*. Febs Letters, 1994. **342(2)**: p. 109-114.
21. Aldridge, D.C., et al., *Demethoxyviridin and Demethoxyviridiol - New Fungal Metabolites*. Journal of the Chemical Society-Perkin Transactions 1, 1975(10): p. 943-945.
22. Marion, F., et al., *Liphagal, a Selective Inhibitor of PI3 Kinase alpha Isolated from the Sponge Aka coralliphaga: Structure Elucidation and Biomimetic Synthesis*. Organic Letters, 2006. **8(2)**: p. 321-324.
23. R. Béliveau and D. Gingras, *Foods to fight cancer*, published in Great Britain in 2007 by Dorling Kindersley Limited, 80 Strand, London WC2R 0RL, Penguin Group (UK).
24. Frojdo, S., et al., *Resveratrol is a class IA phosphoinositide 3-kinase inhibitor*. Biochemical Journal, 2007. **406**: p. 511-518.
25. Srivastava, A.K., *Inhibition of phosphorylase kinase, and tyrosine protein kinase activities by quercetin*. Biochemical and Biophysical Research Communications, 1985. **131(1)**: p. 1-5.
26. Gschwendt, M., et al., *Inhibition of the calcium- and phospholipid-dependent protein kinase activity from mouse brain cytosol by quercetin*. Biochemical and Biophysical Research Communications, 1983. **117(2)**: p. 444-447.
27. Walker, E.H., et al., *Structural Determinants of Phosphoinositide 3-Kinase Inhibition by Wortmannin, LY294002, Quercetin, Myricetin, and Staurosporine*. Molecular Cell, 2000. **6(4)**: p. 909-919.
28. Su, J.D., et al., *PTEN and Phosphatidylinositol 3'-Kinase Inhibitors Up-Regulate p53 and Block Tumor-induced Angiogenesis: Evidence for an Effect on the Tumor and Endothelial Compartment*. Cancer Res, 2003. **63(13)**: p. 3585-3592.

29. Hu, L., et al., *In Vivo and in Vitro Ovarian Carcinoma Growth Inhibition by a Phosphatidylinositol 3-Kinase Inhibitor (LY294002)*. *Clinical Cancer Research*, 2000. **6**(3): p. 880-886.
30. Jackson, S.P., et al., *PI 3-kinase p110 beta: a new target for antithrombotic therapy*. *Nature Medicine*, 2005. **11**(5): p. 507-514.
31. Sadhu, C., et al., *Essential Role of Phosphoinositide 3-Kinase $\{\delta\}$ in Neutrophil Directional Movement*. *J Immunol*, 2003. **170**(5): p. 2647-2654.
32. Puri, K.D., et al., *Mechanisms and implications of phosphoinositide 3-kinase $\{\delta\}$ in promoting neutrophil trafficking into inflamed tissue*. *Blood*, 2004. **103**(9): p. 3448-3456.
33. Billottet, C., et al., *A selective inhibitor of the p110 $\{\delta\}$ isoform of PI 3-kinase inhibits AML cell proliferation and survival and increases the cytotoxic effects of VP16*. *Oncogene*, 2006. **25**(50): p. 6648-6659.
34. Knight, Z.A., et al., *A Pharmacological Map of the PI3-K Family Defines a Role for p110 α in Insulin Signaling*. 2006. **125**(4): p. 733-747.
35. Fan, Q.-W., et al., *A dual PI3 kinase/mTOR inhibitor reveals emergent efficacy in glioma*. 2006. **9**(5): p. 341-349.
36. Raynaud, F.I., et al., *Pharmacologic Characterization of a Potent Inhibitor of Class I Phosphatidylinositide 3-Kinases*. *Cancer Res*, 2007. **67**(12): p. 5840-5850.
37. Hayakawa, M., et al., *Synthesis and biological evaluation of pyrido[3',2':4,5]furo[3,2-d]pyrimidine derivatives as novel PI3 kinase p110 α inhibitors* *Bioorganic & Medicinal Chemistry Letters*, 2007. **17**(9): p. 2438-2442
38. Hayakawa, M., et al., *Synthesis and biological evaluation of 4-morpholino-2-phenylquinazolines and related derivatives as novel PI3 kinase p110 α inhibitors*. *Bioorganic & Medicinal Chemistry*, 2006. **14**(20): p. 6847-6858.
39. Dexin Kong and T. Yamori, *Advances in Development of Phosphatidylinositol 3-Kinase Inhibitors*. *Curr Med Chem*, 2009. **16**(22): p. 2839-2854.
40. Camps, M., et al., *Blockade of PI3K γ suppresses joint inflammation and damage in mouse models of rheumatoid arthritis*. *Nat Med*, 2005. **11**(9): p. 936-943.
41. Pomel, V., et al., *Furan-2-ylmethylene thiazolidinediones as novel, potent, and selective inhibitors of phosphoinositide 3-kinase γ* . *Journal of Medicinal Chemistry*, 2006. **49**(13): p. 3857-3871.
42. Yaguchi, S.-i., et al., *Antitumor Activity of ZSTK474, a New Phosphatidylinositol 3-Kinase Inhibitor*. *J. Natl. Cancer Inst.*, 2006. **98**(8): p. 545-556.
43. Dexin, K. and Y. Takao, *ZSTK474 is an ATP-competitive inhibitor of class I phosphatidylinositol 3 kinase isoforms*. *Cancer Science*, 2007. **98**(10): p. 1638-1642.

44. Crabbe, T., M.J. Welham, and S.G. Ward, *The PI3K inhibitor arsenal: choose your weapon!* Trends in Biochemical Sciences, 2007. **32**(10): p. 450-456.
45. Maira, S.-M., et al., *Identification and characterization of NVP-BEZ235, a new orally available dual phosphatidylinositol 3-kinase/mammalian target of rapamycin inhibitor with potent in vivo antitumor activity.* Molecular Cancer Therapeutics, 2008. **7**(7): p. 1851-1863.
46. Serra, V., et al., *NVP-BEZ235, a Dual PI3K/mTOR Inhibitor, Prevents PI3K Signaling and Inhibits the Growth of Cancer Cells with Activating PI3K Mutations.* Cancer Res, 2008. **68**(19): p. 8022-8030.
47. Burger, A., *Isosterism and Bioisosterism in Drug Design.* Prog. Drug. Res., 1991. **37**: p. 287-371.
48. Patani, G.A. and E.J. LaVoie, *Bioisosterism: A Rational Approach in Drug Design.* Chemical Reviews, 1996. **96**(8): p. 3147-3176.
49. Cohen, M.S., et al., *Structural Bioinformatics-Based Design of Selective, Irreversible Kinase Inhibitors.* Science, 2005. **308**(5726): p. 1318-1321.
50. Zvelebil, M.J., M.D. Waterfield, and S.J. Shuttleworth, *Structural analysis of PI3-kinase isoforms: Identification of residues enabling selective inhibition by small molecule ATP-competitive inhibitors.* Archives of Biochemistry and Biophysics, 2008. **477**(2): p. 404-410.
51. Hans-Joachim, B., et al., *Fluorine in Medicinal Chemistry.* ChemBioChem, 2004. **5**(5): p. 637-643.
52. Rainer, E.M., et al., *Remote Modulation of Amine Basicity by a Phenylsulfone and a Phenylthio Group.* ChemMedChem, 2007. **2**(3): p. 285-287.
53. *ACD/pKa, LogP, LogD, Aqueous Solubility Version 8.02.* Head Office, Advanced Chemistry Development, Inc., 110 Young Street, 14th floor, Toronto, ON, Canada M5C 1T4; <http://www.acdlabs.com>.
54. Smith, A.J.T., et al., *Beyond Picomolar Affinities: Quantitative Aspects of Noncovalent and Covalent Binding of Drugs to Proteins.* Journal of Medicinal Chemistry, 2008. **52**(2): p. 225-233.
55. Rabindran, S.K., et al., *Antitumor Activity of HKI-272, an Orally Active, Irreversible Inhibitor of the HER-2 Tyrosine Kinase.* Cancer Res, 2004. **64**(11): p. 3958-3965.
56. Arora, A. and E.M. Scholar, *Role of Tyrosine Kinase Inhibitors in Cancer Therapy.* Journal of Pharmacology and Experimental Therapeutics, 2005. **315**(3): p. 971-979.
57. Zhengying, P., et al., *Discovery of Selective Irreversible Inhibitors for Bruton's Tyrosine Kinase.* ChemMedChem, 2007. **2**(1): p. 58-61.
58. Crespo, A., X. Zhang, and A. Fernández, *Redesigning Kinase Inhibitors to Enhance Specificity.* Journal of Medicinal Chemistry, 2008. **51**(16): p. 4890-4898.

59. Zhou, W., et al., *A Structure-Guided Approach to Creating Covalent FGFR Inhibitors*. 2010. **17**(3): p. 285-295.
60. Wipf, P. and R.J. Halter, *Chemistry and biology of wortmannin*. Organic & Biomolecular Chemistry, 2005. **3**(11): p. 2053-2061.
61. <http://www.mayoclinic.org/glioma/glioblastoma.html>.
62. H. Christopher Lawson, et al., *Interstitial chemotherapy for malignant gliomas: the Johns Hopkins experience*. Journal of Neuro-Oncology, 2007. **83**(1): p. 61-70.
63. Robert, C., Y.W. Patrick, and S. David, *Novel Therapies for Malignant Gliomas*. Neurologic clinics, 2007. **25**(4): p. 1141-1171.
64. <http://www.invitrogen.com/site/us/en/home.html>.
65. *The Cancer Genome Atlas Research Network. Comprehensive genomic characterization defines human glioblastoma genes and core pathways*. Nature, 2008. **455**(7216): p. 1061-1068.
66. Christine, K.C., F. Qi-Wen, and A.W. William, *PI3K Signaling in Glioma*; *Animal Models and Therapeutic Challenges*. Brain Pathology, 2009. **19**(1): p. 112-120.
67. Opel, D., et al., *Phosphatidylinositol 3-Kinase Inhibition Broadly Sensitizes Glioblastoma Cells to Death Receptor- and Drug-Induced Apoptosis*. Cancer Res, 2008. **68**(15): p. 6271-6280.
68. Westhoff, M.A., et al., *The pyridinylfuranopyrimidine inhibitor, PI-103, chemosensitizes glioblastoma cells for apoptosis by inhibiting DNA repair*. Oncogene, 2009. **28**(40): p. 3586-3596.
69. Koul, D., et al., *Cellular and in vivo activity of a novel PI3K inhibitor, PX-866, against human glioblastoma*. NEURO ONCOL, 2010: p. n0p058.
70. Ihle, N.T., et al., *Molecular pharmacology and antitumor activity of PX-866, a novel inhibitor of phosphoinositide-3-kinase signaling*. Molecular Cancer Therapeutics, 2004. **3**(7): p. 763-772.
71. Pirola, L., et al., *Activation Loop Sequences Confer Substrate Specificity to Phosphoinositide 3-Kinase alpha (PI3K α)*. FUNCTIONS OF LIPID KINASE-DEFICIENT PI3K α IN SIGNALING. J. Biol. Chem., 2001. **276**(24): p. 21544-21554.
72. Jones, G., et al., *Development and validation of a genetic algorithm for flexible docking*. Journal of Molecular Biology, 1997. **267**(3): p. 727-748.
73. Leslie, A.G.W., *Joint CCP4 and ESF-EACMB (Daresbury Laboratory, Warrington, UK)*. Newsletter on Protein Crystallography, 1992. **26**.

74. Kabsch, W., *Automatic processing of rotation diffraction data from crystals of initially unknown symmetry and cell constants*. Journal of Applied Crystallography, 1993. **26**: p. 795-800.
75. *CCP4, 1994, Acta Crystallogr. D, 50, 760-763.*
76. McCoy, A.J., *Solving structures of protein complexes by molecular replacement with Phaser*. Acta Crystallographica, Section D, Biological Crystallography, 2007. **63**: p. 32-41.
77. Murshudov, Acta Crystallogr. D, 1997. **53**: p. 240-255.
78. Emsley and Cowtan, Acta Crystallogr. D, 2004. **60**: p. 2126-32.
79. Schuttelkopf and v. Aalten, Acta Crystallogr D Biol Crystallogr, 2004. **60**(1355-63).

Curriculum Vitae, Natasa Cmiljanovic

Natasa Cmiljanovic, born January 8, 1981 in Kragujevac, Serbia; Languages: fluent in Serbian and English; good in German: written and spoken.

Education, Professional Experience

- 2007 – 2010 Doctoral student, Institute for Organic Chemistry, Center for Biomedicine, University of Basel, Basel Switzerland (Prof. B. Giese and Prof. M. P. Wymann): *Development of Novel, Potent and Selective Small Molecular Weight PI3K/mTOR Inhibitors for the Treatment of Cancer*.
- 2000 – 2006 University of Kragujevac, Kragujevac, Serbia; Diploma in Natural Sciences, Master of Science in Chemistry, October 2006, the highest mark (10.0). Major subjects: organic chemistry, medicinal chemistry, biochemistry.
- 1996 - 2000 Gymnasium, Kragujevac, Serbia.
- 1988 - 1996 Primary school, Kragujevac, Serbia.

Teaching, Student Supervision

- 2007 - 2009 Practical course in general chemistry, 1st year biology students, 2 days/week (summer semester).
- 2007 - 2009 Practical courses in advanced organic chemistry, advanced Master students in chemistry, 8 weeks/semester.
- 2007 - 2009 Master practical courses in organic chemistry, Master students, 6 months tutoring/1 student.

Publications and Patents

Relation between electron and energy contents of hexagons in pericondensed benzenoid hydrocarbons.

I. Gutman*, S. Milosavljevic, B. Furtula, N. Cmiljanovic. *Indian Journal of Chemistry* 2005: Vol. 44A, pp. 13-17.

Dependence of total π -electron energy on a large number of non- bonding molecular orbitals.

I. Gutman*, D. Stevanovic, S. Radenkovic, S. Milosavljevic, N. Cmiljanovic. *Journal of the Serbian Chemical Society* 2004: Vol. 69, pp. 777-782.

Dependence of total π -electron energy on the number of non-bonding molecular orbitals.

I. Gutman*, N. Cmiljanovic, S. Milosavljevic, S. Radenkovic. *Monatshefte für Chemie* 2004: Vol. 135, n^o7, pp. 765-772.

Effect of non-bonding molecular orbitals on total π -electron energy.

I. Gutman*, N. Cmiljanovic, S. Milosavljevic, S. Radenkovic. *Chemical Physics Letters* 2004: Vol. 383, n^o1-2, pp. 171-175.

Graph energy-A useful molecular structure-descriptor.

I. Gutman*, D. Vidovic, N. Cmiljanovic, S. Milosavljevic, S. Radenkovic. *Indian Journal of Chemistry* 2003: Vol. 42A, pp. 1309-1311.

Piperazinotriazines (2010).

Cmiljanovic V, Cmiljanovic N, Giese B, Wymann MP. UK patent application.

Spirocyclic compounds and their use as therapeutic agents and diagnostic probes (2010).

Cmiljanovic V, Cmiljanovic N, Giese B, Wymann MP. UK patent application.

Triazine, pyrimidine and pyridine analogs and their use as therapeutic agents and diagnostic probes (2009).

Cmiljanovic V, Cmiljanovic N, Giese B, Wymann MP. International patent application, PCT/IB2009/007404.

Triazine, pyrimidine and pyridine analogs and their use as therapeutic agents and diagnostic probes (2008).

Cmiljanovic V, Cmiljanovic N, Giese B, Wymann MP. UK patent application, GB 0821219.3.

Development of Novel, Potent and Selective Small Molecular Weight PI3K/mTOR Inhibitors for the Treatment of Cancer